

Tree-Based Diffusion Schrödinger Bridge with Applications to Wasserstein Barycenters

Maxence Noble*

CMAP, CNRS, École polytechnique,
Institut Polytechnique de Paris,
91120 Palaiseau, France

Valentin De Bortoli

Computer Science Department,
ENS, CNRS, PSL University

Arnaud Doucet

Department of Statistics,
University of Oxford, UK

Alain Olivier Durmus

CMAP, CNRS, École polytechnique,
Institut Polytechnique de Paris,
91120 Palaiseau, France

Abstract

Multi-marginal Optimal Transport (mOT), a generalization of OT, aims at minimizing the integral of a cost function with respect to a distribution with some prescribed marginals. In this paper, we consider an entropic version of mOT with a tree-structured quadratic cost, i.e., a function that can be written as a sum of pairwise cost functions between the nodes of a tree. To address this problem, we develop Tree-based Diffusion Schrödinger Bridge (TreeDSB), an extension of the Diffusion Schrödinger Bridge (DSB) algorithm. TreeDSB corresponds to a dynamic and continuous state-space counterpart of the multimarginal Sinkhorn algorithm. A notable use case of our methodology is to compute Wasserstein barycenters which can be recast as the solution of a mOT problem on a star-shaped tree. We demonstrate that our methodology can be applied in high-dimensional settings such as image interpolation and Bayesian fusion.

1 Introduction

In the last decade, computational Optimal Transport (OT) has shown great success with applications in various fields such as biology (Schiebinger et al., 2019; Bunne et al., 2022), shape correspondence (Su et al., 2015; Feydy et al., 2017; Eisenberger et al., 2020), control theory (Bayraktar et al., 2018; Acciaio et al., 2019) and computer vision (Schmitz et al., 2018; Carion et al., 2020). In this paper, we consider the *multi-marginal* OT (mOT) problem, an extension of OT, which is defined as follows. Let $\ell \in \mathbb{N}^*$. Given a cost function $c : (\mathbb{R}^d)^{\ell+1} \rightarrow \mathbb{R}$, a subset $S \subset \{0, \dots, \ell\}$ and a family of probability measures $\{\mu_i\}_{i \in S}$, mOT consists in solving

$$\pi^* = \arg \min \left\{ \int c(x_{0:\ell}) d\pi(x_{0:\ell}) : \pi \in \mathcal{P}^{(\ell+1)}, \pi_i = \mu_i, \forall i \in S \right\}, \quad (\text{mOT})$$

where $\mathcal{P}^{(\ell+1)}$ is the set of probability measures defined on $(\mathbb{R}^d)^{\ell+1}$ and π_i is the i -th marginal of π , i.e., $\pi_i(A) = \pi(\text{proj}_i^{-1}(A))$ for any $A \in \mathcal{B}(\mathbb{R}^d)$, with $\text{proj}_i : x_{0:\ell} \mapsto x_i$. This extension of OT has notably been considered in quantum chemistry (Cotar et al., 2013), clustering (Cuturi & Doucet, 2014) and statistical inference (Srivastava et al., 2018). In particular, given some weights $(w_i)_{i \in \{1, \dots, \ell\}} \in (\mathbb{R}_+)^{\ell}$, an application of interest in machine learning is the computation of the Wasserstein barycenter between the measures $\{\mu_i\}_{i \in S}$ (Peyré et al., 2019), given by π_0^* in (mOT), in

*Corresponding author. Contact at: maxence.noble-bourillot@polytechnique.edu

the case where $S = \{1, \dots, \ell\}$ and $c(x_{0:\ell}) = \sum_{i=1}^{\ell} w_i \|x_0 - x_i\|^2$. In this setting, with $w_i = 1/\ell$, the distribution π_0^* can be regarded as the Fréchet mean (Karcher, 2014) of the measures $\{\mu_i\}_{i \in S}$ for the Wasserstein distance of order 2 (Peyré et al., 2019).

In this work, similarly to Haasler et al. (2021), we consider a multimarginal cost which writes as the sum of interaction energies onto a tree structure and restrict our study to the quadratic setting. More precisely, given an undirected tree $T = (V, E)$, with vertices V (identified with $\{0, \dots, \ell\}$) and edges E , we consider cost functions of the form

$$c(x_{0:\ell}) = \sum_{\{v, v'\} \in E} w_{v, v'} \|x_v - x_{v'}\|_2^2, \quad (1)$$

where $w_{v, v'}$ is a weight on the edge $\{v, v'\}$, which links v to v' (and v' to v). We emphasize that this problem is different from an OT problem defined on the space of graphs (Chen et al., 2016). In our setting, each node represents a probability distribution (observed or to be inferred) and each edge represents a coupling between two distributions.

Interior point methods can be used to solve OT and mOT problems but they come with computational challenges (Pele & Werman, 2009). In order to mitigate these limitations, one often considers an *entropic regularization* of OT, known as Entropic OT (EOT), which can be efficiently solved using the Sinkhorn algorithm (Cuturi, 2013; Knight, 2008; Sinkhorn & Knopp, 1967). Similarly, (mOT) can be relaxed using the following entropic regularization

$$\pi^* = \arg \min \left\{ \int c(x_{0:\ell}) d\pi(x_{0:\ell}) + \varepsilon \text{KL}(\pi | \nu) : \pi \in \mathcal{P}^{(\ell+1)}, \pi_i = \mu_i, \forall i \in S \right\}, \quad (\text{EmOT})$$

where $\varepsilon > 0$ is a hyperparameter and $\text{KL}(\pi | \nu)$ is the Kullback-Leibler divergence between π and ν . In the case of a quadratic cost, EOT can be seen as the *static* counterpart of a *dynamic* formulation: the Schrödinger Bridge (SB) problem. The SB framework naturally arises in stochastic control (Dai Pra, 1991) where one aims at controlling the marginal distribution of a stochastic process at a fixed time. Recently, De Bortoli et al. (2021) introduced Diffusion Schrödinger Bridge (DSB), see also (Vargas et al., 2021; Chen et al., 2022). This approach leverages advances in the field of denoising diffusion models (Song et al., 2021; Ho et al., 2020) in order to derive an efficient and scalable scheme to solve SB.

In this work, we introduce a new methodology based on DSB to approximate the solutions of (EmOT) for a tree-based quadratic cost given by (1) in the case where S coincides with the set of the leaves of T . Our algorithm, TreeDSB, works as follows. First, we pick (i) $r \in S$ to be the root of T and (ii) $\ell \in S \setminus \{r\}$ to be a *target* leaf. Then, we compute the *forward* diffusion (defined by the cost c) going from r to ℓ and learn how to reverse it. Then, we set the ℓ to be the new root of T and pick a new leaf $\ell' \in S \setminus \{\ell\}$ to be the new target leaf. We repeat this process by cycling over the leaves of T . The whole procedure is illustrated in Figure 1. We prove the convergence of our method by extending results on the convergence of Sinkhorn algorithm in the multi-marginal setting. Even though our approach can be applied to any tree-structured cost, we focus on Wasserstein barycenter applications and illustrate our approach on several examples from statistical inference and image processing.

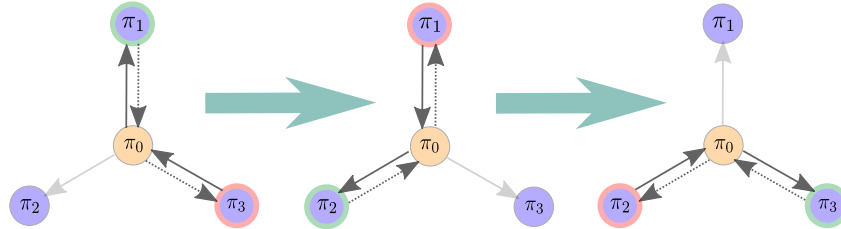


Figure 1: The root is chosen at the node π_3 (red circle) and we pick the leaf π_1 (green circle). The forward process goes from $\pi_3 \rightarrow \pi_1$ and we learn the time-reversal $\pi_1 \rightarrow \pi_3$. Then, we set π_1 to be the root, choose the leaf π_2 and learn the flow $\pi_2 \rightarrow \pi_1$ given the flow $\pi_1 \rightarrow \pi_2$. Finally, we learn the flow $\pi_3 \rightarrow \pi_2$ given the flow $\pi_2 \rightarrow \pi_3$. We cycle through these three iterations. After convergence, the node π_0 approximates the regularized Wasserstein barycenter between π_1, π_2 and π_3 .

Notation. For any measurable space (X, \mathcal{X}) , we denote by $\mathcal{P}(X)$ the space of probability measures defined on (X, \mathcal{X}) . For any $\ell \in \mathbb{N}$, let $\mathcal{P}^{(\ell)} = \mathcal{P}((\mathbb{R}^d)^\ell)$; we will denote $\mathcal{P}^{(1)}$ by \mathcal{P} . Assume that $X = (\mathbb{R}^d)^\ell$ for some $\ell \in \mathbb{N}$. For any $x \in X$ and any $m, n \in \{0, \dots, \ell\}$ such that $m \leq n$, let $x_{m:n} = (x_m, x_{m+1}, \dots, x_n)$. Let Leb be the Lebesgue measure. For any non-negative function $f : X \rightarrow \mathbb{R}_+$, such that $\int_X f d\text{Leb} < +\infty$, define $H(f) = -\int_X f \log f d\text{Leb} \in (-\infty, +\infty]$. For any distribution $\mu \in \mathcal{P}(X)$, we define the entropy of μ as $H(\mu) = H(d\mu/d\text{Leb})$ if $\mu \ll \text{Leb}$ and $H(\mu) = +\infty$ otherwise. For any two arbitrary measures μ and ν defined on (X, \mathcal{X}) , define the Kullback–Leibler divergence between μ and ν as $\text{KL}(\mu|\nu) = \int_X \log(d\mu/d\nu) d\mu - \int_X d\mu + \int_X d\nu$ if $\mu \ll \nu$ and $\text{KL}(\mu|\nu) = +\infty$ otherwise. For any undirected tree $T = (V, E)$ with vertices V and edges E , we denote by $\{v, v'\}$ (or $\{v', v\}$) the edge between $v \in V$ and $v' \in V$, if it exists. Given $r \in V$, we denote by $T_r = (V, E_r)$ the directed version of T rooted in r , where the directed edges E_r are uniquely defined from the edges E , see Appendix B for further details. In this case, the edge linking $v \in V$ to $v' \in V$ in T_r is denoted by (v, v') .

2 Background and setting

Schrödinger Bridges and EOT. We first recall the relationship between Schrödinger Bridges and EOT. Given $T > 0$, \mathbb{Q} a (reference) path measure, *i.e.*, $\mathbb{Q} \in \mathcal{P}(C([0, T], \mathbb{R}^d))$ and two measures $\mu_0, \mu_1 \in \mathcal{P}(\mathbb{R}^d)$, solving the Schrödinger Bridge (SB) problem amounts to finding \mathbb{P}^* such that

$$\mathbb{P}^* = \operatorname{argmin}\{\text{KL}(\mathbb{P}|\mathbb{Q}) : \mathbb{P} \in \mathcal{P}(C([0, T], \mathbb{R}^d)), \mathbb{P}_0 = \mu_0, \mathbb{P}_T = \mu_1\}. \quad (\text{SB})$$

If \mathbb{Q} is associated with a Stochastic Differential Equation (SDE)², of the form $d\mathbf{X}_t = -a\mathbf{X}_t dt + d\mathbf{B}_t$, with $a \geq 0$, then it can be shown, see (Léonard, 2014, Proposition 1) that

$$\mathbb{P}_{0,T}^* = \operatorname{argmin}\{\text{KL}(\pi|\mathbb{Q}_{0,T}) : \pi \in \mathcal{P}^{(2)}, \pi_0 = \mu_0, \pi_1 = \mu_1\}. \quad (\text{static-SB})$$

This is called the *static* formulation of SB. It can be shown that solving (static-SB) is equivalent to solving EOT with regularization $\Phi(a, T) = 2 \sinh(aT)/a$ if $a > 0$ and $2T$ if $a = 0$. Finally, since $\mathbb{P}^* = \mathbb{P}_{0,T}^* \otimes \mathbb{Q}_{|0,T}$, where $\mathbb{Q}_{|0,T}$ is the measure \mathbb{Q} conditioned on an initial and terminal condition, solving the *dynamic* problem (SB) is equivalent to solving the *static* problem (static-SB).

Diffusion Schrödinger Bridge. Recently De Bortoli et al. (2021) introduced Diffusion Schrödinger Bridge (DSB), a numerical scheme to solve (SB). It approximates the so-called *Iterative Proportional Fitting* (IPF) iterates (called Sinkhorn iterates when the measures are discrete) (Sinkhorn & Knopp, 1967; Knight, 2008; Peyré et al., 2019; Cuturi & Doucet, 2014). The IPF algorithm can be described as follows: consider a sequence $(\mathbb{P}^n)_{n \in \mathbb{N}}$ such that $\mathbb{P}^0 = \mathbb{Q}$ and for any $n \in \mathbb{N}$

$$\mathbb{P}^{2n+1} = \operatorname{argmin}\{\text{KL}(\mathbb{P}|\mathbb{P}^{2n}) : \mathbb{P}_T = \mu_1\}, \quad \mathbb{P}^{2n+2} = \operatorname{argmin}\{\text{KL}(\mathbb{P}|\mathbb{P}^{2n+1}) : \mathbb{P}_0 = \mu_0\}.$$

This procedure alternatively projects between the measures with fixed initial distribution and the ones with fixed terminal distribution. For the first iteration, we get that $\mathbb{P}^1 = \mu_1 \otimes \mathbb{Q}_{|T}$. Assuming that \mathbb{Q} is given by $d\mathbf{X}_t = f_t(\mathbf{X}_t)dt + d\mathbf{B}_t$, with $f : [0, T] \times \mathbb{R}^d \rightarrow \mathbb{R}^d$, then \mathbb{P}^1 is associated with the *time-reversal* of this SDE initialized at μ_1 . The time-reversal of an SDE has been derived under mild assumptions on the drift and diffusion coefficients (Haussmann & Pardoux, 1986; Cattiaux et al., 2021). In this case, we have $(\mathbf{Y}_{T-t})_{t \in [0, T]} \sim \mathbb{P}^1$, with $\mathbf{Y}_0 \sim \mu_1$ and

$$d\mathbf{Y}_t = \{-f_{T-t}(\mathbf{Y}_t) + \nabla \log p_{T-t}(\mathbf{Y}_t)\}dt + d\mathbf{B}_t,$$

where p_t is the density of \mathbb{P}_t^0 w.r.t. the Lebesgue measure. The score $\nabla \log p_t$ is estimated using score matching techniques (Hyvärinen, 2005; Vincent, 2011). The first iterate of DSB, \mathbb{P}^1 , corresponds to a *denoising diffusion model* (Ho et al., 2020; Song et al., 2021). DSB iterates further and not only parameterize the backward process but also the forward process. It can therefore be seen as a refinement of diffusion models drawing a bridge between generative modeling and optimal transport.

Link between (EmOT) and Schrödinger Bridge. In this work, we consider a Schrödinger Bridge formulation of (EmOT). Given $\ell \in \mathbb{N}^*$, we follow the framework of Haasler et al. (2021) and consider an undirected tree $T = (V, E)$, where V is identified with $\{0, \dots, \ell\}$. In this case, (EmOT) can be easily rewritten in a *static* SB fashion

$$\pi^* = \operatorname{argmin}\{\text{KL}(\pi|\pi^0) : \pi \in \mathcal{P}^{(|V|)}, \pi_i = \mu_i, \forall i \in S\}, \quad (\text{TreeSB})$$

²We refer to Appendix C for details on solutions of SDEs and associated measures.

with $(d\pi^0/d\text{Leb})(x_{0:\ell}) \propto \exp[-c(x_{0:\ell})/\varepsilon](d\nu/d\text{Leb})(x_{0:\ell})$, where π^0 is the *reference* measure of the SB problem. Although no specific structure on the cost c is assumed in (EmOT), several works consider the case where c can be written as a sum of interaction of energies, see Haasler et al. (2021); Solomon et al. (2015, 2014), for instance. In this case, π^0 factorizes along T due to the form of c .

Our framework. In this work, we restrict our study of (TreeSB), or equivalently (EmOT), to the case where c is the tree-structured quadratic cost derived from T , as defined in (1). Furthermore, as in Haasler et al. (2021), we choose S , *i.e.*, the set of fixed marginals, to coincide with the set of probability measures on the *leaves* of T . This framework, recovers important applications, from Wasserstein barycenters to Wasserstein propagation, see Section 5. We choose π^0 to be a *probability* measure which factorizes along $\mathsf{T}_r = (\mathsf{V}, \mathsf{E}_r)$, the directed version of T rooted in r

$$\pi^0 = \pi_r^0 \bigotimes_{(v,v') \in \mathsf{E}_r} \pi_{v'|v}^0, \quad (2)$$

where $\pi_{v'|v}^0(\cdot | x_v) = \mathcal{N}(x_v, \varepsilon/(2w_{v,v'})\mathbf{I}_d)$ and $\pi_r^0 \ll \text{Leb}$ with density φ_r . In what follows, we define K as the number of leaves of T , denoting $\mathsf{S} = \{i_0, \dots, i_{K-1}\}$, and define $T_{v,v'} = \varepsilon/(2w_{v,v'})$ for any $\{v, v'\} \in \mathsf{E}$. In the next section, we present Tree-Based Diffusion Schrödinger Bridge.

3 Tree-based Diffusion Schrödinger Bridge

In this section, we present a method to solve (TreeSB) in the case where $r \in \mathsf{S}$, *i.e.*, the potential φ_r defining π^0 in (2) corresponds to a leaf of T . We refer to Appendix E for the extension to the case where $r \in \mathsf{V} \setminus \mathsf{S}$. Without loss of generality, see Appendix E, we assume that $r = i_{K-1}$ and choose $\varphi_r = d\mu_{i_{K-1}}/d\text{Leb}$, such that $\pi_{i_{K-1}}^0 = \mu_{i_{K-1}}$.

In order to approximate solutions of (TreeSB), we consider the *multimarginal* extension of the Iterative Proportional Fitting algorithm. Namely, we define $(\pi^n)_{n \in \mathbb{N}}$ such that for any $n \in \mathbb{N}$

$$\pi^{n+1} = \operatorname{argmin}\{\text{KL}(\pi | \pi^n) : \pi \in \mathcal{P}(|\mathsf{V}|), \pi_{i_{k+1}} = \mu_{i_{k+1}}\}, \quad (\text{mIPF})$$

with $k = (n-1) \bmod(K)$ and $k+1$ is identified with $n \bmod(K)$.

Although (TreeSB) is a *static* problem, our methodology relies on the fact that $\pi^0 \in \mathcal{P}(|\mathsf{V}|)$ can be obtained in a *dynamic* fashion. For any path measure $\mathbb{P} \in \mathcal{P}(C([0, T], \mathbb{R}^d))$ we denote by $\text{Ext}(\mathbb{P}) \in \mathcal{P}^{(2)}$, with $\text{Ext}(\mathbb{P}) = \mathbb{P}_{0,T}$, the coupling between the *extremal* (initial and terminal) distributions of the path measure, see Figure 2. The following proposition establishes this *static-dynamic* correspondence.

Proposition 1. *Let $\mathsf{T}_{K-1} = (\mathsf{V}, \mathsf{E}_{K-1})$, the directed tree associated with $\mathsf{T} = (\mathsf{V}, \mathsf{E})$ and root i_{K-1} . Then, for any $(v, v') \in \mathsf{E}_{K-1}$, there exists $\mathbb{P}_{(v,v')}^0 \in \mathcal{P}(C([0, T_{v,v'}], \mathbb{R}^d))$ with $\text{Ext}(\mathbb{P}_{(v,v')}^0) = \pi_{(v,v')}^0$ and such that $\mathbb{P}_{(v,v')}^0|_0$ is the distribution of $(\mathbf{B}_t)_{t \in [0, T_{v,v'}]}$, recalling that $T_{v,v'} = \varepsilon/(2w_{v,v'})$.*

Proposition 1 shows that in order to sample from π^0 we can use the following procedure: (i) sample from $\mu_{i_{K-1}}$ at the root i_{K-1} , (ii) propagate along each edge $(v, v') \in \mathsf{E}_{K-1}$, using $(\mathbf{B}_t)_{t \in [0, T_{v,v'}]}$. We emphasize that this *dynamic* description of π^0 is not unique. In particular, we could have replaced the Brownian motions by an Ornstein–Uhlenbeck process with different hyperparameters. The key property of the dynamics is that its extremal coupling is the same as the static one. The next proposition shows that this *dynamic* formulation of π^0 is still valid for the (mIPF) iterates.

Proposition 2. *Let $n \in \mathbb{N}$, $k = (n-1) \bmod(K)$, $\mathsf{T}_k = (\mathsf{V}, \mathsf{E}_k)$, the directed tree with root i_k . Then, for any $(v, v') \in \mathsf{E}_k$, there exists $\mathbb{P}_{(v,v')}^n \in \mathcal{P}(C([0, T_{v,v'}], \mathbb{R}^d))$ with $\text{Ext}(\mathbb{P}_{(v,v')}^n) = \pi_{(v,v')}^n$.*

Based on the previous proposition, we show that these path measures can be updated iteratively. The key observation is that each update can be done on a *path* of a (directed) tree.

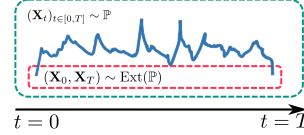


Figure 2: Path $(\mathbf{X}_t)_{t \in [0, T]}$ and the Ext operator.

Proposition 3. Let $n \in \mathbb{N}$, $k = (n-1) \bmod(K)$. Consider the path $P = \{(v_j, v_{j+1})\}_{j=1}^J$ in $T_k = (V, E_k)$, the directed tree with root i_k , such that $v_1 = i_k$ and $v_{J+1} = i_{k+1}$. Then, for any $(v, v') \in E_{k+1}$ either $(v', v) \in P$ or $(v, v') \in E_k \setminus P$. In addition, we have for any $(v, v') \in E_{k+1}$

- (a) if $(v, v') \in E_k \setminus P$ then $\mathbb{P}_{(v,v')}^{n+1} = \pi_v^{n+1} \otimes \mathbb{P}_{(v,v')}^n|_0$,
- (b) if $(v', v) \in P$ then $\mathbb{P}_{(v,v')}^{n+1} = \pi_v^{n+1} \otimes (\mathbb{P}_{(v',v)}^n)^R$,

where \mathbb{P}^R is the time-reversal of the path measure \mathbb{P} .

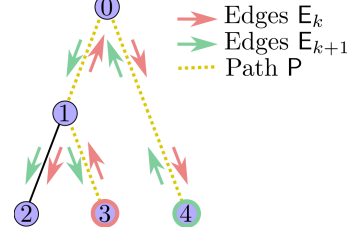


Figure 3: Illustration of Proposition 3

Figure 3 illustrates Proposition 3 in the case where $K = 3$, $i_k = 3$ and $i_{k+1} = 4$. Since $\pi_{i_{k+1}}^{n+1} = \mu_{i_{k+1}}$, the path measures $\{\mathbb{P}_{(v,v')}^{n+1}\}_{(v,v') \in E_{k+1}}$ are defined recursively on the vertices by following a breadth-first search in T_{k+1} , starting from its root i_{k+1} . Moreover, the time reversal in Proposition 3-(b) can be computed explicitly, see Haussmann & Pardoux (1986) for instance. Indeed, assuming that $\mathbb{P}_{(v,v')}^n$ is associated with $d\mathbf{X}_t = f_{t,v,v'}(\mathbf{X}_t)dt + d\mathbf{B}_t$ with $\mathbf{X}_0 \sim \pi_v^n$, then, under mild conditions, its time-reversal $(\mathbb{P}_{(v,v')}^n)^R$ is associated with $d\mathbf{Y}_t = \{-f_{T-t,v,v'} + \nabla \log p_{v,v',T-t}(\mathbf{Y}_t)\}dt + d\mathbf{B}_t$ with $\mathbf{Y}_0 \sim \pi_{v'}^{n+1}$, where $p_{v,v',t}$ is the density of $\mathbb{P}_{(v,v'),t}^n$ w.r.t. the Lebesgue measure. The score $\nabla \log p_{v,v',T-t}$ can then be approximated using score-matching techniques (Hyvärinen, 2005; Vincent, 2011) which are now ubiquitous in diffusion models (Song et al., 2021) and used in DSB De Bortoli et al. (2021). Therefore, the update (b) is similar to the one of DSB for each edge on the path joining i_k and i_{k+1} , with $k = (n-1) \bmod(K)$. In practice, we parameterize the drifts $f_{t,v,v'}$ for any $\{v, v'\} \in E$ with neural networks $f_{t,\theta_{v,v'}}$ and use the mean-matching loss introduced in De Bortoli et al. (2021). Note that doing so we obtain $2|E|$ neural networks. We call this algorithm *Tree-based Diffusion Schrödinger Bridge* (TreeDSB), see Algorithm 1.

Algorithm 1 Tree Diffusion Schrödinger Bridge (Training)

```

1: Input:  $T = (V, E)$ ,  $\{\mu_i\}_{i \in S}$ ,  $\{\theta_{(v,v')}\}_{(v,v') \in E}$ ,  $N \in \mathbb{N}$ 
2: for  $n = 0, \dots, N$  do
3:   Let  $k = (n-1) \bmod(K)$ 
4:   Get path between  $i_k$  and  $i_{k+1}$ ,  $P = \{v_j, v_{j+1}\}_{j=1}^J$ 
5:   while not converged do
6:     for  $j = 1, \dots, J$  do
7:       Sample from  $\mathbb{P}_{v_j, v_{j+1}}^n$  (Euler-Maruyama)
8:       Compute mean matching loss  $\ell(\theta_{v_{j+1}, v_j})$ 
9:        $\theta_{v_{j+1}, v_j} \leftarrow \text{Gradient Step}(\ell(\theta_{v_{j+1}, v_j}))$ 
10:      Update  $f_{t, \theta_{v_{j+1}, v_j}}$ 
11:     end for
12:   end while
13: end for
14: Output:  $\{\theta_{(v,v')}\}_{(v,v') \in E}$ 

```

The algorithm is initialized with $f_{t, \theta_{v,v'}} = 0$ for all $(v, v') \in E$. This corresponds to Brownian motion dynamics when sampling at the first iteration of TreeDSB, see Proposition 1. Note that in Algorithm 1, when we sample from $\mathbb{P}_{(v_j, v_{j+1})}^n$, we update $f_{t, \theta_{v_{j+1}, v_j}}$ which will be used to sample from $\mathbb{P}_{(v_{j+1}, v_j)}^{n+1}$ in the next iterations. In order to sample from the dynamics $\mathbb{P}_{(v_j, v_{j+1})}^n$, we consider its Euler-Maruyama discretization, see Appendix F for more details. We describe the different steps of the algorithm in the case of a toy example below, see Figure 1 for an illustration.

We consider a star-shaped tree with three leaves denoted $\{1, 2, 3\}$ and its central node $\{0\}$. For ease of exposition, we choose $w_{v,v'} = 1/2$ for any $\{v, v'\} \in E$ such that $T_{v,v'} = \varepsilon/(2w_{v,v'}) = T$ where $T = \varepsilon$. We consider a measure π^0 as defined in (2) with $r = 3$ and such that $\varphi_r = (d\mu_3/d\text{Leb})$, i.e.,

$$\begin{aligned}
(d\pi^0/d\text{Leb})(x_{0:3}) &\propto (d\mu_3/d\text{Leb})(x_3) \exp[-\|x_0 - x_3\|^2/(2\varepsilon)] \\
&\quad \exp[-\|x_1 - x_0\|^2/(2\varepsilon)] \exp[-\|x_2 - x_0\|^2/(2\varepsilon)].
\end{aligned}$$

Hence, in order to sample from π^0 , we first sample from μ_3 , then follow the Brownian motion up to time T along the edge $3 \rightarrow 0$. Then, we follow two (independent) Brownian motions along the edges $0 \rightarrow 1$ and $0 \rightarrow 2$ up until time T . During the first iteration of TreeDSB, we follow the path from 3 to 1, i.e., $3 \rightarrow 0 \rightarrow 1$, and using samples from π^0 , we compute $f_{t, \theta_{0,3}}$ and $f_{t, \theta_{1,0}}$ for any $t \in [0, T]$. We then reroot the tree at 1. In order to sample from π^1 , we first sample from μ_1 . Then, we follow the dynamics $d\mathbf{X}_t^{1,0} = f_{t, \theta_{1,0}}(\mathbf{X}_t^{1,0})dt + d\mathbf{B}_t$ up to time T . We get that $(\mathbf{X}_T^{1,0}, \mathbf{X}_0^{1,0})$ is a sample from $\pi_{0,1}^1$. Then, we follow the two dynamics $d\mathbf{X}_t^{0,2} = d\mathbf{B}_t$ and $d\mathbf{X}_t^{0,3} = f_{t, \theta_{0,3}}(\mathbf{X}_t^{0,3})dt + d\mathbf{B}_t$ with initial conditions $\mathbf{X}_0^{0,2} = \mathbf{X}_0^{0,3} = \mathbf{X}_T^{1,0}$. We get that

$(\mathbf{X}_T^{1,0}, \mathbf{X}_0^{1,0}, \mathbf{X}_T^{0,2}, \mathbf{X}_T^{0,3})$ is sampled approximately³ from π^1 . We repeat the procedure to estimate π^2 and the following iterates. Combining Proposition 7 and Proposition 8, we show that $(\pi_0^n)_{n \in \mathbb{N}}$ converges to a (regularized) Wasserstein barycenter.

4 Theoretical properties of Tree DSB

Using Proposition 2, we have that for any edge $\{v, v'\} \in E$ and $n \in \mathbb{N}$, $\mathbb{P}_{(v,v')}^n = \text{Ext}(\pi_{(v,v')}^n)$, where $(\pi^n)_{n \in \mathbb{N}}$ is given by (mIPF). Based on this equivalence, we now study some of the theoretical properties of $(\pi^n)_{n \in \mathbb{N}}$, and its limits. In the case where the cost is bounded, the convergence of (mIPF) was recently studied in Marino & Gerolin (2020); Carlier (2022). Our setting does not satisfy their assumptions, since our transport cost is quadratic and the measures are defined on \mathbb{R}^d . In what follows, we provide the first non-quantitative convergence results for (mIPF) to solve (TreeSB).

For the rest of the section, we consider a formulation of the multi-marginal Schrödinger bridge problem which is more general than the one derived from a tree-structured cost

$$\pi^* = \text{argmin}\{\text{KL}(\pi | \pi^0) : \pi \in \mathcal{P}^{(\ell+1)}, \pi_i = \mu_i, \forall i \in S\}, \quad (\text{mSB})$$

where $S \subset \{0, \dots, \ell\}$, $\pi^0 \in \mathcal{P}$, $\{\mu_i\}_{i \in S} \in \mathcal{P}^{|S|}$. We consider the following set of assumptions.

- A1.** *There exists a family of measures $\{\nu_i\}_{i \in \{0, \dots, \ell\}}$ defined on $(\mathbb{R}^d, \mathcal{B}(\mathbb{R}^d))$ such that $\pi^0 \ll \bigotimes_{i=0}^{\ell} \nu_i$ with density $h = d\pi^0 / (d \bigotimes_{i=0}^{\ell} \nu_i)$ and $\mu_i \ll \nu_i$ with density $r_i = d\mu_i / d\nu_i$ for any $i \in S$.*
- A2.** $\{\pi \in \mathcal{P}^{(\ell+1)} : \text{KL}(\pi | \pi^0) < \infty, \pi_i = \mu_i, \forall i \in S\} \neq \emptyset$.
- A3.** *There exists a family of probability measures $\{\tilde{\mu}_j\}_{j \in \{0, \dots, \ell\} \setminus S}$ such that $\pi^0 \sim \tilde{\pi}^0$, where $\tilde{\pi}^0 = \bigotimes_{i \in S} \mu_i \bigotimes_{j \in \{0, \dots, \ell\} \setminus S} \tilde{\mu}_j$.*

In particular, (mSB) recovers (TreeSB) by considering $\nu_i = \text{Leb}$ for any $i \in \{0, \dots, \ell\}$ and $h(x_{0:\ell}) = \varphi_r(x_r) \exp[-c(x_{0:\ell})/\varepsilon]$ in A1. We detail in Appendix D how A2 and A3 can be met in (TreeSB). Under these assumptions, the multimarginal Schrödinger Bridge exists.

Proposition 4. *Assume A1 and A2. Then, there exists a unique solution π^* to (mSB). In addition, assume A3. Then, there exists a family $\{\psi_i^*\}_{i \in S}$ of measurable functions $\psi_i^* : \mathbb{R}^d \rightarrow \mathbb{R}$ such that*

$$(d\pi^* / d\pi^0) = \exp[\bigoplus_{i \in S} \psi_i^*] \quad \pi^0\text{-a.s.}$$

In order to establish the existence and uniqueness result of Proposition 4, we extend results from Nutz (2021) to the multimarginal setting. A consequence of Proposition 4 is that the iterations of (mIPF) can be described using potentials.

Corollary 5. *Assume A1, A2 and A3. Let $(\pi^n)_{n \in \mathbb{N}}$ be the sequence given by (mIPF). Then, for any $n \in \mathbb{N}^*$ with $k = (n-1) \bmod(K)$ and $q \in \mathbb{N}$ such that $n = qK + k + 1$, there exists a family of measurable functions $\{\psi_{i_0}^{q+1}, \dots, \psi_{i_k}^{q+1}, \psi_{i_{k+1}}^q, \dots, \psi_{i_{K-1}}^q\}$ such that*

$$(d\pi^n / d\pi^0)(x_{0:\ell}) = \exp[\bigoplus_{j=0}^k \psi_{i_j}^{q+1}(x_{i_j}) \bigoplus_{j=k+1}^{K-1} \psi_{i_j}^q(x_{i_j})] \quad \pi^0\text{-a.s.}$$

We now prove that the marginal π_i^n converges to μ_i for any $i \in S$, as n goes to infinity, i.e., we have marginal convergence on the leaves of T.

Proposition 6. *Assume A1 and A2. Let $(\pi^n)_{n \in \mathbb{N}}$ be the sequence given by (mIPF). Then, we have $\lim_{n \rightarrow \infty} \|\pi_i^n - \mu_i\|_{\text{TV}} = 0$ for any $i \in S$.*

The previous result does not ensure the convergence of $(\pi^n)_{n \in \mathbb{N}}$ to the solution to (mSB). In particular, Proposition 6 does not provide the convergence of the marginals on the nodes $v \in V \setminus S$, which is key to compute regularized Wasserstein barycenters with Tree-DSB. Relying on additional assumptions, we now derive the convergence of (mIPF).

A4. $\bigoplus_{i \in S} L^1(\mu_i) \subset L^1(\pi^*)$ is closed.

A5. *There exist $\bar{c} \in (0, \infty)$ such that $\exp(\psi_{i_k}^n - \psi_{i_k}^{n+1}) \leq \bar{c}$, for any $n \in \mathbb{N}$, any $k \in \{0, \dots, K-2\}$.*

³There is no approximation if the neural networks $f_{t, \theta_{v,v'}}$ are global minimizers of their loss functions.

These assumptions can be seen as multimarginal extensions of the ones of [Ruschendorf \(1995\)](#), see [Appendix D](#) for a discussion and examples.

Proposition 7. *Assume [A1](#), [A2](#), [A3](#), [A4](#) and [A5](#). Let $(\pi^n)_{n \in \mathbb{N}}$ be the sequence given by [\(mIPF\)](#). Then, we have $\lim_{n \rightarrow \infty} \|\pi^n - \pi^*\|_{TV} = 0$, where π^* is given in [Proposition 4](#).*

To the best of our knowledge, [Proposition 7](#) is the first convergence result of [\(mIPF\)](#) without assuming that the space is compact or that the cost is bounded. We highlight that traditional techniques to prove the convergence of the IPF cannot be easily extended to the multimarginal setting as pointed by [Carlier \(2022\)](#). In the case of bounded cost, quantitative results exist ([Marino & Gerolin, 2020](#); [Carlier, 2022](#)). We leave the study of such results in the *unbounded* cost setting for future work.

5 Application to Wasserstein barycenters

Although [Algorithm 1](#) can be applied to trees T with fixed marginals on the leaves, one case of particular interest is star-shaped trees, *i.e.*, trees with a central node, denoted by index 0, and such that $S = \{1, \dots, \ell\}$ (see [Figure 1](#) for an illustration with $\ell = 3$). In this section, we draw a link between [\(TreeSB\)](#) and regularized Wasserstein barycenters. We recall the definition of the Wasserstein distance of order 2 with ε -entropic regularization between μ and ν ([Peyré et al., 2019](#), Chapter 4)

$$W_{2,\varepsilon}^2(\mu, \nu) = \inf \left\{ \int \|x_1 - x_0\|^2 d\pi(x_0, x_1) - \varepsilon H(\pi) : \pi \in \mathcal{P}^{(2)}, \pi_0 = \mu, \pi_1 = \nu \right\}. \quad (3)$$

In this work, we consider the doubly-regularized Wasserstein-2 barycenter problem defined as follows

$$\mu_\varepsilon^* = \arg \min \left\{ \sum_{i=1}^{\ell} w_i W_{2,\varepsilon/w_i}^2(\mu, \mu_i) + \ell \varepsilon H(\mu) + \varepsilon \text{KL}(\mu | \mu_0) : \mu \in \mathcal{P} \right\}, \quad (\mu_0\text{-regWB})$$

where $(w_i)_{i \in \{1, \dots, \ell\}} \in (0, +\infty)^\ell$, $\mu_0 \in \mathcal{P}$ is a reference measure. In the case where $\mu_0 = N(0, \sigma_0^2 I_d)$, letting $\sigma_0 \rightarrow \infty$ and setting $w_i = 1/\ell$, we recover the $(\ell\varepsilon, (\ell-1)\varepsilon)$ -doubly regularized Wasserstein barycenter problem introduced in [Chizat \(2023\)](#). [Proposition 8](#) shows the equivalence between the barycenter problem $(\mu_0\text{-regWB})$ and the multi-marginal Schrödinger bridge problem [\(TreeSB\)](#) over T . The proof of this result is postponed to [Appendix D](#).

Proposition 8. *Let $\varepsilon > 0$ and $\mu_0 \in \mathcal{P}$ such that $\mu_0 \ll \text{Leb}$. Assume $r = 0$ and $\varphi_r = d\mu_0/d\text{Leb} > 0$ in [\(2\)](#). Under [A2](#), $(\mu_0\text{-regWB})$ has a unique solution π_0^* , where π^* is the solution to [\(TreeSB\)](#).*

More generally, we show in [Appendix D](#) that, for any tree T , [\(TreeSB\)](#) is equivalent to a regularized version of the Wasserstein propagation problem ([Solomon et al., 2014, 2015](#)). Thus, we can use [TreeDSB](#) to estimate the solution of the regularized Wasserstein barycenter problem $(\mu_0\text{-regWB})$. We provide practical guidelines to set the regularization parameter μ_0 in [Appendix F](#).

6 Related work

Diffusion Schrödinger Bridge. Schrödinger Bridges ([Schrödinger, 1932](#)) have been extensively studied using tools from stochastic control and probability theory ([Léonard, 2014](#); [Dai Pra, 1991](#); [Chen et al., 2021](#)). More recently, algorithms were proposed to efficiently approximate such bridges in the context of machine learning. In particular, [De Bortoli et al. \(2021\)](#) proposed DSB while [Vargas et al. \(2021\)](#); [Chen et al. \(2022\)](#) developed related algorithms. In [Chen et al. \(2023\)](#), the authors study a multimarginal version of DSB. In their setting, the graph is linear tree $T = (V, E)$ and the set of observed nodes is the whole set of vertices V . However, contrary to our setting, [Chen et al. \(2023\)](#) introduced a momentum variable. This allows for smoother trajectories which are desirable for single-cell trajectories applications and correspond to some spline interpolation in the space of probability measures ([Chen et al., 2018](#)). A general framework for Schrödinger Bridges on trees was given in [Haasler et al. \(2021\)](#). In this work, we follow this framework, see [Appendix D](#) for more a thorough comparison, to define multimarginal IPF leading to its numerical counterpart [TreeDSB](#).

Wasserstein barycenters. The notion of Wasserstein barycenter was first introduced in [Rabin et al. \(2012\)](#) and then later studied in [Agueh & Carlier \(2011\)](#). The algorithms to solve this problem can be split into two families: the in-sample based approaches and the parametric ones. In-sample approaches require access to all the measures μ_i which are assumed to be empirical measures [Cuturi & Doucet \(2014\)](#); [Benamou et al. \(2015\)](#); [Solomon et al. \(2015\)](#). Related to this class of algorithms is the semi-discrete approach, which aims at computing a Wasserstein barycenter between continuous distribution but rely on a discretization of the barycenter ([Claici et al., 2018](#); [Staib et al., 2017](#); [Mi](#)

et al., 2020). Most recent approaches do not rely on a discrete representation of the barycenter, but instead parameterize it using neural networks. These approaches can be further split into two categories. First, *measure-based optimization* approaches parameterize the measures using a neural network. This is the case of Cohen et al. (2020), where the barycenter is given by a generative model, which is then optimized. Fan et al. (2020) introduce an optimization procedure which relies on a *min-max-min* problem using the framework of Makuva et al. (2020). More recently, Korotin et al. (2022) considered a fixed point-based algorithm introduced in Álvarez-Esteban et al. (2016) to update a generative model parametrizing the barycenter. On the one hand, *potential based methods* rely on a dual formulation of the barycenter. Korotin et al. (2021) parameterized the dual potentials using Input Convex Neural Network and considered regularizing losses imposing conjugacy and congruency. On the other hand, Li et al. (2020) consider a dual version of the *regularized* Wasserstein barycenter problem contrary to other works. Our approach applied to start-shaped tree also approximates a *regularized* Wasserstein barycenter. However, contrary to Li et al. (2020), we do not consider a parameterization of the potentials in the *static* setting but instead, parameterize the drift of an associated *dynamic* formulation using Schrödinger bridges. To the best of our knowledge TreeDSB is the first approach leveraging DSB-like algorithms to compute Wasserstein barycenters.

7 Experiments

In our experiments⁴, we illustrate the performance of TreeDSB to compute entropic regularized Wasserstein barycenters for various tasks. We choose to compare our method with state-of-the-art regularized algorithms: (i) fast free-support Wasserstein barycenter (fsWB) (Cuturi & Doucet, 2014), and continuous regularized Wasserstein barycenter (crWB) (Li et al., 2020). In all of our settings, we consider a star-shaped tree with K leaves and edge weights that are equal to $1/K$. This results in a sequential training procedure over $2K$ neural networks. The initial diffusion is always a Brownian motion starting from the central node and diffusing to each leaf up to time $T = K\varepsilon/2$, according to Proposition 1. The order of the leaves is randomly shuffled between IPF cycles. We consider 50 steps for the time discretization on $[0, T]$. We refer to Appendix G for details on the choice of the schedule, the architecture of the neural networks and the settings of our experiments.

Synthetic two dimensional datasets. We start by illustrating our procedure in a synthetic two dimensional setting. We consider three different datasets Swiss-roll (vertex 1), circle (vertex 2) and moons (vertex 3) and compute their Wasserstein barycenter by running TreeDSB for 20 IPF cycles with $\varepsilon = 0.2$. In Figure 4, we show the estimated densities given by our model on the leaves of the tree, *i.e.*, the original datasets (we emphasize that the distributions plotted on each leaf are generated from the central barycenter measure). In Figure 5, we observe the consistency between the barycenters generated from the different leaves.

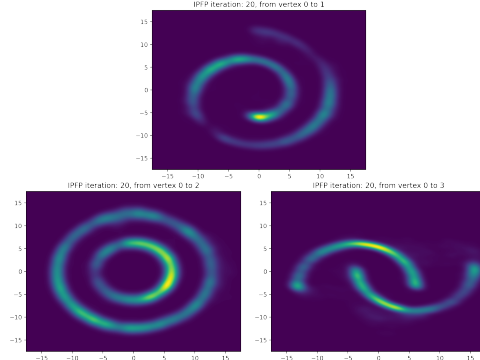


Figure 4: Estimated densities on the leaves.

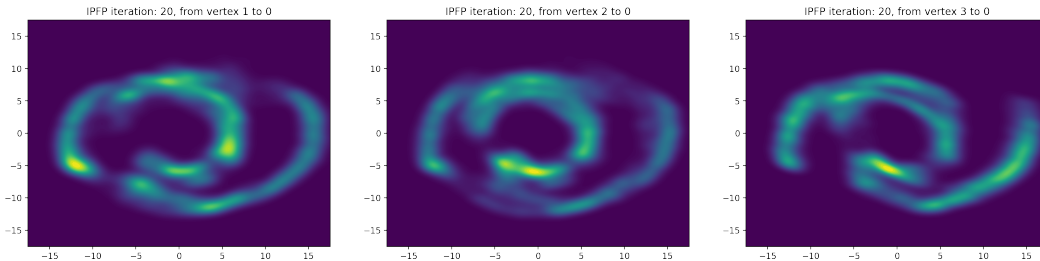


Figure 5: From left to right: barycenter estimated from the leaves Swiss-roll, circle and moons.

⁴Code available at <https://github.com/maxencenoble/tree-diffusion-schrodinger-bridge>.

Synthetic Gaussian datasets. Next, we consider three independent Gaussian distributions with zero mean and random non-diagonal covariance matrices whose conditional number is less than 10, following Fan et al. (2020). In this case, the non-regularized barycenter can be exactly computed. To evaluate the performance of the algorithms, we use the Bures-Wasserstein Unexplained Variance Percentage (UVP), following (Korotin et al., 2021, Section 5). Given a target distribution $\mu^* \in \mathcal{P}$ and some approximation $\mu \in \mathcal{P}$, we define

$$\text{BW}_2^2\text{-UVP}(\mu, \mu^*) = 100 \cdot 2 \text{BW}_2^2(\mu, \mu^*) / \text{Var}(\mu^*)\%,$$

where $\text{BW}_2^2(\mu, \mu^*) = W_2^2(\mathcal{N}(\mathbb{E}[\mu], \text{Cov}(\mu)), \mathcal{N}(\mathbb{E}[\mu^*], \text{Cov}(\mu^*)))$.

| Method | $d = 2$ | $d = 16$ | $d = 64$ | $d = 128$ | $d = 256$ |
|------------------------------|-----------------------------------|-----------------------------------|-----------------------------------|-----------------------------------|-----------------------------------|
| fsWB (Cuturi & Doucet, 2014) | 0.06 ± 0.01 | 2.86 ± 0.06 | 11.12 ± 0.06 | 14.47 ± 0.07 | 17.41 ± 0.05 |
| crWB (Li et al., 2020) | 0.02 ± 0.01 | 1.52 ± 0.11 | 11.41 ± 0.73 | 5.75 ± 0.02 | 18.27 ± 0.54 |
| Tree DSB | 0.63 ± 0.26 | 1.07 ± 0.58 | 1.39 ± 0.07 | 1.92 ± 0.02 | 2.62 ± 0.07 |

Table 1: Gaussian setting: comparison with the regularized methods crWB and fsWB.

In this setting, we choose μ^* to be the non-regularized barycenter and assess the dependency w.r.t. the dimension of the algorithms using the $\text{BW}_2^2\text{-UVP}$ metric. In Table 1, we compare ourselves with the two regularized methods Li et al. (2020) (L_2 -reg. equal to 10^{-4}) and Cuturi & Doucet (2014). We run TreeDSB for 10 IPF cycles with $\varepsilon = 0.2$. Bold numbers represent the best values up to statistical significance. While Li et al. (2020) and Cuturi & Doucet (2014) enjoy better performance in low dimensions ($d = 2$), TreeDSB outperforms these methods as the dimension increases.

MNIST Wasserstein barycenter. We then turn to an image experiment and compare ourselves with Li et al. (2020) as well as Fan et al. (2020); Korotin et al. (2021) which compute *non-regularized* Wasserstein barycenter. For TreeDSB, we set $\varepsilon = 0.5$ and show the results obtained after 3 IPF cycles. In Figure 6, we compare ourselves with Li et al. (2020), Fan et al. (2020) and Korotin et al. (2021) in the MNIST setting (LeCun, 1998) by computing a Wasserstein barycenter between the digits 0 and 1. Our results are on par with the non-regularized methods Fan et al. (2020); Korotin et al. (2021) while outperforming Li et al. (2020). Furthermore, we compute the Wasserstein barycenter between the digits 4 and 6 and 2 in Figure 7. This illustrates the capabilities of TreeDSB to scale two more than two terminal distributions.

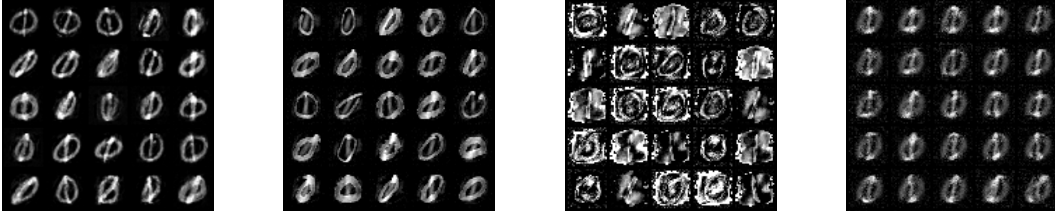


Figure 6: From left to right: Fan et al. (2020), Korotin et al. (2021), Li et al. (2020) and TreeDSB.

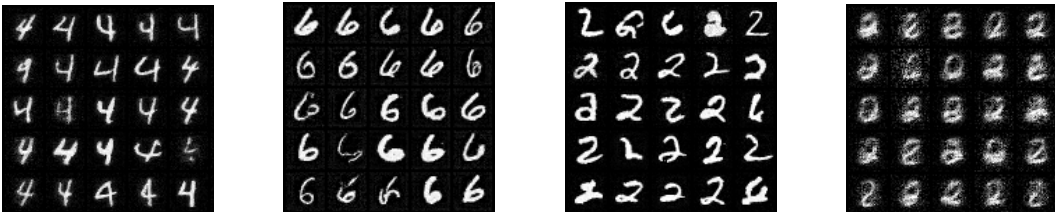


Figure 7: Reconstructed measures and regularized Wasserstein barycenter (right).

Subset posterior aggregation. Finally, we evaluate TreeDSB in the context of *Bayesian fusion* (Srivastava et al., 2018). We consider the posterior aggregation task for the logistic regression model applied to the wine dataset⁵ ($d = 42$), which is splitted into 3 datasets with or without heterogeneity.

⁵<https://archive.ics.uci.edu/ml/datasets/wine>

We estimate the parameters on each shard of the data and then draw samples from the obtained logistic distribution to define μ_1, μ_2, μ_3 . The true posterior is estimated on the full dataset. As in the synthetic Gaussian experiment, we run TreeDSB for 10 IPF cycles $\varepsilon = 0.2$ and we compare ourselves with Li et al. (2020) (L_2 -reg. equal to 10^{-4}) and Cuturi & Doucet (2014). We evaluate the methods using the BW_2^2 -UVP metric, where μ^* is the estimated full data posterior, and report the results in Table 2. In both settings, we observe that our method outperforms existing regularized methods to compute Wasserstein barycenters.

| Method | Without heterogeneity | With heterogeneity |
|------------------------------|---------------------------------|---------------------------------|
| fsWB (Cuturi & Doucet, 2014) | 12.95 \pm 0.35 | 14.43 \pm 0.51 |
| crWB (Li et al., 2020) | 20.66 \pm 0.71 | 23.06 \pm 0.12 |
| Tree DSB | 8.69\pm0.12 | 8.90\pm0.68 |

Table 2: Bayesian fusion setting: comparison with the regularized methods crWB and fsWB.

Limitations. One of the main limitation of entropic regularized OT approach is that their behavior is usually badly conditioned as $\varepsilon \rightarrow 0$. In our setting, we observe that if ε , or equivalently T , is too low then the algorithm becomes less stable as the training of the models slows down. In the future, we plan to mitigate this issue by incorporating fixed point techniques like the one used in Korotin et al. (2022). Finally, since our algorithm is based on DSB (De Bortoli et al., 2021), it suffers from the same limitations. In particular, training different neural networks iteratively incurs some bias in the SDE which is harmful for large number of IPF iterations.

8 Discussion

In this paper, we introduced Tree Diffusion Schrödinger Bridge (TreeDSB) a scalable scheme to approximate solutions of entropy-regularized multimarginal Optimal Transport problems. Our methodology leverages tools from the diffusion model literature and extends Diffusion Schrödinger Bridge (De Bortoli et al., 2021). In particular it approximates the iterates of the multimarginal Iterative Proportional Fitting algorithm. We prove the convergence of this algorithm under mild assumptions and illustrate the efficiency of TreeDSB in an image setting and in the case of Bayesian fusion using a link between multimarginal OT and Wasserstein barycenters.

In future work, we would like to investigate quantitative convergence bounds for (mIPF) in the *unbounded* cost setting. Another line of work would be to scale TreeDSB to higher dimensional problems building on recent developments in the diffusion model and flow matching community (Lipman et al., 2023; Peluchetti, 2023; Shi et al., 2023).

Acknowledgment

We thank James Thornton for the DSB codebase⁶ and useful discussions. Alain Durmus acknowledges support from the Lagrange Mathematics and Computing Research Center.

References

- Acciaio, B., Backhoff-Veraguas, J., and Carmona, R. Extended mean field control problems: stochastic maximum principle and transport perspective. *SIAM journal on Control and Optimization*, 57(6):3666–3693, 2019.
- Agueh, M. and Carlier, G. Barycenters in the Wasserstein space. *SIAM Journal on Mathematical Analysis*, 43(2):904–924, 2011.
- Álvarez-Esteban, P. C., Del Barrio, E., Cuesta-Albertos, J., and Matrán, C. A fixed-point approach to barycenters in Wasserstein space. *Journal of Mathematical Analysis and Applications*, 441(2): 744–762, 2016.

⁶https://github.com/JTT94/diffusion_schrodinger_bridge

- Bayraktar, E., Cox, A. M., and Stoev, Y. Martingale optimal transport with stopping. *SIAM Journal on Control and Optimization*, 56(1):417–433, 2018.
- Benamou, J.-D., Carlier, G., Cuturi, M., Nenna, L., and Peyré, G. Iterative Bregman projections for regularized transportation problems. *SIAM Journal on Scientific Computing*, 37(2):A1111–A1138, 2015.
- Bunne, C., Papaxanthos, L., Krause, A., and Cuturi, M. Proximal optimal transport modeling of population dynamics. In *International Conference on Artificial Intelligence and Statistics*, pp. 6511–6528. PMLR, 2022.
- Carion, N., Massa, F., Synnaeve, G., Usunier, N., Kirillov, A., and Zagoruyko, S. End-to-end object detection with transformers. In *Computer Vision—ECCV 2020: 16th European Conference, Glasgow, UK, August 23–28, 2020, Proceedings, Part I 16*, pp. 213–229. Springer, 2020.
- Carlier, G. On the linear convergence of the multimarginal Sinkhorn algorithm. *SIAM Journal on Optimization*, 32(2):786–794, 2022.
- Cattiaux, P., Conforti, G., Gentil, I., and Léonard, C. Time reversal of diffusion processes under a finite entropy condition. *arXiv preprint arXiv:2104.07708*, 2021.
- Chen, T., Liu, G.-H., and Theodorou, E. A. Likelihood training of Schrödinger bridge using forward-backward sdes theory. *International Conference on Learning Representations*, 2022.
- Chen, T., Liu, G.-H., Tao, M., and Theodorou, E. A. Deep momentum multi-marginal Schrödinger bridge. 2023. doi: 10.48550/ARXIV.2303.01751.
- Chen, Y., Georgiou, T., Pavon, M., and Tannenbaum, A. Robust transport over networks. *IEEE Transactions on Automatic Control*, 62(9):4675–4682, 2016.
- Chen, Y., Conforti, G., and Georgiou, T. T. Measure-valued spline curves: An optimal transport viewpoint. *SIAM Journal on Mathematical Analysis*, 50(6):5947–5968, 2018.
- Chen, Y., Georgiou, T. T., and Pavon, M. Optimal transport in systems and control. *Annual Review of Control, Robotics, and Autonomous Systems*, 4, 2021.
- Chizat, L. Doubly regularized entropic Wasserstein barycenters. *arXiv preprint arXiv:2303.11844*, 2023.
- Claici, S., Chien, E., and Solomon, J. Stochastic Wasserstein barycenters. In *International Conference on Machine Learning*, pp. 999–1008. PMLR, 2018.
- Cohen, S., Arbel, M., and Deisenroth, M. P. Estimating barycenters of measures in high dimensions. *arXiv preprint arXiv:2007.07105*, 2020.
- Cotar, C., Friesecke, G., and Klüppelberg, C. Density functional theory and optimal transportation with coulomb cost. *Communications on Pure and Applied Mathematics*, 66(4):548–599, 2013.
- Csiszár, I. I-divergence geometry of probability distributions and minimization problems. *The annals of probability*, pp. 146–158, 1975.
- Cuturi, M. Sinkhorn distances: Lightspeed computation of optimal transport. *Advances in neural information processing systems*, 26, 2013.
- Cuturi, M. and Doucet, A. Fast computation of Wasserstein barycenters. In *International conference on machine learning*, pp. 685–693. PMLR, 2014.
- Dai Pra, P. A stochastic control approach to reciprocal diffusion processes. *Applied Mathematics and Optimization*, 23(1):313–329, 1991.
- De Bortoli, V., Thornton, J., Heng, J., and Doucet, A. Diffusion Schrödinger bridge with applications to score-based generative modeling. *Advances in Neural Information Processing Systems*, 34: 17695–17709, 2021.

- Dupuis, P. and Ellis, R. S. *A weak convergence approach to the theory of large deviations*. John Wiley & Sons, 2011.
- Eisenberger, M., Toker, A., Leal-Taixé, L., and Cremers, D. Deep shells: Unsupervised shape correspondence with optimal transport. *Advances in Neural information processing systems*, 33: 10491–10502, 2020.
- Fan, J., Taghvaei, A., and Chen, Y. Scalable computations of Wasserstein barycenter via input convex neural networks. *arXiv preprint arXiv:2007.04462*, 2020.
- Feydy, J., Charlier, B., Vialard, F.-X., and Peyré, G. Optimal transport for diffeomorphic registration. In *Medical Image Computing and Computer Assisted Intervention- MICCAI 2017: 20th International Conference, Quebec City, QC, Canada, September 11-13, 2017, Proceedings, Part I 20*, pp. 291–299. Springer, 2017.
- Flamary, R., Courty, N., Gramfort, A., Alaya, M. Z., Boisbunon, A., Chambon, S., Chapel, L., Corenflos, A., Fatras, K., Fournier, N., et al. Pot: Python optimal transport. *The Journal of Machine Learning Research*, 22(1):3571–3578, 2021.
- Haasler, I., Ringh, A., Chen, Y., and Karlsson, J. Multimarginal optimal transport with a tree-structured cost and the Schrödinger bridge problem. *SIAM Journal on Control and Optimization*, 59(4):2428–2453, 2021.
- Hausmann, U. G. and Pardoux, E. Time reversal of diffusions. *The Annals of Probability*, pp. 1188–1205, 1986.
- Ho, J., Jain, A., and Abbeel, P. Denoising diffusion probabilistic models. *Advances in Neural Information Processing Systems*, 33:6840–6851, 2020.
- Hyvärinen, A. Estimation of non-normalized statistical models by score matching. *Journal of Machine Learning Research*, 6(4), 2005.
- Karcher, H. Riemannian center of mass and so called Karcher mean. *arXiv preprint arXiv:1407.2087*, 2014.
- Kingma, D. P. and Ba, J. Adam: A method for stochastic optimization. *arXiv preprint arXiv:1412.6980*, 2014.
- Knight, P. A. The Sinkhorn–Knopp algorithm: convergence and applications. *SIAM Journal on Matrix Analysis and Applications*, 30(1):261–275, 2008.
- Kober, H. A theorem on Banach spaces. *Compositio Mathematica*, 7:135–140, 1940.
- Koller, D. and Friedman, N. *Probabilistic Graphical Models: Principles and Techniques*. MIT press, 2009.
- Korotin, A., Li, L., Solomon, J., and Burnaev, E. Continuous Wasserstein-2 barycenter estimation without minimax optimization. *arXiv preprint arXiv:2102.01752*, 2021.
- Korotin, A., Egiazarian, V., Li, L., and Burnaev, E. Wasserstein iterative networks for barycenter estimation. *arXiv preprint arXiv:2201.12245*, 2022.
- LeCun, Y. The mnist database of handwritten digits. <http://yann.lecun.com/exdb/mnist/>, 1998.
- Léonard, C. A survey of the Schrödinger problem and some of its connections with optimal transport. *Discrete & Continuous Dynamical Systems-A*, 34(4):1533–1574, 2014.
- Li, L., Genevay, A., Yurochkin, M., and Solomon, J. M. Continuous regularized Wasserstein barycenters. *Advances in Neural Information Processing Systems*, 33:17755–17765, 2020.
- Lipman, Y., Chen, R. T., Ben-Hamu, H., Nickel, M., and Le, M. Flow matching for generative modeling. *International Conference on Learning Representations*, 2023.
- Luo, Z.-Q. and Tseng, P. On the convergence of the coordinate descent method for convex differentiable minimization. *Journal of Optimization Theory and Applications*, 72(1):7–35, 1992.

- Makkuva, A., Taghvaei, A., Oh, S., and Lee, J. Optimal transport mapping via input convex neural networks. In *International Conference on Machine Learning*, pp. 6672–6681. PMLR, 2020.
- Marino, S. D. and Gerolin, A. An optimal transport approach for the schrödinger bridge problem and convergence of Sinkhorn algorithm. *Journal of Scientific Computing*, 85(2):27, 2020.
- Mi, L., Yu, T., Bento, J., Zhang, W., Li, B., and Wang, Y. Variational Wasserstein barycenters for geometric clustering. *arXiv preprint arXiv:2002.10543*, 2020.
- Minsker, S., Srivastava, S., Lin, L., and Dunson, D. Scalable and robust Bayesian inference via the median posterior. In *International Conference on Machine Learning*, pp. 1656–1664. PMLR, 2014.
- Nichol, A. Q. and Dhariwal, P. Improved denoising diffusion probabilistic models. In *International Conference on Machine Learning*, pp. 8162–8171, 2021.
- Nutz, M. Introduction to entropic optimal transport, 2021.
- Pele, O. and Werman, M. Fast and robust earth mover’s distances. In *2009 IEEE 12th International Conference on Computer Vision*, pp. 460–467. IEEE, 2009.
- Peluchetti, S. Diffusion bridge mixture transports, Schrödinger bridge problems and generative modeling. *arXiv preprint arXiv:2304.00917*, 2023.
- Peyré, G., Cuturi, M., et al. Computational optimal transport: With applications to data science. *Foundations and Trends® in Machine Learning*, 11(5-6):355–607, 2019.
- Rabin, J., Peyré, G., Delon, J., and Bernot, M. Wasserstein barycenter and its application to texture mixing. In *Scale Space and Variational Methods in Computer Vision: Third International Conference, SSVM 2011, Ein-Gedi, Israel, May 29–June 2, 2011, Revised Selected Papers 3*, pp. 435–446. Springer, 2012.
- Ruschendorf, L. Convergence of the iterative proportional fitting procedure. *The Annals of Statistics*, pp. 1160–1174, 1995.
- Schiebinger, G., Shu, J., Tabaka, M., Cleary, B., Subramanian, V., Solomon, A., Gould, J., Liu, S., Lin, S., Berube, P., et al. Optimal-transport analysis of single-cell gene expression identifies developmental trajectories in reprogramming. *Cell*, 176(4):928–943, 2019.
- Schmitz, M. A., Heitz, M., Bonneel, N., Ngole, F., Coeurjolly, D., Cuturi, M., Peyré, G., and Starck, J.-L. Wasserstein dictionary learning: Optimal transport-based unsupervised nonlinear dictionary learning. *SIAM Journal on Imaging Sciences*, 11(1):643–678, 2018.
- Schrödinger, E. Sur la théorie relativiste de l’électron et l’interprétation de la mécanique quantique. *Annales de l’Institut Henri Poincaré*, 2(4):269–310, 1932.
- Shi, Y., De Bortoli, V., Campbell, A., and Doucet, A. Diffusion Schrödinger bridge matching. *arXiv preprint arXiv:2303.16852*, 2023.
- Sinkhorn, R. and Knopp, P. Concerning nonnegative matrices and doubly stochastic matrices. *Pacific Journal of Mathematics*, 21(2):343–348, 1967.
- Solomon, J., Rustamov, R., Guibas, L., and Butscher, A. Wasserstein propagation for semi-supervised learning. In *International Conference on Machine Learning*, pp. 306–314. PMLR, 2014.
- Solomon, J., De Goes, F., Peyré, G., Cuturi, M., Butscher, A., Nguyen, A., Du, T., and Guibas, L. Convolutional Wasserstein distances: Efficient optimal transportation on geometric domains. *ACM Transactions on Graphics (ToG)*, 34(4):1–11, 2015.
- Song, Y., Sohl-Dickstein, J., Kingma, D. P., Kumar, A., Ermon, S., and Poole, B. Score-based generative modeling through stochastic differential equations. *International Conference on Learning Representations*, 2021.
- Srivastava, S., Li, C., and Dunson, D. B. Scalable Bayes via barycenter in Wasserstein space. *The Journal of Machine Learning Research*, 19(1):312–346, 2018.

- Staib, M., Claici, S., Solomon, J. M., and Jegelka, S. Parallel streaming Wasserstein barycenters. *Advances in Neural Information Processing Systems*, 30, 2017.
- Stroock, D. W. and Varadhan, S. S. *Multidimensional diffusion processes*, volume 233. Springer Science & Business Media, 1997.
- Su, Z., Wang, Y., Shi, R., Zeng, W., Sun, J., Luo, F., and Gu, X. Optimal mass transport for shape matching and comparison. *IEEE Transactions on Pattern Analysis and Machine Intelligence*, 37(11):2246–2259, 2015.
- Valiente, G. *Algorithms on Trees and Graphs*, volume 112. Springer, 2002.
- Vargas, F., Thodoroff, P., Lamacraft, A., and Lawrence, N. Solving schrödinger bridges via maximum likelihood. *Entropy*, 23(9):1134, 2021.
- Vaswani, A., Shazeer, N., Parmar, N., Uszkoreit, J., Jones, L., Gomez, A. N., Kaiser, Ł., and Polosukhin, I. Attention is all you need. *Advances in Neural Information Processing Systems*, 30, 2017.
- Vincent, P. A connection between score matching and denoising autoencoders. *Neural computation*, 23(7):1661–1674, 2011.

Appendix organization

First, additional notation is introduced in Appendix A. Then, we briefly recall some notions on undirected and directed trees in Appendix B. Similarly, martingale problems are introduced in Appendix C. The proofs of the main manuscript and additional theoretical results on Tree Schrödinger Bridges are given in Appendix D. Additional details on the algorithm TreeDSB are described in Appendix E. Details on the implementation of TreeDSB are given in Appendix F and the experiments are investigated in Appendix G.

A Additional notation

For any finite set E , we equivalently refer to the cardinal of E as $\text{card}(E)$ or $|E|$. Let (X, \mathcal{X}) be a measurable space. For any $x \in (\mathbb{R}^d)^{\ell+1}$ and any $m \in \{0, \dots, \ell\}$, let $x_{-m} = (x_0, \dots, x_{m-1}, x_{m+1}, \dots, x_\ell)$. For any family of measures $\{\nu_j\}_{j \in \{0, \dots, \ell\}}$ defined on (X, \mathcal{X}) and any $i \in \{0, \dots, \ell\}$, let $\nu_{-i} = \bigotimes_{j \in \{0, \dots, \ell\} \setminus \{i\}} \nu_j$. Let $I = \{i_1, \dots, i_q\} \subset \{1, \dots, \ell\}$ and $\mu \in \mathcal{P}^{(\ell)}$ such that $\mu \ll \text{Leb}$. We define $I^c = \{1, \dots, \ell\} \setminus I$ and denote it by $\{i_1^c, \dots, i_{\bar{q}}^c\}$ where $\bar{q} = \ell - q$. We denote the marginal of μ along I by μ_I , i.e., $\mu_I \in \mathcal{P}^{(q)}$ and we have for any $A \in \mathcal{B}((\mathbb{R}^d)^q)$, $\mu_I(A) = \int_X \mu(x) \prod_{j=1}^q \delta_{x_{i_j}}(A_j) dx$. In addition, note that $\mu_I \ll \text{Leb}$. We denote the conditional distribution of μ given I by $\mu_{|I}(\cdot|\cdot)$, i.e., $\mu_{|I}(\cdot|\cdot) \in \mathcal{P}^{(\bar{q})} \times (\mathbb{R}^d)^q$ and we have for any $y \in (\mathbb{R}^d)^q$ and any $A \in \mathcal{B}((\mathbb{R}^d)^{\bar{q}})$, $\mu_{|I}(A|y) = \int_X \mu(x) / \mu_I(y) \prod_{j=1}^q \delta(x_{i_j} - y_j) \prod_{j'=1}^{\bar{q}} \delta_{x_{i_{j'}^c}}(A_{j'}) dx$. Remark that for any $y \in (\mathbb{R}^d)^q$, $\mu_{|I}(\cdot|y) \ll \text{Leb}$. For any subset $J \subset I^c$ with $\text{card}(J) = q_J$, we also define $\mu_{J||}(\cdot|\cdot) \in \mathcal{P}^{(q_J)} \times (\mathbb{R}^d)^q$ such that for any $y \in (\mathbb{R}^d)^q$, $\mu_{J||}(\cdot|y) = \{\mu_{|I}(\cdot|y)\}_J$. For a collection of functions $\{f_i\}_{i \in I}$, with $I \subset \{1, \dots, n\}$ and $n \in \mathbb{N}$ such that $f_i : \mathbb{R}^d \rightarrow \mathbb{R}$, we define $\oplus_{i \in I} f_i : (\mathbb{R}^d)^n \rightarrow \mathbb{R}$ such that for any $x = (x_1, \dots, x_n) \in (\mathbb{R}^d)^n$, $\oplus_{i \in I} f_i(x) = \sum_{i \in I} f_i(x_i)$.

B Introduction to trees

Undirected tree. An undirected graph $T = (V, E)$, with vertices V and edges E , is said to be an *undirected tree* if it is *acyclic* and *connected* (Valiente, 2002, Definition 1.19.). In particular, we have $\text{card}(E) = \text{card}(V) - 1$. The undirected edge between two nodes v_1 and v_2 is similarly denoted by $\{v_1, v_2\}$ or $\{v_2, v_1\}$. We say that $T' = (V', E')$ is a *sub-tree* of T if T' is an undirected tree with vertices $V' \subset V$ and edges $E' \subset E$. For any vertex $v \in V$, we define the set of its *neighbours* N_v as the set of vertices $v' \in V$ such that $\{v, v'\} \in E$. The integer $\text{card}(N_v)$ is referred to as the degree of v . The vertices with degree 1 are called *leaves*, and we denote the set of leaves by $V_L \subset V$. The (unique) *path* in T between two vertices v and v' is the sequence of two-by-two distinct edges $\{\{v_i, v_{i+1}\}\}_{i=1}^n$ (with $n \geq 1$) such that $v_k = v_{k+1}$ for any $k \in \{1, \dots, n\}$ such that $k \equiv 0 \pmod{2}$, $v_1 = v$ and $v_{n+1} = v'$. This path can be seen as a linear sub-tree of T , and we define n as the *length* of this path. We say that T is *weighted* if there exists a map $w : E \mapsto \mathbb{R}_+$; in this case, $w(\{v_1, v_2\})$, or equivalently $w(\{v_2, v_1\})$ (also denoted by w_{v_1, v_2} or w_{v_2, v_1}) is called the weight of the edge $\{v_1, v_2\}$. The tree T is said to be *rooted* in $r \in V$ if r defines a partial ordering $\leq_{T, r} \subset V \times V$ such that for any $v_1, v_2 \in V$, $v_1 \leq_{T, r} v_2$ if the node v_1 lies on the unique path between r and v_2 .

Directed tree. Consider a directed graph $T_r = (V, E_r)$ rooted in $r \in V$. Any directed edge $e \in E_r$ from $v_1 \in V$ to $v_2 \in V$ is denoted by (v_1, v_2) . T_r is said to be a *directed tree* rooted in r if (i) the underlying undirected graph $T = (V, E)$ is an undirected tree rooted in r and (ii) any $(v_1, v_2) \in E_r$ is directed according to the partial ordering $\leq_{T, r}$, i.e., $\{v_1, v_2\} \in E$ and $v_1 \leq_{T, r} v_2$. For any vertices $(v, v') \in V \times V$ such that $v \leq_{T, r} v'$, the (unique) *path* in T_r from v to v' , denoted by $\text{path}_{T_r}(v, v')$, is defined as the directed version of the path in T between v and v' (viewed as a sub-tree of T), which is rooted in v . We say that T_r is *weighted*, if T is weighted and the edges of T_r have the same weights as the corresponding undirected edges of T . For any $(v_1, v_2) \in E_r$, we denote this weight by w_{v_1, v_2} . We say that T_r is the (unique) *directed version* of T rooted in r . It is endowed with a canonical vertex numbering $\zeta : V \rightarrow \{0, \dots, \text{card}(V) - 1\}$, corresponding to a depth-first traversal of its nodes, starting from the root r (Valiente, 2002, Definition 3.1.). This numbering is consistent with the partial ordering on T , i.e., if $v_1 \leq_{T, r} v_2$, $\zeta(v_1) \leq \zeta(v_2)$, and satisfies $\zeta(r) = 0$. In the rest of the paper, we will write in an equivalent manner v or $\zeta(v)$.

For any vertices $(v_1, v_2) \in E \times E$ such that $v_1 \leq_{T,r} v_2$, $\text{path}_{T,r}(v_1, v_2)$ corresponds to the ordered set of edges in E_r which define the ordered path between two vertices v_1 and v_2 . For any vertex $v \in V$, we define:

- (a) the set of its *children* C_v as the set of vertices $v' \in V$ such that $(v, v') \in E_r$. In particular, for any $v \in V_L$, the set of leaves, one has $C_v = \emptyset$.
- (b) its *parent* as the unique vertex $p(v)$ such that $(p(v), v) \in E_r$, if $v \neq r$ (the parent of the root is not defined).

Note that $N_r = C_r$ and, for any vertex $v \in V \setminus \{r\}$, $N_v = \{p(v)\} \cup C_v$.

Definition 9 (Tree-structured directed Probabilistic Graphical Model (PGM)). *Consider a directed tree $T_r = (V, E_r)$. The directed PGM induced by T_r (Koller & Friedman, 2009, Definition 3.4.), denoted by \mathcal{P}_{T_r} , is the family of distributions $\pi \in \mathcal{P}^{(|V|)}$ which have a Markovian factorization along T_r , i.e.,*

$$\mathcal{P}_{T_r} = \left\{ \pi \in \mathcal{P}^{(|V|)} : \pi = \pi_r \bigotimes_{(v,v') \in E_r} \pi_{v'|v} \right\}.$$

Lemma 10. *Consider an undirected tree $T = (V, E)$. Let $(r, r') \in V \times V$. Let T' be a sub-tree of T with vertices V' such that $r' \in V'$. Denote by $T'_{r'}$ the directed version of T' rooted in r' . Then, for any $\pi \in \mathcal{P}_{T_r}$, we have $\pi_{V'} \in \mathcal{P}_{T'_{r'}}$.*

Proof. Let $(r, r') \in V \times V$. We denote by $T_r = (V, E_r)$, respectively $T_{r'} = (V, E_{r'})$, the directed version of T rooted in r , respectively r' . We define the paths $P_{r,r'} = \text{path}_{T_r}(r, r') \subset E_r$ and $P_{r',r} = \text{path}_{T_{r'}}(r', r) \subset E_{r'}$. It is easy to see that

- (a) $E_r \setminus P_{r,r'} = E_{r'} \setminus P_{r',r}$,
- (b) $P_{r,r'} = \{(v_2, v_1) : (v_1, v_2) \in P_{r',r}\}$,
- (c) $P_{r',r} = \{(v_2, v_1) : (v_1, v_2) \in P_{r,r'}\}$.

Let $\pi \in \mathcal{P}_{T_r}$. First note that for any $(v_1, v_2) \in E_r$, we have by Bayes decomposition $\pi_{v_1} \pi_{v_2|v_1} = \pi_{v_2} \pi_{v_1|v_2} = \pi_{v_1, v_2}$. Then it comes

$$\begin{aligned} \pi &= \pi_r \bigotimes_{(v_1, v_2) \in E_r} \pi_{v_2|v_1} \\ &= \pi_r \bigotimes_{(v_1, v_2) \in P_{r,r'}} \pi_{v_2|v_1} \bigotimes_{(v_1, v_2) \in E_r \setminus P_{r,r'}} \pi_{v_2|v_1} \\ &= \pi_r \bigotimes_{(v_2, v_1) \in P_{r',r}} \pi_{v_2|v_1} \bigotimes_{(v_1, v_2) \in E_r \setminus P_{r',r}} \pi_{v_2|v_1} \\ &= \pi_{r'} \bigotimes_{(v_1, v_2) \in P_{r',r}} \pi_{v_2|v_1} \bigotimes_{(v_1, v_2) \in E_{r'} \setminus P_{r',r}} \pi_{v_2|v_1} \\ &= \pi_{r'} \bigotimes_{(v_1, v_2) \in E_{r'}} \pi_{v_2|v_1}, \end{aligned}$$

and therefore, we have $\pi \in \mathcal{P}_{T_{r'}}$.

Let T' be a sub-tree of T with vertices V' such that $r' \in V'$. First note that $E'_{r'} \subset E_{r'}$. Using the previous computation, we have for any $A \in \mathcal{B}((\mathbb{R}^d)^{|V'|})$,

$$\begin{aligned} \pi_{V'}(A) &= \int_{(\mathbb{R}^d)^{|V|}} \pi_{r'}(x_{r'}) \bigotimes_{(v_1, v_2) \in E_{r'}} \pi_{v_2|v_1}(x_{v_2}|x_{v_1}) \prod_{v' \in V'} \delta_{x_{v'}}(A_{v'}) dx \\ &= \int_{(\mathbb{R}^d)^{|V| - |V'|}} \{ \pi_{r'}(A_{r'}) \bigotimes_{(v_1, v_2) \in E'_{r'}} \pi_{v_2|v_1}(A_{v_2}|x_{v_1}) \} \bigotimes_{(v_1, v_2) \in E_{r'} \setminus E'_{r'}} \pi_{v_2|v_1}(x_{v_2}|x_{v_1}) dx_{V \setminus V'} \\ &= \{ \pi_{r'} \bigotimes_{(v_1, v_2) \in E'_{r'}} \pi_{v_2|v_1} \}(A), \end{aligned}$$

which proves that $\pi_{V'} \in \mathcal{P}_{T'_{r'}}$. □

Discretized undirected tree. Let $N \geq 1$. Consider an undirected tree $T = (V, E)$ with weights w . We say that $T^{(N)} = (V^{(N)}, E^{(N)})$ is a N -discretized version of T if it is an undirected tree with weights $w^{(N)}$ such that

- (a) $V^{(N)} = V \bigsqcup \bigcup_{e \in E, k \in \{1, \dots, N-1\}} \{v_e^k\}$,

- (b) $E^{(N)} = \cup_{e \in E} \cup_{k=0, \dots, N-1} \{\{v_e^k, v_e^{k+1}\}\}$ with the convention that the vertices v_e^N and v_e^N are defined such that $\{v_e^0, v_e^N\} = e$,
- (c) $\sum_{e \in \text{path}_T(v, v')} 1/w_e^{(N)} = 1/w_{v, v'}$, if $\{v, v'\} \in E$.

Remark that the leaves of $T^{(N)}$ are exactly the original leaves of T and that $T^{(1)} = T$. The non-uniqueness of $T^{(N)}$ comes from the freedom of choice on the weights of its edges.

Discretized directed tree. Let $N \geq 1$. Consider a directed tree $T_r = (V, E_r)$ rooted in $r \in V$ with weights w . We say that $T_r^{(N)} = (V^{(N)}, E_r^{(N)})$ is a N -discretized version of T_r if it is the directed version of $T^{(N)}$ rooted in r , where $T^{(N)}$ is a N -discretized version of the underlying undirected tree of T_r .

C Background on martingale problems

In this section, we introduce the background on Stochastic Differential Equations (SDEs) and weak solutions of SDEs following the framework of (Stroock & Varadhan, 1997, Section 10.1, page 249). We recall that $C_0^\infty(\mathbb{R}^d)$ is the space of infinitely differentiable real-valued functions which vanish at infinity. In addition, we have that \mathcal{S}_+^d is the space of $d \times d$, symmetric, non-negative matrices.

Definition 11. Let $T > 0$ or $T = +\infty$, $\sigma : [0, T) \times \mathbb{R}^d \rightarrow \mathcal{S}_+^d$ and $b : [0, T) \times \mathbb{R}^d \rightarrow \mathbb{R}^d$, locally bounded measurable functions. We define the infinitesimal generator, \mathcal{A} , given for any $f \in C_0^\infty(\mathbb{R}^d)$, $t \in [0, T)$ and $x \in \mathbb{R}^d$ by

$$\mathcal{A}_t(f)(x) = \langle b_t(x), \nabla f(x) \rangle + \frac{1}{2} \langle \sigma_t(x) \sigma_t(x)^\top, \nabla^2 f(x) \rangle. \quad (4)$$

We say that a probability measure \mathbb{P} satisfies the martingale problem for \mathcal{A} if for any $t \in [0, T)$ and $f \in C_0^\infty(\mathbb{R}^d)$, we have that $(f(\mathbf{X}_t) - \int_0^t \mathcal{A}_s(f)(\mathbf{X}_s) ds)_{s \in [0, t]}$ is a \mathbb{P} -martingale.

In the main document, see Section 2, we say that “a path measure \mathbb{P} is associated with $d\mathbf{X}_t = b(t, \mathbf{X}_t)dt + \sigma(t, \mathbf{X}_t)d\mathbf{B}_t$ with $(\mathbf{B}_t)_{t \geq 0}$ a d -dimensional Brownian motion” if \mathbb{P} solves the martingale problem associated with \mathcal{A} given by (4). Unless specified, we always assume that such a path measure exists and is unique. Below, we recall the following theorem, see (Stroock & Varadhan, 1997, Theorem 10.2.2), which gives sufficient conditions for the existence and uniqueness of solutions to the martingale problem.

Theorem 12. Assume that for any $x \in \mathbb{R}^d$ we have

$$\inf\{\langle \theta, \sigma \sigma^\top(s, x) \theta \rangle : \theta \in \mathbb{R}^d, \|\theta\| = 1, s \in [0, T]\} > 0, \\ \lim_{y \rightarrow x} \sup\{\|\sigma(s, x) - \sigma(s, y)\| : s \in [0, T]\} = 0.$$

In addition, assume that there exists $C > 0$ such that for any $x \in \mathbb{R}^d$

$$\sup\{\|\sigma \sigma^\top(t, x)\| : s \in [0, T]\} + \sup\{\langle x, b(t, x) \rangle : s \in [0, T]\} \leq C(1 + \|x\|^2).$$

Then, there exists a unique solution to the martingale problem with initialization $x_0 \in \mathbb{R}^d$.

D Theoretical results on Tree Schrödinger Bridges

We respectively provide in Appendix D.1, Appendix D.2 and Appendix D.3 the proofs of the results of the main manuscript respectively presented in Section 3, Section 4 and Section 5. Finally, we make a detailed comparison between our setting and the framework of Haasler et al. (2021) in Appendix D.4. In the rest of this section, we consider an undirected tree $T = (V, E)$, where $|V| = \ell + 1$, and some subset $S \subset V$ which we denote by $S = \{i_0, \dots, i_{K-1}\}$. We define $S^c = V \setminus S$.

D.1 Proofs of Section 3

Proposition 1 is straightforward to obtain by combining the definition of the Brownian motion with the definition of π^0 given in (2). Proposition 2 is a consequence of Lemma 13-(i).

Lemma 13. Let $(\pi^n)_{n \in \mathbb{N}}$ be the sequence given by (mIPF). Let $n \in \mathbb{N}$, $k = (n-1) \bmod(K)$, $k+1 = n \bmod(K)$. Denote by T_k , respectively T_{k+1} with edges E_{k+1} , the directed version of T rooted in i_k , respectively in i_{k+1} . Then, (i) $\pi^n \in \mathcal{P}_{\mathsf{T}_k}$ and (ii) for any edge $(v, v') \in \mathsf{E}_{k+1}$, we have $\pi_{v'|v}^{n+1} = \pi_{v'|v}^n$.

Proof. We show the result (i) by recursion on $n \in \mathbb{N}$, and will deduce (ii) from the proof. Using (2), we first have $\pi^0 \in \mathcal{P}_{\mathsf{T}_r}$, where r is chosen as i_{K-1} , see Section 3. Thus, we obtain the result (i) at step $n = 0$. Assume now that $\pi^n \in \mathcal{P}_{\mathsf{T}_k}$ for some $n \in \mathbb{N}$ with $k = (n-1) \bmod(K)$.

Consider the paths $\mathsf{P}_k = \text{path}_{\mathsf{T}_k}(i_k, i_{k+1})$ and $\mathsf{P}_{k+1} = \text{path}_{\mathsf{T}_{k+1}}(i_{k+1}, i_k)$. Note that these two paths have the same length, denoted by J , and contain the same vertices, denoted by V_k . Let $\pi \in \mathcal{P}^{(J+1)}$ such that $\text{KL}(\pi|\pi^n) < +\infty$. We have the following decomposition

$$\text{KL}(\pi|\pi^n) = \text{KL}(\pi_{\mathsf{V}_k}|\pi_{\mathsf{V}_k}^n) + \int_{(\mathbb{R}^d)^{J+1}} \text{KL}(\pi_{\mathsf{V}_k}|\pi_{\mathsf{V}_k}^n) d\pi_{\mathsf{V}_k}(x_{\mathsf{V}_k}).$$

Hence, the $(n+1)$ -th iterate of (mIPF) is given by $\pi^{n+1} = \pi_{\mathsf{V}_k}^{n+1} \otimes \pi_{\mathsf{V}_k}^n$, with

$$\pi_{\mathsf{V}_k}^{n+1} = \text{argmin}\{\text{KL}(\pi|\pi_{\mathsf{V}_k}^n) : \pi \in \mathcal{P}^{(J+1)}, \pi_{i_{k+1}} = \mu_{i_{k+1}}\}.$$

Since $\pi^n \in \mathcal{P}_{\mathsf{T}_k}$, we have (i) $\pi_{\mathsf{V}_k}^n = \bigotimes_{(v,v') \in \mathsf{E}_k \setminus \mathsf{P}_k} \pi_{v'|v}^n$ and (ii) $\pi_{\mathsf{V}_k}^n \in \mathcal{P}_{\mathsf{P}_{k+1}}$ by Lemma 10, where P_{k+1} is viewed as a directed tree rooted in i_{k+1} . Defining $\mathsf{V}_{k+1} = \mathsf{V}_k \setminus \{i_{k+1}\}$, we thus have $\pi_{\mathsf{V}_k}^n = \pi_{i_{k+1}}^n \otimes \pi_{\mathsf{V}_{k+1}|i_{k+1}}^n$ where $\pi_{\mathsf{V}_{k+1}|i_{k+1}}^n = \bigotimes_{(v,v') \in \mathsf{P}_{k+1}} \pi_{v'|v}^n$.

Let $\pi \in \mathcal{P}^{(J+1)}$ such that $\pi_{i_{k+1}} = \mu_{i_{k+1}}$ and $\text{KL}(\pi|\pi_{\mathsf{V}_k}^n) < +\infty$. Similarly to the previous computation, we have the following decomposition

$$\begin{aligned} \text{KL}(\pi|\pi_{\mathsf{V}_k}^n) &= \text{KL}(\pi_{i_{k+1}}|\pi_{i_{k+1}}^n) + \int_{\mathbb{R}^d} \text{KL}(\pi_{\mathsf{V}_{k+1}|i_{k+1}}|\pi_{\mathsf{V}_{k+1}|i_{k+1}}^n) d\pi_{i_{k+1}}(x_{i_{k+1}}) \\ &= \text{KL}(\mu_{i_{k+1}}|\pi_{i_{k+1}}^n) + \int_{\mathbb{R}^d} \text{KL}(\pi_{\mathsf{V}_{k+1}|i_{k+1}}|\pi_{\mathsf{V}_{k+1}|i_{k+1}}^n) d\mu_{i_{k+1}}(x_{i_{k+1}}). \end{aligned}$$

Therefore, we obtain

$$\pi_{\mathsf{V}_k}^{n+1} = \mu_{i_{k+1}} \otimes \pi_{\mathsf{V}_{k+1}|i_{k+1}}^n = \mu_{i_{k+1}} \bigotimes_{(v,v') \in \mathsf{P}_{k+1}} \pi_{v'|v}^n.$$

Noting that $\mathsf{E}_k \setminus \mathsf{P}_k = \mathsf{E}_{k+1} \setminus \mathsf{P}_{k+1}$ and recalling that $\pi^{n+1} = \pi_{\mathsf{V}_k}^{n+1} \otimes \pi_{\mathsf{V}_k}^n$, it finally comes

$$\pi^{n+1} = \mu_{i_{k+1}} \bigotimes_{(v,v') \in \mathsf{P}_{k+1}} \pi_{v'|v}^n \bigotimes_{(v,v') \in \mathsf{E}_{k+1} \setminus \mathsf{P}_{k+1}} \pi_{v'|v}^n = \mu_{i_{k+1}} \bigotimes_{(v,v') \in \mathsf{E}_{k+1}} \pi_{v'|v}^n.$$

Therefore, $\pi^{n+1} \in \mathcal{P}_{\mathsf{T}_{k+1}}$, which achieves the recursion. In particular, we have $\pi_{v'|v}^{n+1} = \pi_{v'|v}^n$ for any edge $(v, v') \in \mathsf{E}_{k+1}$ by definition of π^{n+1} . \square

We now provide the proof of Proposition 3.

Proof of Proposition 3. Let $n \in \mathbb{N}$, $k = (n-1) \bmod(K)$, $k+1 = n \bmod(K)$. Denote by T_k with edges E_k , respectively T_{k+1} with edges E_{k+1} , the directed version of T rooted in i_k , respectively in i_{k+1} . We know from Lemma 13-(ii) that $\pi_{v'|v}^{n+1} = \pi_{v'|v}^n$ for any edge $(v, v') \in \mathsf{E}_{k+1}$. Consider path measures $\{\mathbb{P}_{(v,v')}^n\}_{(v,v') \in \mathsf{E}_k}$ and $\{\mathbb{P}_{(v,v')}^{n+1}\}_{(v,v') \in \mathsf{E}_{k+1}}$ as given by Proposition 2. Define the path $\mathsf{P} = \text{path}_{\mathsf{T}_k}(i_k, i_{k+1})$.

Let $(v, v') \in \mathsf{E}_{k+1}$. We first turn to the proof of (a). If $(v, v') \in \mathsf{E}_k \setminus \mathsf{P}$, we get that

$$\mathbb{P}_{(v,v'), T|0}^{n+1} = \pi_{v'|v}^{n+1} = \pi_{v'|v}^n = \mathbb{P}_{(v,v'), T|0}^n,$$

which gives the result. If $(v', v) \in \mathsf{P}$, we get that

$$\mathbb{P}_{(v,v'), T|0}^{n+1} = \pi_{v'|v}^{n+1} = \pi_{v'|v}^n = (\mathbb{P}_{(v',v), T|0}^n)^R,$$

which concludes the proof of (b). \square

D.2 Proofs of Section 4

Remark on assumption A1. Although **A1** is not needed to establish the result of Proposition 4, Corollary 5 and Proposition 6, it is however crucial in the proof of convergence (mIPF) stated in Proposition 7. Nevertheless, we choose to keep **A1** as an assumption in the statement of every theoretical result presented in Section 4 for sake of clarity.

Additional definitions. We define the set $\mathcal{P}_S = \cap_{i \in S} \mathcal{P}_i$, where $\mathcal{P}_i = \{\pi \in \mathcal{P}^{(\ell+1)} : \pi_i = \mu_i\}$, i.e., \mathcal{P}_S is the set of all probability measures $\pi \in \mathcal{P}^{(\ell+1)}$ which verify

$$\int_{(\mathbb{R}^d)^{\ell+1}} f_i(x_i) d\pi(x_{0:\ell}) = \int_{\mathbb{R}^d} f_i(x_i) d\mu_i(x_i) ,$$

for any family of bounded measurable functions $\{f_i\}_{i \in S} \in C(\mathbb{R}^d, \mathbb{R})^K$. Since \mathbb{R}^d is separable, there exists a dense family of functions $\{f_i^k\}_{k \in \mathbb{N}^*, i \in S}$, with $f_i^k \in L^\infty(\mu_i)$ for any $k \in \mathbb{N}^*$ and any $i \in S$, such that $\pi \in \mathcal{P}_S$ if and only if

$$\int_{(\mathbb{R}^d)^{\ell+1}} f_i^k(x_i) d\pi(x_{0:\ell}) = \int_{\mathbb{R}^d} f_i^k(x_i) d\mu_i(x_i)$$

or equivalently, upon centering f_i^k ,

$$\int_{(\mathbb{R}^d)^{\ell+1}} f_i^k(x_i) d\pi(x_{0:\ell}) = 0 .$$

In the rest of the section, we consider such family $\{f_i^k\}_{k \in \mathbb{N}^*, i \in S}$.

For any $n \in \mathbb{N}^*$, we also define $\mathcal{P}_S^n = \cap_{i \in S} \mathcal{P}_i^n$, where $\mathcal{P}_i^n = \{\pi \in \mathcal{P}^{(\ell+1)} : \int_{(\mathbb{R}^d)^{\ell+1}} f_i^k(x_i) d\pi(x_{0:\ell}) = 0, \forall k \in \{1, \dots, n\}\}$. In particular, we have

$$\mathcal{P}_S = \cap_{n \in \mathbb{N}^*} \mathcal{P}_S^n . \quad (5)$$

Finally, (mSB) can be rewritten as

$$\pi^* = \operatorname{argmin}\{\operatorname{KL}(\pi \mid \pi^0) : \pi \in \mathcal{P}_S\} . \quad (6)$$

Proof of Proposition 4 and Corollary 5. In this part of the section, we present an extension of the theoretical results from Nutz (2021) to the multi-marginal setting. We first present two technical results, Lemma 14 and Lemma 15, which are respectively adapted from (Nutz, 2021, Lemma 2.10.) and (Nutz, 2021, Lemma 2.11.).

Lemma 14. Let $\{\tilde{\mu}_j\}_{j \in S^c}$ be a family of probability measures defined on $(\mathbb{R}^d, \mathcal{B}(\mathbb{R}^d))$. We define $\tilde{\pi}^0 = \bigotimes_{i \in S} \mu_i \bigotimes_{j \in S^c} \tilde{\mu}_j$. Let $A \in \bigotimes_{m=0}^\ell \mathcal{B}(\mathbb{R}^d)$ such that $\tilde{\pi}^0(A) = 1$. Then, for $\tilde{\pi}^0$ -almost any $x^* \in A$, there exists a family of sets $\{X_m^0\}_{m=0}^\ell \subset (\mathbb{R}^d)^{\ell+1}$ such that

(a) $\mu_i(X_i^0) = 1$ for any $i \in S$, and $\tilde{\mu}_j(X_j^0) = 1$ for any $j \in S^c$,

(b) $A^0 = A \cap (\prod_{m=0}^\ell X_m^0)$ satisfies $x^* \in A^0$ and

$$(x_0^*, \dots, x_{m-1}^*, x_m, x_{m+1}^*, \dots, x_\ell^*) \in A^0, \forall x \in A^0, \forall m \in \{0, \dots, \ell\} .$$

Proof. Consider such set A . We define for any $m \in \{0, \dots, \ell\}$ the set

$$X_m = \{u \in \mathbb{R}^d : \tilde{\pi}_{-m}^0(A_m^u) = 1\} ,$$

where $A_m^u = \{y \in (\mathbb{R}^d)^\ell : (y_0, \dots, y_{m-1}, u, y_m, \dots, y_{\ell-1}) \in A\}$.

Take $i \in S$. Assume that $\mu_i(X_i) < 1$. We recall that $\tilde{\pi}^0 = \tilde{\pi}_{-i}^0 \otimes \mu_i$. Using Fubini's theorem and that $\int_{A_i^{x_i}} d\tilde{\pi}_{-i}^0(x_{-i}) < 1$ for any $x_i \notin X_i$, we have

$$\begin{aligned} 1 = \tilde{\pi}^0(A) &= \int_A d\tilde{\pi}_{-i}^0(x_{-i}) \otimes d\mu_i(x_i) \\ &= \int_{\mathbb{R}^d} \{\int_{A_i^{x_i}} d\tilde{\pi}_{-i}^0(x_{-i})\} d\mu_i(x_i) \\ &= \int_{X_i} \{\int_{A_i^{x_i}} d\tilde{\pi}_{-i}^0(x_{-i})\} d\mu_i(x_i) + \int_{X_i^c} \{\int_{A_i^{x_i}} d\tilde{\pi}_{-i}^0(x_{-i})\} d\mu_i(x_i) \\ &< \mu_i(X_i) + \mu_i(X_i^c) = 1 , \end{aligned}$$

which is absurd. Therefore, we obtain $\mu_i(X_i) = 1$, and similarly, we have $\tilde{\mu}_j(X_j) = 1$ for any $j \in S^c$. For any $y \in (\mathbb{R}^d)^\ell$, any $m \in \{0, \dots, \ell\}$, we define the set

$$\bar{A}_m^y = \{u \in \mathbb{R}^d : (y_0, \dots, y_{m-1}, u, y_m, \dots, y_{\ell-1}) \in A\}.$$

Let $i \in S$. We have by Fubini's theorem

$$\begin{aligned} 1 &= \tilde{\pi}^0(A) = \int_A d\mu_i(x_i) \otimes d\tilde{\pi}_{-i}^0(x_{-i}) \\ &= \int_{(\mathbb{R}^d)^\ell} \left\{ \int_{\bar{A}_i^{x_{-i}}} d\mu_i(x_i) \right\} d\tilde{\pi}_{-i}^0(x_{-i}) \\ &= \int_{\prod_{\substack{m=0 \\ m \neq i}}^\ell X_i} \left\{ \int_{\bar{A}_i^{x_{-i}}} d\mu_i(x_i) \right\} d\tilde{\pi}_{-i}^0(x_{-i}), \end{aligned}$$

where the last equality comes from the fact that $\mu_i(X_i) = 1$ for any $i \in S$, $\tilde{\mu}_j(X_j) = 1$ for any $j \in S^c$ and that $\tilde{\pi}^0 = \bigotimes_{i \in S} \mu_i \bigotimes_{j \in S^c} \tilde{\mu}_j$. Consequently, there exists a measurable set $A_{-i} \subset \prod_{\substack{m=0 \\ m \neq i}}^\ell X_i$ such that the following properties hold: (a) $\mu_i(\bar{A}_i^y) = 1$ for any $y \in A_{-i}$, (b) $\tilde{\pi}_{-i}^0(A_{-i}) = 1$. Similarly, this result holds for any $j \in S^c$, i.e., there exists a measurable set $A_{-j} \subset \prod_{\substack{m=0 \\ m \neq j}}^\ell X_i$ such that the following properties hold: (a) $\tilde{\mu}_j(\bar{A}_j^y) = 1$ for any $y \in A_{-j}$, (b) $\tilde{\pi}_{-j}^0(A_{-j}) = 1$. We consider such sets $\{A_{-m}\}_{m=0}^\ell$ for the rest of the proof and finally define the set

$$\tilde{A} = \bigcap_{m=0}^\ell \tilde{A}_m,$$

where $\tilde{A}_m = A_{-m} \times \{u \in \bar{A}_m^y : y \in A_{-m}\}$. By definition, we have $\tilde{A} \subset A \cap \prod_{m=0}^\ell X_m$, using the fact that $\tilde{A}_m \subset A$ for any $m \in \{0, \dots, \ell\}$. In addition, for any $i \in S$, we get by Fubini's theorem

$$\tilde{\pi}^0(\tilde{A}_i) = \int_{\tilde{A}_i} d\mu_i(x_i) \otimes d\tilde{\pi}_{-i}^0(x_{-i}) = \int_{A_{-i}} \left\{ \int_{\bar{A}_i^{x_{-i}}} d\mu_i(x_i) \right\} d\tilde{\pi}_{-i}^0(x_{-i}) = \tilde{\pi}_{-i}^0(A_{-i}) = 1,$$

and similarly, we get $\tilde{\pi}^0(\tilde{A}_j) = 1$ for any $j \in S^c$. We can deduce that $\tilde{\pi}^0(\tilde{A}) = 1$ since $\tilde{\pi}^0(\tilde{A}^c) \leq \sum_{m=0}^\ell \tilde{\pi}^0(\tilde{A}_m^c) = 0$.

Let $x^* \in \tilde{A}$. In particular, $x^* \in A$. We define the set $A^0 = A \cap (\prod_{m=0}^\ell X_m^0)$, where $X_m^0 = X_m \cap \bar{A}_m^{x^*-m}$ for any $m \in \{0, \dots, \ell\}$. We now establish the result of Lemma 14.

We first prove item (a). Let $i \in S$. Since $x^* \in \tilde{A}$, we have $x^* \in \tilde{A}_i$ and therefore $x_{-i}^* \in A_{-i}$. By definition of A_{-i} , we obtain that $\mu_i(\bar{A}_i^{x_{-i}^*}) = 1$ and thus,

$$\mu_i(\{X_i^0\}^c) \leq \mu_i(X_i^c) + \mu_i(\{\bar{A}_i^{x_{-i}^*}\}^c) = 0,$$

which gives $\mu_i(X_i^0) = 1$, and similarly, we have $\tilde{\mu}_j(X_j^0) = 1$ for any $j \in S^c$.

We now prove item (b). Let $m \in \{0, \dots, \ell\}$. Since $x^* \in \tilde{A} \subset A$, we get $x_m^* \in \bar{A}_m^{x^*-m}$. Using that $\tilde{A} \subset A \cap \prod_{m=0}^\ell X_m$, we get $x^* \in A^0$. Let $x \in A^0$. We denote $x^m = (x_0^*, \dots, x_{m-1}^*, x_m, x_{m+1}^*, \dots, x_\ell^*)$. We need to show that $x^m \in A$ and $x^m \in \prod_{j=1}^\ell X_j^0 = \prod_{j=1}^\ell (X_j \cap \bar{A}_j^{x^*-m})$. First, since $x_j^m = x_j$ or x_j^* for any $j \in \{0, \dots, \ell\}$, and $x \in A^0$ and $x^* \in A^0$, we get that for any $j \in \{0, \dots, \ell\}$, $x_j^m \in X_j$. Similarly, for any $j \in \{0, \dots, \ell-1\}$, $x_j^m \in \bar{A}_j^{x^*-m}$. Therefore, we get that $x^m \in \prod_{j=1}^\ell (X_j \cap \bar{A}_j^{x^*-m})$. Since $x_m \in A_m^{x^*-m}$ (because $x \in \prod_{j=1}^\ell (X_j \cap \bar{A}_j^{x^*-m})$), we get that $x \in A$, which concludes the proof. \square

Lemma 15. Let $A^0 \subset (\mathbb{R}^d)^{\ell+1}$. For any $m \in \{0, \dots, \ell\}$, we denote $X_m^0 = \text{proj}_m(A^0)$. We make the following assumptions.

(a) Assume there exists $x^* \in A^0$ such that for any $x \in A^0$, for any $m \in \{0, \dots, \ell\}$, we have $(x_0^*, \dots, x_{m-1}^*, x_m, x_{m+1}^*, \dots, x_\ell^*) \in A^0$.

(b) Assume there exists a family of functions $\{\varphi_{i_k}^n\}_{n \in \mathbb{N}^*, k \in \{0, \dots, K-1\}}$ with $\varphi_{i_k}^n : X_{i_k}^0 \rightarrow [-\infty, +\infty)$ such that for any $n \in \mathbb{N}^*$ and any $k \in \{0, \dots, K-2\}$, we have $\varphi_{i_k}^n(x_{i_k}^*) = 0$.

(c) Denote $F^n(x) = \sum_{k=0}^{K-1} \varphi_{i_k}^n(x_{i_k})$ for any $x \in A^0$. Assume that for any $x \in A^0$, $F(x) = \lim_{n \rightarrow \infty} F^n(x)$ exists and is such that $F(x) \in [-\infty, +\infty)$ with $F(x^*) \in \mathbb{R}$.

Then, for any $i \in S$, for any $x_i \in X_i^0$, $\varphi_i(x_i) = \lim_{n \rightarrow \infty} \varphi_i^n(x_i)$ exists and is such that $\varphi_i(x_i) \in [-\infty, +\infty)$.

Proof. Consider $A^0 \subset (\mathbb{R}^d)^{\ell+1}$ such that assumptions (a), (b) and (c) hold. Remark that we have $F^n(x^*) = \varphi_{i_{K-1}}^n(x_{i_{K-1}}^*)$.

Let $x \in A^0$. We denote $x^m = (x_1^*, \dots, x_{m-1}^*, x_m, x_{m+1}^*, \dots, x_\ell^*)$ for any $m \in \{0, \dots, \ell\}$. In particular, we have $x^m \in A^0$ by assumption (a). Let us define

$$\begin{aligned} \varphi_{i_k}(x_{i_k}) &= F(x^{i_k}) - F(x^*), \quad \forall k \in \{0, \dots, K-2\}, \\ \varphi_{i_{K-1}}(x_{i_{K-1}}) &= F(x^{i_{K-1}}). \end{aligned}$$

Using assumption (c), we have $\varphi_i(x_i) \in [-\infty, +\infty)$ for any $i \in S$. Let $k \in \{0, \dots, K-2\}$. We have by definition of F^n ,

$$\varphi_{i_k}^n(x_{i_k}) = F^n(x^{i_k}) - \sum_{\substack{m=0 \\ m \neq k}}^{K-1} \varphi_{i_m}^n(x_{i_m}^*) = F^n(x^{i_k}) - F^n(x^*),$$

where we used assumption (b) in the last equality. Since $x^{i_k} \in A^0$ and $x^* \in A^0$, we have by assumption (c),

$$\lim_{n \rightarrow \infty} \varphi_{i_k}^n(x_{i_k}) = F(x^{i_k}) - F(x^*) = \varphi_{i_k}(x_{i_k}).$$

Furthermore, by combining the definition of F^n with assumption (b), we have

$$\lim_{n \rightarrow \infty} \varphi_{i_{K-1}}^n(x_{i_{K-1}}) = F(x^{i_{K-1}}) = \varphi_{i_{K-1}}(x_{i_{K-1}}),$$

which concludes the proof. \square

In what follows, before proving Proposition 4, we respectively show in Proposition 16 and Proposition 17 how A2 and A3 can be satisfied in the case where $\pi^0 \in \mathcal{P}_{T_r}$, as in (2), that is

$$\pi^0 = \pi_r^0 \otimes_{(v,v') \in E_r} \pi_{v'|v}^0.$$

Proposition 16. Let $\pi^0 \in \mathcal{P}_{T_r}$. Assume that $\pi_r^0 = N(m_r, \sigma_r \text{Id})$, with $m_r \in \mathbb{R}^d$ and $\sigma_r > 0$ or $\pi_r^0 = \mu_r$ if $r \in S$. In addition, assume that for any $(v, v') \in E_r$, $\pi_{v'|v}^0(\cdot | x_v) = N(x_v, \sigma_{v,v'} \text{Id})$ with $\sigma_{v,v'} > 0$. Finally, assume that for any $i \in S$, $\int_{\mathbb{R}^d} \|x\|^2 d\mu_i(x) < +\infty$ and $H(\mu_i) < +\infty$. Then A2 is satisfied.

Proof. Let $\pi = \otimes_{i \in S} \mu_i \otimes_{i \in S^c} \nu_i$ with ν_i any Gaussian measure with positive definite covariance matrix. First, we have that

$$\text{KL}(\pi | \pi^0) = \text{KL}(\pi_r | \pi_r^0) + \sum_{(v,v') \in E_r} \int_{\mathbb{R}^d} \text{KL}(\pi_{v'|v} | \pi_{v'|v}^0) d\pi_v.$$

For any $(v, v') \in E_r$, there exists $C_{v,v'} \geq 0$ such that

$$\begin{aligned} \int_{\mathbb{R}^d} \text{KL}(\pi_{v'|v} | \pi_{v'|v}^0) d\pi_v &\leq C_{v,v'} - H(\pi_{v'}) + \int_{\mathbb{R}^d \times \mathbb{R}^d} \|x_v - x_{v'}\|^2 / (2\sigma_{v,v'}^2) d\pi_v \otimes \pi_{v'}(x_v, x_{v'}) \\ &\leq C_{v,v'} - H(\pi_{v'}) + (1/\sigma_{v,v'}^2) \int_{\mathbb{R}^d} \|x_v\|^2 d\pi_v(x_v) + (1/\sigma_{v,v'}^2) \int_{\mathbb{R}^d} \|x_{v'}\|^2 d\pi_{v'}(x_{v'}) < +\infty. \end{aligned}$$

We conclude the proof upon remarking that $\text{KL}(\pi_r | \pi_r^0) < +\infty$. \square

Proposition 17. Let $\pi^0 \in \mathcal{P}_{T_r}$. Assume that $\pi_r^0 = N(m_r, \sigma_r \text{Id})$, with $m_r \in \mathbb{R}^d$ and $\sigma_r > 0$ or $\pi_r^0 = \mu_r$ if $r \in S$. In addition, assume that for any $(v, v') \in E_r$, $\pi_{v'|v}^0(\cdot | x_v) = N(x_v, \sigma_{v,v'} \text{Id})$ with $\sigma_{v,v'} > 0$. Finally, assume that for any $i \in S$, μ_i admits a positive density w.r.t. the Lebesgue measure. Then A3 is satisfied.

Proof. We have that π^0 admits a positive density w.r.t the Lebesgue measure. Letting $\tilde{\pi}^0 = \otimes_{i \in S} \mu_i \otimes_{j \in S^c} \tilde{\mu}_j$ with $\tilde{\mu}_j$ which admits a positive density w.r.t the Lebesgue measure for any $j \in S^c$, we get that $\tilde{\pi}^0$ admits a positive density w.r.t. the Lebesgue measure and therefore $\pi^0 \sim \tilde{\pi}^0$, which concludes the proof. \square

Using the preliminary results presented above, we are now ready to prove Proposition 4.

Proof of Proposition 4. Assume **A1** and **A2**. Since \mathcal{P}_S is convex and closed in total-variation norm, there exists a probability distribution π^* solution to (6), or equivalently to (mSB), by using **A2** with (Csiszár, 1975, Theorem 2.1.). Moreover, this solution is unique by strict convexity of $\text{KL}(\cdot \mid \pi^0)$.

We now turn to the proof of existence of potentials defining $(d\pi^*/d\pi^0)$, by adapting the arguments of (Nutz, 2021, Section 2.3.). Define $\nu^n = \text{argmin}\{\text{KL}(\pi \mid \pi^0) : \pi \in \mathcal{P}_S^n\}$ for any $n \in \mathbb{N}^*$. Since $\{\mathcal{P}_S^n\}_{n \in \mathbb{N}^*} \subset \mathcal{P}^{(\ell+1)}$ is a decreasing sequence of sets that are convex and closed in total-variation norm such that (5) holds, we get from (Nutz, 2021, Proposition 1.17.) with **A2** that

$$\lim_{n \rightarrow \infty} \|\nu^n - \pi^*\|_{\text{TV}} = 0,$$

or equivalently

$$\lim_{n \rightarrow \infty} \|(d\nu^n/d\pi^0) - (d\pi^*/d\pi^0)\|_{L^1(\pi^0)} = 0. \quad (7)$$

Following (Nutz, 2021, Example 1.18), there exists a family of bounded measurable functions $\{\varphi_i^n\}_{n \in \mathbb{N}^*, i \in S}$ with $\varphi_i^n : \mathbb{R}^d \rightarrow \mathbb{R}$ such that for any $n \in \mathbb{N}^*$

$$(d\nu^n/d\pi^0) = \exp[\bigoplus_{i \in S} \varphi_i^n]. \quad (8)$$

We consider such family $\{\varphi_i^n\}_{n \in \mathbb{N}^*, i \in S}$ for the rest of the proof. By combining (7) and (8), we obtain, up to extraction,

$$(d\pi^*/d\pi^0) = \lim_{n \rightarrow \infty} \exp[\bigoplus_{i \in S} \varphi_i^n] \quad \pi^0\text{-a.s.} \quad (9)$$

We now define the following sets

$$\begin{aligned} A^* &= \{x \in (\mathbb{R}^d)^{\ell+1} : \lim_{n \rightarrow \infty} \bigoplus_{i \in S} \varphi_i^n(x_i) \in [-\infty, +\infty)\}, \\ B^* &= \{x \in (\mathbb{R}^d)^{\ell+1} : \lim_{n \rightarrow \infty} \bigoplus_{i \in S} \varphi_i^n(x_i) > -\infty\} \subset A^* \end{aligned}$$

Using (9), we have $\pi^0(A^*) = 1$. Using **A3**, it comes $\tilde{\pi}^0(A^*) = 1$. Moreover, we also get that $\pi^*(B^*) = 1$ by (9). Thus, it comes $\pi^0(B^*) > 0$, and $\tilde{\pi}^0(B^*) > 0$ using **A3**.

We then apply Lemma 14 to $\tilde{\pi}^0$ and $A = A^*$. Since $\tilde{\pi}^0(B^*) > 0$, it implies that there exists $x^* \in B^*$ and a measurable set $A^0 \subset B^*$ verifying the properties (a) and (b). Following (Nutz, 2021, Corollary 2.12), we may assume without loss of generality in the statement of Lemma 14 that the sets X_m^0 are measurable with $\prod_{m=0}^{\ell} X_m^0 \subset A$. In this case, we obtain that $\mu_i(\text{proj}_i(A^0)) = 1$ for any $i \in S$.

We now aim at applying Lemma 15 to the set A^0 . Remark that A^0 directly satisfies assumption (a). For any $n \in \mathbb{N}^*$, consider the following transformation of the functions $\{\varphi_i^n\}_{i \in S}$

$$\begin{aligned} \varphi_{i_k}^n &\leftarrow \varphi_{i_k}^n - \varphi_{i_k}^n(x_{i_k}^*), \quad \forall k \in \{0, \dots, K-2\}, \\ \varphi_{i_{K-1}}^n &\leftarrow \varphi_{i_{K-1}}^n + \sum_{k=0}^{K-2} \varphi_{i_k}^n(x_{i_k}^*). \end{aligned}$$

For any $i \in S$, we restrict $\varphi_{i_k}^n$ to $X_{i_k}^0$, so that the family $\{\varphi_i^n\}_{n \in \mathbb{N}^*, i \in S}$ now verifies assumption (b). Finally, since $A^0 \subset A^*$ and $x^* \in B^*$, we directly obtain assumption (c).

Therefore, Lemma 15 may be applied. It provides us with the family of functions $\{\varphi_i\}_{i \in S}$ defined by $\varphi_i : X_i^0 \rightarrow [-\infty, +\infty)$ with $\varphi_i = \lim_{n \rightarrow \infty} \varphi_i^n$ μ_i -a.s. for any $i \in S$. Since $\mu_i(\text{proj}_i(A^0)) = 1$ for any $i \in S$, we may extend the functions φ_i to \mathbb{R}^d . In particular, we can find a family of functions $\{\psi_i^*\}_{i \in S}$ with $\psi_i^* : \mathbb{R}^d \rightarrow [-\infty, +\infty)$ such that $\psi_i^* = \varphi_i$ μ_i -a.s. Note that these functions are measurable as limits of measurable functions.

Since $\pi^0 \sim \tilde{\pi}^0$ by **A3**, (9) turns into

$$(d\pi^*/d\pi^0) = \exp[\bigoplus_{i \in S} \psi_i^*] \quad \pi^0\text{-a.s.} \quad (10)$$

Finally, we show that the functions ψ_i^* are μ_i -a.s. finite. Let $i \in S$. Let us define $A_i = \{x_i \in \mathbb{R}^d : \psi_i^*(x_i) = -\infty\}$. Using (10), we obtain $(d\pi^*/d\pi^0)(A_i \times (\mathbb{R}^d)^\ell) = 0$. Since $\pi_i^* = \mu_i$, we have

$$\mu_i(A_i) = \pi^*(A_i \times (\mathbb{R}^d)^\ell) = \int_{A_i \times (\mathbb{R}^d)^\ell} (d\pi^*/d\pi^0) d\pi^0 = 0,$$

which gives the result. \square

We now turn to the proof of Corollary 5, which states that the iterates of (mIPF) can be expressed via potentials, in the same manner as the solution π^* to (mSB).

Proof of Corollary 5. Assume A1, A2 and A3. We prove the result of this corollary by recursion on $n \in \mathbb{N}^*$. First take $n = 1$. In this case, the first iteration of (mIPF) is a multi-marginal SB problem of the form (mSB) where $S = \{i_0\}$ with reference measure π^0 . Therefore, using A2 and A3, we can apply Proposition 4 and obtain existence of $\psi_{i_0}^1 : \mathbb{R}^d \rightarrow \mathbb{R}$ such that

$$(d\pi^1/d\pi^0) = \exp[\psi_{i_0}^1] \quad \pi^0\text{-a.s.}$$

By taking $\psi_{i_k}^0 = 0$ for $k \in \{1, \dots, K-1\}$, we thus obtain the result at step $n = 1$.

Now assume that the result is verified for some $n \in \mathbb{N}^*$, with $k = (n-1) \bmod(K)$. We define $k+1 = n \bmod(K)$ and $q \in \mathbb{N}$ as the quotient of the Euclidean division of n by K . In this case, the $(n+1)$ -th iteration of (mIPF) is a multi-marginal SB problem of the form (mSB) where $S = \{i_{k+1}\}$ with reference measure π^n . Using (12), we have that A2 is satisfied for this new (mSB) problem. A1 and A3 are satisfied for this problem, given the form of π^n . Therefore, we can apply Proposition 4 and obtain existence of $\psi_{i_{k+1}}^{q+1} : \mathbb{R}^d \rightarrow \mathbb{R}$ such that

$$(d\pi^{n+1}/d\pi^n) = \exp[\psi_{i_{k+1}}^{q+1}] \quad \pi^n\text{-a.s.} \quad (11)$$

By assumption, we have that $\pi^n \ll \pi^0$. Hence, we obtain $\pi^{n+1} \ll \pi^0$ and thus,

$$(d\pi^{n+1}/d\pi^0) = (d\pi^{n+1}/d\pi^n)(d\pi^n/d\pi^0) \quad \pi^0\text{-a.s.}$$

By combining (11) with the result of the recursion at step n , we directly obtain the result at step $n+1$, which achieves the proof. \square

Proofs of Proposition 6 and Proposition 7. In this part of the section, we establish the proofs of results related to the convergence of (mIPF), respectively Proposition 6 and Proposition 7, which can be seen as a natural extension of (Ruschendorf, 1995, Proposition 2.1.) and (Ruschendorf, 1995, Theorem 3.1.).

Proof of Proposition 6. Under A1 and A2, we obtain by Proposition 4 existence and uniqueness of a solution to (mSB), which we denote by π^* . Since $\pi^* \in \mathcal{P}_S$, using recursively (Csiszár, 1975, Theorem 3.12.), the fact that $\{\pi_{i_k} = \mu_{i_k} : \pi \in \mathcal{P}^{(|V|)}\}$ is convex for any $k \in \{0, \dots, K-1\}$ and (mIPF), we obtain

$$\text{KL}(\pi^* | \pi^0) = \text{KL}(\pi^* | \pi^n) + \sum_{i=1}^n \text{KL}(\pi^i | \pi^{i-1}). \quad (12)$$

Therefore, we have $\sum_{i=1}^\infty \text{KL}(\pi^i | \pi^{i-1}) \leq \text{KL}(\pi^* | \pi^0) < \infty$ and thus,

$$\lim_{i \rightarrow +\infty} \text{KL}(\pi^i | \pi^{i-1}) = 0. \quad (13)$$

Let $n \in \mathbb{N}^*$ with $n > 2K$, $k \in \{0, \dots, K-1\}$ and let $q \in \mathbb{N}$ be the quotient of the Euclidean division of $n-1$ by K . We define $n_k = qK + k + 1$ with $(n_k - 1) = k \bmod(K)$ if $n_k \leq n$. Otherwise, we set $n_k = (q-1)K + k + 1$ with $(n_k - 1) = k \bmod(K)$. Note that we always have $|n - n_k| \leq 2K$. In particular, we have $\pi_{i_k}^{n_k} = \mu_{i_k}$ by definition of (mIPF). Therefore, we obtain

$$\begin{aligned} \|\pi_{i_k}^n - \mu_{i_k}\|_{\text{TV}} &\leq \|\pi^n - \pi^{n_k}\|_{\text{TV}} \\ &\leq \|\pi^n - \pi^{n-1}\|_{\text{TV}} + \dots + \|\pi^{n_k+1} - \pi^{n_k}\|_{\text{TV}} \quad (\text{triangle inequality}) \\ &\leq (2\text{KL}(\pi^n | \pi^{n-1}))^{1/2} + \dots + (2\text{KL}(\pi^{n_k+1} | \pi^{n_k}))^{1/2}, \quad (\text{Pinsker's inequality}) \end{aligned}$$

where each term goes to 0 as $n \rightarrow +\infty$ in the last inequality by (13), which achieves the proof. \square

For the rest of this section, we define, for any $n \in \mathbb{N}$, q_n as the quotient of the Euclidean division of $n-1$ by K (in particular, $q_0 = -1$).

Schrödinger equations. Under **A1**, **A2** and **A3**, we know from Proposition 6 that the unique solution π^* to (mSB) can be π^0 -a.s. written as $(d\pi^*/d\pi^0) = \exp[\bigoplus_{i \in S} \psi_i^*]$, where $\{\psi_i^*\}_{i \in S}$ are measurable potentials, referred to as *Schrödinger potentials*. These functions are determined by the fixed-point *Schrödinger equations*

$$\psi_i^*(x_i) = \log[r_i(x_i) / \int_{(\mathbb{R}^d)^\ell} \exp[\sum_{j \in S \setminus \{i\}} \psi_j^*(x_j)] h(x_{0:\ell}) d\nu_{-i}(x_{-i})] \quad \mu_i\text{-a.s.}, \quad \forall i \in S,$$

which are obtained by marginalising π^* along its constrained marginals. This family of potentials is not unique. Indeed, for any family of real numbers $\{\lambda_{i_k}\}_{k \in \{0, \dots, K-2\}}$, we have

$$(d\pi^*/d\pi^0) = \exp[\bigoplus_{i \in S} \tilde{\psi}_i],$$

where $\tilde{\psi}_{i_k} = \psi_{i_k}^* + \tilde{\lambda}_{i_k}$ for any $k \in \{0, \dots, K-1\}$ with $\tilde{\lambda}_{i_k} = \lambda_{i_k}$ if $k \in \{0, \dots, K-2\}$ and $\tilde{\lambda}_{i_{K-1}} = -\sum_{i=0}^{K-2} \lambda_{i_k}$.

Remark on the initialisation of (mIPF). Consider a probability measure $\bar{\pi}^0 \in \mathcal{P}^{(\ell+1)}$ of the form

$$(d\bar{\pi}^0/d\pi^0) = \exp[\bigoplus_{i \in S} \psi_i^0], \quad (14)$$

where $\{\psi_i^0\}_{i \in S}$ is a family of measurable potentials with $\psi_i^0 : \mathbb{R}^d \rightarrow \mathbb{R}$ such that $|\int_{\mathbb{R}^d} \psi_i^0 d\mu_i| < \infty$ for any $i \in S$. Then, for any $\pi \in \mathcal{P}_S$, we have

$$\text{KL}(\pi | \pi^0) = \text{KL}(\pi | \bar{\pi}^0) + \int_{(\mathbb{R}^d)^K} \bigoplus_{i \in S} \psi_i^0 d\pi = \text{KL}(\pi | \bar{\pi}^0) + \sum_{i \in S} \int_{\mathbb{R}^d} \psi_i^0 d\mu_i.$$

Hence, (mSB) is equivalent to the multi-marginal SB problem

$$\text{argmin}\{\text{KL}(\pi | \bar{\pi}^0) : \pi \in \mathcal{P}^{(\ell+1)}, \pi_i = \mu_i, \forall i \in S\}.$$

We refer to (Peyré et al., 2019, Proposition 4.2) for the EOT counterpart of this result. This means that the solutions of the multimarginal Schrödinger Bridge problem are invariant by multiplication of the reference path measure by potentials on the *fixed* marginals. Consequently, the initialisation of (mIPF) may be chosen as $\bar{\pi}^0$ instead of π^0 . For sake of clarity, we now refer to the reference measure of (mSB) as $\bar{\pi}$ or π^{-1} and the initialisation of (mIPF) as π^0 .

Solving (mIPF) with potentials. We recursively define the sequence of potentials $\{\psi_i^n\}_{n \in \mathbb{N}, i \in S}$ by

$$\begin{aligned} \psi_{i_0}^0 &= \dots = \psi_{i_{K-2}}^0 = 0, \\ \psi_{i_{K-1}}^0(x_{i_{K-1}}) &= \log(r_{i_{K-1}}(x_{i_{K-1}}) / \int_{(\mathbb{R}^d)^\ell} h(x_{0:\ell}) d\nu_{-i_{K-1}}(x_{-i_{K-1}})), \end{aligned} \quad (15)$$

recalling that q_n is the quotient of the Euclidean division of $n-1$ by K , we define for any $n \in \mathbb{N}^*$ and $k \in \{0, \dots, K-1\}$

$$\begin{aligned} \psi_{i_k}^{q_n+1}(x_{i_k}) &= \log[r_{i_k}(x_{i_k}) / \int_{(\mathbb{R}^d)^\ell} \exp[\bigoplus_{\ell=0}^k \psi_{i_\ell}^{q_n+1}(x_{i_\ell}) \bigoplus_{m=k+1}^{K-1} \psi_{i_m}^{q_n}(x_{i_m})] \\ &\quad \times h(x_{0:\ell}) d\nu_{-i_k}(x_{-i_k})]. \end{aligned} \quad (16)$$

We now consider the sequence of probability measures $\{\pi^n\}_{n \in \mathbb{N}}$ given by

$$d\pi^n/d\bar{\pi} = \exp[\bigoplus_{\ell=0}^k \psi_{i_\ell}^{q_n+1} \bigoplus_{m=k+1}^{K-1} \psi_{i_m}^{q_n}], \quad k = (n-1) \bmod(K), \quad n = q_n K + k + 1. \quad (17)$$

In particular, we have $(d\pi^0/d\bar{\pi}) = \exp[\bigoplus_{\ell=0}^{K-1} \psi_{i_\ell}^0] = \exp[\psi_{i_{K-1}}^0]$, and thus $\int_{\mathbb{R}^d} \psi_{i_{K-1}}^0 d\mu_{i_{K-1}} = \text{KL}(\mu_{i_{K-1}} | \bar{\pi}_{i_{K-1}})$. Consequently, π^0 can be chosen as the initialisation of (mIPF) if we assume that $\text{KL}(\mu_{i_{K-1}} | \bar{\pi}_{i_{K-1}}) < \infty$. In (TreeSB) with $r = i_{K-1}$, the latter assumption is directly verified since we choose $\bar{\pi}_{i_{K-1}} = \mu_{i_{K-1}}$.

Let $n \in \mathbb{N}$, with $k = (n-1) \bmod(K)$, $k+1 = n \bmod(K)$. Using (15) and (16), we get that $\pi_{i_k}^n = \mu_{i_k}$. Moreover, we have

$$d\pi^n/d\pi^{n-1} = \exp[\psi_{i_k}^{q_n+1} - \psi_{i_k}^{q_n}], \quad (18)$$

with the convention that $\psi_{i_{K-1}}^{-1} = 0$, which implies that $\pi_{i_{k+1}}^{n+1} = \pi_{i_{k+1}}^n$. Therefore, we have $\pi^{n+1} = \mu_{i_{k+1}} \pi_{i_k}^n$, which proves that the sequence $(\pi^n)_{n \in \mathbb{N}}$ solves (mIPF), see Lemma 13. Finally, since $\pi_{i_k}^n = \mu_{i_k}$, we get that

$$\text{KL}(\pi^n | \pi^{n-1}) = \int_{\mathbb{R}^d} (\psi_{i_k}^{q_n+1} - \psi_{i_k}^{q_n}) d\mu_{i_k}. \quad (19)$$

Before proving a multimarginal counterpart to (Ruschendorf, 1995, Lemma 4.1), we state and prove the following result.

Proposition 18. Let π_0, π_1 two probability measures on \mathbb{R}^d such that $\pi_0 \ll \pi_1$. Then, denoting $f = d\pi_0/d\pi_1$, the following assertions are equivalent:

- (a) $\text{KL}(\pi_0 \mid \pi_1) < +\infty$
- (b) $\int_{\mathbb{R}^d} |\log(f)(x)| d\pi_0(x) < +\infty$
- (c) $\int_{\mathbb{R}^d} \log(f)(x) \mathbb{1}_{f(x) > 1} d\pi_0(x) < +\infty$

If one of these conditions is satisfied then $\int_{\mathbb{R}^d} |\log(f)(x)| d\pi_0 \leq \text{KL}(\pi_0 \mid \pi_1) + 2/e$.

Proof. First, note that

$$\int_{\mathbb{R}^d} |\log(f)(x)| \mathbb{1}_{f < 1} d\pi_0(x) \leq \int_{\mathbb{R}^d} |\log(f)(x)f(x)| \mathbb{1}_{f < 1} d\pi_1(x) \leq 1/e, \quad (20)$$

where we have used that for any $u \in [0, 1]$, $|u \log(u)| \leq 1/e$. We have that (b) implies (c). Using the previous result we have that (c) implies (b). Hence (c) and (b) are equivalent. In addition, it is clear that (b) implies (a). Finally (this is more of a convention), we have that $\text{KL}(\pi_0 \mid \pi_1) = \int_{\mathbb{R}^d} \log(f)(x) \mathbb{1}_{f(x) > 1} d\pi_0(x) + \int_{\mathbb{R}^d} \log(f)(x) \mathbb{1}_{f(x) < 1} d\pi_0(x) < +\infty$. Using (20) this implies (c). Finally, we have

$$\begin{aligned} \int_{\mathbb{R}^d} |\log(f)(x)| d\pi_0(x) &= \int_{\mathbb{R}^d} \log(f)(x) d\pi_0(x) - 2 \int_{\mathbb{R}^d} \log(f)(x) \mathbb{1}_{f(x) < 1} d\pi_0(x) \\ &\leq \text{KL}(\pi_0 \mid \pi_1) + 2/e, \end{aligned}$$

which concludes the proof. \square

We begin with the following lemma which controls the integral of the potentials uniformly w.r.t. $n \in \mathbb{N}$. It can be seen as the *multimarginal* counterpart of (Ruschendorf, 1995, Lemma 4.1).

Lemma 19. Assume A4. There exist $\{c_i\}_{i \in S} \in (0, +\infty)^K$ such that for any function $f : (\mathbb{R}^d)^{\ell+1} \rightarrow \mathbb{R}$ of the form $f = \bigoplus_{i \in S} f_i$, we have

$$c_i \|f\|_{L^1(\pi^*)} \geq \|f_i\|_{L^1(\mu_i)}, \quad \forall i \in S. \quad (21)$$

For any $n \in \mathbb{N}^*$, we have

- (a) $\sum_{i \in S} \int_{\mathbb{R}^d} \psi_i^n d\mu_i \leq \text{KL}(\pi^* \mid \bar{\pi}) < \infty$,
- (b) $\int_{(\mathbb{R}^d)^{\ell+1}} (\bigoplus_{i \in S} \psi_i^* - \bigoplus_{i \in S} \psi_i^n) d\pi^* \leq \text{KL}(\pi^* \mid \bar{\pi}) < \infty$,
- (c) $\sup_{n \in \mathbb{N}} \int_{\mathbb{R}^d} |\psi_i^n| d\mu_i < \infty, \quad \forall i \in S$.

Proof. First, we have that (21) is a direct consequence of (Kober, 1940, Theorem 1) and A4. Let us now prove item (a). Using (19), we have

$$\begin{aligned} \sum_{m=0}^{Kn} \text{KL}(\pi^m \mid \pi^{m-1}) &= \sum_{\ell=0}^{n-1} \sum_{k=0}^{K-1} \text{KL}(\pi^{\ell K+k+1} \mid \pi^{\ell K+k}) + \text{KL}(\pi^0 \mid \pi^{-1}) \\ &= \sum_{\ell=0}^{n-1} \sum_{i \in S} \int_{\mathbb{R}^d} (\psi_i^{\ell+1} - \psi_i^\ell) d\mu_i + \int_{\mathbb{R}^d} (\psi_{i_{K-1}}^0 - \psi_{i_{K-1}}^{-1}) d\mu_{i_{K-1}} \\ &= \sum_{i \in S} \sum_{\ell=0}^{n-1} \int_{\mathbb{R}^d} (\psi_i^{\ell+1} - \psi_i^\ell) d\mu_i + \int_{\mathbb{R}^d} (\psi_{i_{K-1}}^0 - \psi_{i_{K-1}}^{-1}) d\mu_{i_{K-1}} \\ &= \sum_{i \in S} \int_{\mathbb{R}^d} (\psi_i^n - \psi_i^0) d\mu_i + \int_{\mathbb{R}^d} (\psi_{i_{K-1}}^0 - \psi_{i_{K-1}}^{-1}) d\mu_{i_{K-1}} \\ &= \sum_{i \in S} \int_{\mathbb{R}^d} \psi_i^n d\mu_i \leq \text{KL}(\pi^* \mid \bar{\pi}). \end{aligned}$$

where the last inequality follows the proof of Proposition 6.

Since the first term in inequality of item (b) is equal to $\text{KL}(\pi^* \mid \pi^{nK})$, we obtain item (b) using that $\text{KL}(\pi^* \mid \pi^{nK}) \leq \text{KL}(\pi^* \mid \bar{\pi})$ following the proof of Proposition 6.

Let us now prove item (c). Since $\text{KL}(\pi^* \mid \bar{\pi}) < \infty$, using Proposition 18, we have that $\bigoplus_{i \in S} \psi_i^* \in L^1(\pi^*)$. From item (b) and Proposition 18, we also get that $\bigoplus_{i \in S} (\psi_i^* - \psi_i^n) \in L^1(\pi^*)$, and thus $\int_{(\mathbb{R}^d)^{\ell+1}} |\bigoplus_{i \in S} (\psi_i^* - \psi_i^n)| d\pi^* \leq C_0$ with $C_0 > 0$. Therefore, we have

$$\int_{(\mathbb{R}^d)^{\ell+1}} |\bigoplus_{i \in S} \psi_i^n| d\pi^* \leq \int_{(\mathbb{R}^d)^{\ell+1}} |\bigoplus_{i \in S} \psi_i^*| d\pi^* + \int_{(\mathbb{R}^d)^{\ell+1}} |\bigoplus_{i \in S} (\psi_i^* - \psi_i^n)| d\pi^* \leq 2C_0.$$

Using (21), we conclude with A4 that for any $i \in S$, we have

$$\int_{\mathbb{R}^d} |\psi_i^n| d\mu_i \leq 2c_i C_0 ,$$

which concludes the proof of item (c). \square

The next lemma gives an explicit expression for $\text{KL}(\pi^n | \bar{\pi})$. It can be seen as the *multimarginal* counterpart of (Ruschendorf, 1995, Lemma 4.2).

Lemma 20. *For any $n \in \mathbb{N}$, with $k = (n - 1) \bmod(K)$, we have*

$$\begin{aligned} \text{KL}(\pi^n | \bar{\pi}) &= \int_{\mathbb{R}^d} \psi_{i_k}^{q_n+1} d\mu_{i_k} + \sum_{\ell=0}^{k-1} \int_{\mathbb{R}^d} \psi_{i_\ell}^{q_n+1} \exp[\psi_{i_\ell}^{q_n+1} - \psi_{i_\ell}^{q_n+2}] d\mu_{i_\ell} \\ &\quad + \sum_{m=k+1}^{K-1} \int_{\mathbb{R}^d} \psi_{i_m}^{q_n} \exp[\psi_{i_m}^{q_n} - \psi_{i_m}^{q_n+1}] d\mu_{i_m} . \end{aligned}$$

Proof. Let $n \in \mathbb{N}$, with $k = (n - 1) \bmod(K)$. Using (17), we have

$$\text{KL}(\pi^n | \bar{\pi}) = \int_{\mathbb{R}^d} \psi_{i_k}^{q_n+1} d\mu_{i_k} + \sum_{\ell=0}^{k-1} \int_{\mathbb{R}^d} \psi_{i_\ell}^{q_n+1} d\pi_{i_\ell}^n + \sum_{m=k+1}^{K-1} \int_{\mathbb{R}^d} \psi_{i_m}^{q_n} d\pi_{i_m}^n . \quad (22)$$

Consider $m \in \{k+1, \dots, K-1\}$. Let m_n be the closest integer to n such that $m_n > n$ and $m = (m_n - 1) \bmod(K)$. By (18), we have

$$d\pi^n = \exp[\bigoplus_{j=k+1}^m \psi_{i_j}^{q_n} - \psi_{i_j}^{q_n+1}] d\pi^{m_n} .$$

Using (18) recursively, we obtain

$$d\pi_{i_m}^n = \exp[\psi_{i_m}^{q_n} - \psi_{i_m}^{q_n+1}] d\pi_{i_m}^{m_n} , \quad (23)$$

where we recall that $\pi_{i_m}^{m_n} = \mu_{i_m}$.

Consider now $\ell \in \{0, \dots, k-1\}$. Let ℓ_n be the closest integer to n such that $\ell_n > n$ and $\ell = (\ell_n - 1) \bmod(K)$. By (18), we have

$$d\pi^n = \exp[\bigoplus_{j=k+1}^{K-1} \{\psi_{i_j}^{q_n} - \psi_{i_j}^{q_n+1}\} \bigoplus_{j'=0}^{\ell} \{\psi_{i_{j'}}^{q_n+1} - \psi_{i_{j'}}^{q_n+2}\}] d\pi^{\ell_n} ,$$

and using (18) recursively, we obtain

$$d\pi_{i_\ell}^n = \exp[\psi_{i_\ell}^{q_n+1} - \psi_{i_\ell}^{q_n+2}] d\pi_{i_\ell}^{\ell_n} , \quad (24)$$

where we recall that $\pi_{i_\ell}^{\ell_n} = \mu_{i_\ell}$. We conclude the proof upon combining (22), (23) and (24). \square

We are now ready to prove a *uniform integrability* result which is the multimarginal counterpart of (Ruschendorf, 1995, Lemma 4.4). Before stating Lemma 22, we prove the following well-known lemma. We recall that a sequence $(\Psi_n)_{n \in \mathbb{N}}$ such that for any $n \in \mathbb{N}$, $\Psi_n \in L^1(\mu)$, is *uniformly integrable* w.r.t. μ if (i) $\sup_{n \in \mathbb{N}} \int_{\mathbb{R}^d} |\Psi_n| d\mu < +\infty$ (ii) for any $\varepsilon > 0$, there exists $K > 0$ such that for any $n \in \mathbb{N}$, $\int_{\overline{B}(0,K)^c} |\Psi_n| d\mu \leq \varepsilon$.

Lemma 21. *Let $f : \mathbb{R} \rightarrow \mathbb{R}$, convex and non-decreasing on $[A, +\infty)$ with $A > 0$ and $\lim_{x \rightarrow +\infty} f(x)/x = +\infty$. Assume that $\sup_{n \in \mathbb{N}} \int_{\mathbb{R}^d} f(|\Psi_n|) d\mu < +\infty$. Then, $(\Psi_n)_{n \in \mathbb{N}}$ is uniformly integrable w.r.t. μ .*

Proof. Since f is convex, using Jensen's inequality, we get that $\sup_{n \in \mathbb{N}} f(\int_{\mathbb{R}^d} |\Psi_n| d\mu) < +\infty$ and since $\lim_{x \rightarrow +\infty} f(x)/x = +\infty$ we have $\sup_{n \in \mathbb{N}} \int_{\mathbb{R}^d} |\Psi_n| d\mu < +\infty$. Let $\varepsilon > 0$, there exists $K > 0$ such that for any $x > K$, $x \leq \varepsilon f(x)/B$ with $B = \sup_{n \in \mathbb{N}} \int_{\mathbb{R}^d} f(|\Psi_n|) d\mu < +\infty$. Therefore, we have for any $n \in \mathbb{N}$

$$\int_{\overline{B}(0,K)^c} |\Psi_n| d\mu \leq (\varepsilon/B) \int_{\overline{B}(0,K)^c} f(|\Psi_n|) d\mu \leq \varepsilon ,$$

which concludes the proof. \square

Lemma 22. *Assume A4 and A5. Then, $\{\exp[\bigoplus_{i \in S} \psi_i^n]\}_{n \in \mathbb{N}}$ is uniformly integrable w.r.t. $\bar{\pi}$.*

Proof. It is enough to show that the sequence $\{f(\exp[\bigoplus_{i \in S} \psi_i^n])\}_{n \in \mathbb{N}}$ is bounded in $L^1(\bar{\pi})$, where $f : u \mapsto u \log(u)$ is continuous, convex and such that $\lim_{u \rightarrow \infty} f(u)/u = +\infty$, see Lemma 21. Let $n \in \mathbb{N}$. We have

$$\begin{aligned}
\int_{(\mathbb{R}^d)^{\ell+1}} f(\exp[\bigoplus_{i \in S} \psi_i^n]) d\bar{\pi} &= \text{KL}(\pi^{nK} \mid \bar{\pi}) \\
&= \int_{\mathbb{R}^d} \psi_{i_{K-1}}^n d\mu_{i_{K-1}} + \sum_{k=0}^{K-2} \int_{\mathbb{R}^d} \psi_{i_k}^n \exp[\psi_{i_k}^n - \psi_{i_k}^{n+1}] d\mu_{i_k} \quad (\text{Lemma 20}) \\
&= \sum_{k=0}^{K-1} \int_{\mathbb{R}^d} \psi_{i_k}^n d\mu_{i_k} + \sum_{k=0}^{K-2} \int_{\mathbb{R}^d} \psi_{i_k}^n \{\exp[\psi_{i_k}^n - \psi_{i_k}^{n+1}] - 1\} d\mu_{i_k} \\
&\leq \text{KL}(\pi^* \mid \bar{\pi}) + (\bar{c} + 1) \sum_{k=0}^{K-2} \int_{\mathbb{R}^d} \psi_{i_k}^n d\mu_{i_k} \quad (\text{Lemma 19-(a), A5}) \\
&\leq \text{KL}(\pi^* \mid \bar{\pi}) + (\bar{c} + 1) \sum_{k=0}^{K-2} \sup_{n \in \mathbb{N}} \int_{\mathbb{R}^d} |\psi_{i_k}^n| d\mu_{i_k} < \infty. \quad (\text{Lemma 19-(c)})
\end{aligned}$$

□

With the preliminary results stated above, we are now ready to prove Proposition 7.

Proof of Proposition 7. Using A4 and A5, we have, by Lemma 22, uniform integrability of $\{\exp[\bigoplus_{i \in S} \psi_i^n]\}_{n \in \mathbb{N}}$ in $L^1(\bar{\pi})$. Therefore, the sequence $\{\pi^{nK}\}_{n \in \mathbb{N}}$ is relatively compact with respect to the weak topology of $\sigma(L^1(\bar{\pi}), L^\infty(\bar{\pi}))$, denoted as the τ -topology. We recall that $\lim_{n \rightarrow \infty} \text{KL}(\pi^{nK+1} \mid \pi^{nK}) = 0$. This implies that $\{\pi^{nK+1}\}_{n \in \mathbb{N}}$ is also relatively τ -compact. By trivial recursion, we obtain that the sequences $\{\pi^{nK+k}\}_{n \in \mathbb{N}}$, where $k \in \{2, \dots, K-1\}$ are also relatively τ -compact. Therefore, $\{\pi^n\}_{n \in \mathbb{N}}$ is relatively τ -compact and τ -sequentially compact.

We consider an increasing function $\Phi : \mathbb{N} \rightarrow \mathbb{N}$ such that $\{\pi^m\}_{m \in \Phi(\mathbb{N})}$ is a τ -convergent subsequence, and we denote by $\tilde{\pi}$ its limit for this topology. In particular, $\tilde{\pi} \in \mathcal{P}_S$ by Proposition 6. We assume without loss of generality that $\Phi(\mathbb{N}) \subset K\mathbb{N}$.

Using the lower semi-continuity of the Kullback-Leibler divergence (Dupuis & Ellis, 2011, Lemma 1.4.3), we get

$$\text{KL}(\tilde{\pi} \mid \bar{\pi}) \leq \liminf \text{KL}(\pi^m \mid \bar{\pi}) \leq \limsup \text{KL}(\pi^m \mid \bar{\pi}).$$

Consider $k \in \{0, \dots, K-2\}$. By (18), we have

$$\frac{d\mu_{i_k}}{d\pi_{i_k}^{nK+k}} = \frac{d\pi_{i_k}^{nK+k+1}}{d\pi_{i_k}^{nK+k}} = \frac{d\pi^{nK+k+1}}{d\pi^{nK+k}} = \exp[\psi_{i_k}^{n+1} - \psi_{i_k}^n],$$

and thus,

$$\|\mu_{i_k} - \pi_{i_k}^{nK+k}\|_{\text{TV}} = (1/2) \int_{\mathbb{R}^d} |d\pi_{i_k}^{nK+k}/d\mu_{i_k} - 1| d\mu_{i_k} = (1/2) \int_{\mathbb{R}^d} |\exp[\psi_{i_k}^n - \psi_{i_k}^{n+1}] - 1| d\mu_{i_k}.$$

With Proposition 6, we obtain that $\{\exp[\psi_{i_k}^n - \psi_{i_k}^{n+1}]\}_{n \in \mathbb{N}}$ converges to 1 in $L^1(\mu_{i_k})$. In addition using the uniform integrability of $\{\psi_{i_k}^n\}_{n \in \mathbb{N}}$ and A5, we get

$$\limsup_{n \rightarrow +\infty} \int_{\mathbb{R}^d} \psi_{i_k}^n \exp[\psi_{i_k}^n - \psi_{i_k}^{n+1}] d\mu_{i_k} = \limsup_{n \rightarrow +\infty} \int_{\mathbb{R}^d} \psi_{i_k}^n d\mu_{i_k}.$$

We denote $m = K\ell$. Since $\text{KL}(\pi^m \mid \bar{\pi}) = \int_{\mathbb{R}^d} \psi_{i_{K-1}}^\ell d\mu_{i_{K-1}} + \sum_{k=0}^{K-2} \int_{\mathbb{R}^d} \psi_{i_k}^\ell \exp[\psi_{i_k}^\ell - \psi_{i_k}^{\ell+1}] d\mu_{i_k}$ by Lemma 20, we finally have

$$\text{KL}(\tilde{\pi} \mid \bar{\pi}) \leq \limsup \left\{ \sum_{k=0}^{K-1} \int_{\mathbb{R}^d} \psi_{i_k}^\ell d\mu_{i_k} \right\} \leq \text{KL}(\pi^* \mid \bar{\pi})$$

where the last inequality comes from Lemma 19.

Since $\tilde{\pi}_i = \mu_i$ for any $i \in S$, using Proposition 6, we have $\tilde{\pi} = \pi^*$ by uniqueness of π^* . Hence, π^* is the only limit point of $\{\pi^n\}_{n \in \mathbb{N}}$ in the τ -topology. In particular, $\text{KL}(\pi^n \mid \bar{\pi}) \rightarrow \text{KL}(\pi^* \mid \bar{\pi})$. Since \mathcal{P}_S is convex, this last result implies $\|\pi^* - \pi^n\|_{\text{TV}} \rightarrow 0$, see the proof of Theorem 2.1 in Csiszár (1975). □

We finish this section by highlighting that A5 is stronger than (Ruschendorf, 1995, B1). A natural extension of the latter assumption would consist of having a guarantee on the $(K-1)$ first potentials given by (16), as presented below.

A6. *There exist $0 < \underline{c} \leq \bar{c}$ such that for any $k \in \{0, \dots, K-2\}$, we have $\underline{c} \leq \exp(-\psi_{i_k}^1) \leq \bar{c}$.*

However, the adaptation of (Ruschendorf, 1995, Lemma 4.3) under **A6** only yield non-vacuous bounds in the case $K = 2$, as we show below.

Lemma 23. Assume **A6**. Then, for any $n \in \mathbb{N}^*$

(a) for any $k \in \{0, \dots, K-2\}$, there exists $\alpha_{n,k} \in \mathbb{N}$ such that

$$\underline{c} \cdot (\underline{c}/\bar{c})^{\alpha_{n,k}(K-2)} \leq \exp[\psi_{i_k}^{n-1} - \psi_{i_k}^n] \leq \bar{c} \cdot (\bar{c}/\underline{c})^{\alpha_{n,k}(K-2)}$$

(b) there exists $\alpha_{n,K-1} \in \mathbb{N}$ such that

$$1/\bar{c}^{K-1} \cdot (\underline{c}/\bar{c})^{\alpha_{n,K-1}(K-2)} \leq \exp[\psi_{i_{K-1}}^{n-1} - \psi_{i_{K-1}}^n] \leq 1/\underline{c}^{K-1} \cdot (\bar{c}/\underline{c})^{\alpha_{n,K-1}(K-2)}$$

where $\{\alpha_{n,k}\}_{n \in \mathbb{N}^*, k \in \{0, \dots, K-1\}}$ is a strictly increasing sequence that can be explicitly defined.

Proof. We prove the result by recursion on $n \in \mathbb{N}^*$.

Take $n = 1$. Let $k \in \{0, \dots, K-2\}$. We define $\alpha_{1,k} = 0$ and directly obtain (a) by **A5** since $\psi_{i_k}^0 = 0$. Let us prove item (b). We have by (16)

$$\begin{aligned} \exp[\psi_{i_{K-1}}^0 - \psi_{i_{K-1}}^1] &= \frac{\int_{(\mathbb{R}^d)^\ell} \exp[\bigoplus_{k=0}^{K-2} \psi_{i_k}^1] h d\nu_{-i_{K-1}}}{\int_{(\mathbb{R}^d)^\ell} \exp[\bigoplus_{k=0}^{K-2} \psi_{i_k}^0] h d\nu_{-i_{K-1}}} \\ &= \frac{\int_{(\mathbb{R}^d)^\ell} \exp[\bigoplus_{k=0}^{K-2} \{\psi_{i_k}^1 - \psi_{i_k}^0\} + \bigoplus_{k=0}^{K-2} \psi_{i_k}^0] h d\nu_{-i_{K-1}}}{\int_{(\mathbb{R}^d)^\ell} \exp[\bigoplus_{k=0}^{K-2} \psi_{i_k}^0] h d\nu_{-i_{K-1}}}. \end{aligned}$$

Using item (a) at rank $n = 1$, we have

$$1/\bar{c}^{K-1} \leq \exp[\bigoplus_{k=0}^{K-2} \{\psi_{i_k}^1 - \psi_{i_k}^0\}] \leq 1/\underline{c}^{K-1},$$

and therefore, we obtain item (b) by taking $\alpha_{1,K-1} = 0$. Let us assume that the result is verified for some $n \in \mathbb{N}^*$. We have

$$\begin{aligned} \exp[\psi_{i_0}^n - \psi_{i_0}^{n+1}] &= \frac{\int \exp[\bigoplus_{k=1}^{K-1} \psi_{i_k}^n] h d\nu_{-i_0}}{\int \exp[\bigoplus_{k=1}^{K-1} \psi_{i_k}^{n-1}] h d\nu_{-i_0}} \\ &= \frac{\int \exp[\bigoplus_{k=1}^{K-2} \{\psi_{i_k}^n - \psi_{i_k}^{n-1}\} \oplus \{\psi_{i_{K-1}}^n - \psi_{i_{K-1}}^{n-1}\} + \bigoplus_{k=1}^{K-1} \psi_{i_k}^{n-1}] h d\nu_{-i_0}}{\int \exp[\bigoplus_{k=1}^{K-1} \psi_{i_k}^{n-1}] h d\nu_{-i_0}} \end{aligned}$$

Using item (a) and item (b) at rank n , we have

$$\begin{aligned} 1/\bar{c}^{K-2} \cdot (\underline{c}/\bar{c})^{(K-2) \sum_{k=1}^{K-2} \alpha_{n,k}} &\leq \exp[\bigoplus_{k=1}^{K-2} \{\psi_{i_k}^n - \psi_{i_k}^{n-1}\}] \\ &\leq 1/\underline{c}^{K-2} \cdot (\bar{c}/\underline{c})^{(K-2) \sum_{k=1}^{K-2} \alpha_{n,k}}, \\ \underline{c}^{K-1} \cdot (\underline{c}/\bar{c})^{\alpha_{n,K-1}(K-2)} &\leq \exp[\psi_{i_{K-1}}^n - \psi_{i_{K-1}}^{n-1}] \leq \bar{c}^{K-1} \cdot (\bar{c}/\underline{c})^{\alpha_{n,K-1}(K-2)}. \end{aligned}$$

Therefore, we obtain

$$\begin{aligned} \underline{c} \cdot (\underline{c}/\bar{c})^{(K-2) \sum_{k=1}^{K-1} \alpha_{n,k}} &\leq \exp[\bigoplus_{k=1}^{K-2} \{\psi_{i_k}^n - \psi_{i_k}^{n-1}\} \oplus \{\psi_{i_{K-1}}^n - \psi_{i_{K-1}}^{n-1}\}] \\ &\leq \bar{c} \cdot (\bar{c}/\underline{c})^{(K-2) \sum_{k=1}^{K-1} \alpha_{n,k}}, \\ \underline{c} \cdot (\underline{c}/\bar{c})^{(K-2) \sum_{k=1}^{K-1} \alpha_{n,k}} &\leq \exp[\psi_{i_0}^n - \psi_{i_0}^{n+1}] \leq \bar{c} \cdot (\bar{c}/\underline{c})^{(K-2) \sum_{k=1}^{K-1} \alpha_{n,k}}. \end{aligned}$$

Now, we define $\alpha_{n+1,0} = \sum_{k=1}^{K-1} \alpha_{n,k}$ to obtain item (a) for $k = 0$. Consider now $k \in \{1, \dots, K-2\}$. Following the same steps as above, we recursively define

$$\alpha_{n+1,k} = \sum_{j=0}^{k-1} \alpha_{n+1,j} + \sum_{j'=k+1}^{K-1} \alpha_{n,j'},$$

which gives item (a) at rank $n+1$. Let us now prove item (b) at rank $n+1$. We have

$$\begin{aligned} \exp[\psi_{i_{K-1}}^n - \psi_{i_{K-1}}^{n+1}] &= \frac{\int \exp[\bigoplus_{k=0}^{K-2} \psi_{i_k}^{n+1}] h d\nu_{-i_{K-1}}}{\int \exp[\bigoplus_{k=0}^{K-2} \psi_{i_k}^n] h d\nu_{-i_{K-1}}} \\ &= \frac{\int \exp[\bigoplus_{k=0}^{K-2} \{\psi_{i_k}^{n+1} - \psi_{i_k}^n\} + \bigoplus_{k=0}^{K-2} \psi_{i_k}^n] h d\nu_{-i_{K-1}}}{\int \exp[\bigoplus_{k=0}^{K-2} \psi_{i_k}^n] h d\nu_{-i_{K-1}}}. \end{aligned}$$

Using item (a) at rank $n+1$, we obtain

$$\begin{aligned} 1/\bar{c}^{K-1} \cdot (\underline{c}/\bar{c})^{(K-2) \sum_{k=0}^{K-2} \alpha_{n+1,k}} &\leq \exp[\bigoplus_{k=0}^{K-2} \{\psi_{i_k}^{n+1} - \psi_{i_k}^n\}] \\ &\leq 1/\underline{c}^{K-1} \cdot (\bar{c}/\underline{c})^{(K-2) \sum_{k=0}^{K-2} \alpha_{n+1,k}}. \end{aligned}$$

Therefore, by taking $\alpha_{n+1,K-1} = \sum_{k=0}^{K-2} \alpha_{n+1,k}$, we obtain item (b), which concludes the proof. \square

D.3 Proof of Section 5

For the rest of this section, we consider the multi-marginal Schrödinger bridge problem given by (TreeSB) and establish in Proposition 25 the correspondence with the regularized Wasserstein propagation problem presented in Solomon et al. (2014, 2015). We first state a technical result.

Lemma 24. *Let $\varepsilon > 0$. Assume that π^0 is given by (2), where $r \in \mathcal{V}$ is chosen arbitrarily. Then, for any $\pi \in \mathcal{P}_{T_r}$, we have*

$$\begin{aligned} \varepsilon \text{KL}(\pi \mid \pi^0) &= \sum_{(v,v') \in E_r} \{w_{v,v'} \mathbb{E}_{\pi_{v,v'}} [\|X_v - X_{v'}\|^2] - \varepsilon H(\pi_{v,v'})\} \\ &\quad + \varepsilon \sum_{v \in \mathcal{V}} \text{card}(C_v) H(\pi_v) + \varepsilon \text{KL}(\pi_r \mid \pi_r^0), \end{aligned}$$

where we recall that $C_v = \{v' \in \mathcal{V} : (v, v') \in E_r\}$.

Proof. Since $\pi, \pi^0 \in \mathcal{P}_{T_r}$, we obtain the following decomposition

$$\begin{aligned} \text{KL}(\pi \mid \pi^0) &= \text{KL}(\pi_r \prod_{(v,v') \in E_r} \pi_{v'|v} \mid \pi_r^0 \prod_{(v,v') \in E_r} \pi_{v'|v}^0) \\ &= \text{KL}(\pi_r \mid \pi_r^0) + \sum_{(v,v') \in E_r} \int_{\mathbb{R}^d} \text{KL}(\pi_{v'|v}(\cdot \mid x_v) \mid \pi_{v'|v}^0(\cdot \mid x_v)) d\pi_v(x_v) \\ &= \text{KL}(\pi_r \mid \pi_r^0) - \sum_{(v,v') \in E_r} \int_{\mathbb{R}^d \times \mathbb{R}^d} \log \pi_{v'|v}^0 d\pi_{v,v'} - \sum_{(v,v') \in E_r} \int_{\mathbb{R}^d} H(\pi_{v'|v}(\cdot \mid x_v)) d\pi_v(x_v). \end{aligned}$$

We finally obtain the result by using the definition of π^0 and noticing that $\int_{\mathbb{R}^d} H(\pi_{v'|v}(\cdot \mid x_v)) d\pi_v(x_v) = H(\pi_{v,v'}) - H(\pi_v)$ for any $(v, v') \in E_r$. \square

Proposition 25. *Let $\varepsilon > 0$ and $\mu_0 \in \mathcal{P}$ such that $\mu_0 \ll \text{Leb}$. Assume that π^0 is given by (2), where $r \in \mathcal{V}$ is chosen arbitrarily, and that $\varphi_r = d\mu_0/d\text{Leb}$. Also assume A2. Then, the set of marginals of the solution to (TreeSB) is exactly the solution to the entropic-regularized Wasserstein Propagation problem (Solomon et al., 2014, 2015) defined by*

$$\begin{aligned} \arg \min \{ \sum_{(v,v') \in E_r} w_{v,v'} W_{2,\varepsilon/w_{v,v'}}^2(\nu_v, \nu_{v'}) + \varepsilon \sum_{v \in \mathcal{V}} \text{card}(C_v) H(\nu_v) + \varepsilon \text{KL}(\nu_r \mid \mu_0) : (\text{WP}) \\ \{\nu_v\}_{v \in \mathcal{V}} \in \mathcal{P}^{\ell+1}, \nu_i = \mu_i, \forall i \in \mathcal{S} \}, \end{aligned}$$

where we recall that $C_v = \{v' \in \mathcal{V} : (v, v') \in E_r\}$.

Proof. Assume that π^0 is given by (2), where $r \in \mathcal{V}$ is chosen arbitrarily, and that $\varphi_r = d\mu_0/d\text{Leb}$. In particular, we have $\pi_r^0 = \mu_0$. Moreover, it is clear that π^0 verifies A1, and A3 by Proposition 17.

Let $\{\nu_v\}_{v \in \mathcal{V}} \in \mathcal{P}^{\ell+1}$ and $\{\nu^{(v,v')}\}_{(v,v') \in E_r} \in (\mathcal{P}^{(2)})^{|E_r|}$. We define

$$\begin{aligned} F(\{\nu_v\}) &= \sum_{(v,v') \in E_r} w_{v,v'} W_{2,\varepsilon/w_{v,v'}}^2(\nu_v, \nu_{v'}) + \varepsilon \sum_{v \in \mathcal{V}} \text{card}(C_v) H(\nu_v) + \varepsilon \text{KL}(\nu_r \mid \mu_0), \\ G(\nu_r, \{\nu^{(v,v')}\}) &= \sum_{(v,v') \in E_r} \{w_{v,v'} \mathbb{E}_{\nu^{(v,v')}} [\|X_v - X_{v'}\|^2] - \varepsilon H(\nu^{(v,v')})\} \\ &\quad + \varepsilon \sum_{(v,v') \in E_r} H(\nu_v^{(v,v')}) + \varepsilon \text{KL}(\nu_r \mid \mu_0). \end{aligned}$$

By definition of the regularized Wasserstein distance given in (3), we have for any $\{\nu_v\}_{v \in \mathcal{V}} \in \mathcal{P}^{\ell+1}$

$$F(\{\nu_v\}) = \min \{ G(\nu_r, \{\nu^{(v,v')}\}) : \nu^{(v,v')} \in \mathcal{P}^{(2)}, \nu_v^{(v,v')} = \nu_v, \nu_{v'}^{(v,v')} = \nu_{v'}, \forall (v, v') \in E_r \}. \quad (25)$$

In particular, we have $F(\{\pi_v\}) \leq G(\pi_r, \{\pi_{v,v'}\})$ for any $\pi \in \mathcal{P}^{(\ell+1)}$. We now prove the result of Proposition 25 in two steps denoted by Step 1 and Step 2.

Step 1. Let us not assume A2 for now. In this case, we prove in Step 1.a and Step 1.b that solving (WP) is equivalent to solving a modified version of (TreeSB) given by

$$\pi^* = \arg \min \{ \text{KL}(\pi \mid \pi^0) : \pi \in \mathcal{P}_{T_r}, \pi_i = \mu_i, \forall i \in \mathcal{S} \}. \quad (T_r\text{-TreeSB})$$

Remark that any solution to (T_r-TreeSB) is a solution to (TreeSB), but the converse result may not be true.

Step 1.a: (WP) \implies (\mathbf{T}_r -TreeSB). Consider a solution $\{\nu_v^*\}_{v \in V}$ to (WP). For any $(v, v') \in E_r$, $W_{2,\varepsilon/w_{v,v'}}^2(\nu_v^*, \nu_{v'}^*)$ is well defined and thus, there exists $\nu^{(v,v')} \in \Pi(\nu_v^*, \nu_{v'}^*)$ such that

$$\nu^{(v,v')} \in \operatorname{argmin}\{\mathbb{E}_\pi[\|X_v - X_{v'}\|^2] - (\varepsilon/w_{v,v'})H(\pi) : \pi \in \Pi(\nu_v^*, \nu_{v'}^*)\}. \quad (26)$$

Using the gluing lemma, we build the probability measure $\pi^* = \nu_r^* \prod_{(v,v') \in E_r} \nu_{v'|v}^{(v,v')}$ such that (i) $\pi^* \in \mathcal{P}_{T_r}$, and (ii) $\pi_{v,v'}^*$ and $\nu^{(v,v')}$ have the same distribution for any $(v, v') \in E_r$. In particular, we have $\pi_i^* = \mu_i$ for any $i \in S$.

Let us show now that π^* is a solution to (\mathbf{T}_r -TreeSB). Let $\pi \in \mathcal{P}_{T_r}$ such that $\pi_i = \mu_i$ for any $i \in S$. We have

$$\begin{aligned} \epsilon \text{KL}(\pi \mid \pi^0) &= G(\pi_r, \{\pi_{v,v'}\}) && \text{(Lemma 24)} \\ &\geq F(\{\pi_v\}) \\ &\geq F(\{\nu_v^*\}) && \text{(definition of } \nu^*) \\ &= G(\nu_r^*, \{\nu^{(v,v')}\}) && \text{(see (26))} \\ &= G(\pi_r^*, \{\pi_{v,v'}^*\}) && \text{(definition of } \pi^*) \\ &= \epsilon \text{KL}(\pi^* \mid \pi^0). && \text{(Lemma 24)} \end{aligned}$$

Therefore, π^* is a solution to (\mathbf{T}_r -TreeSB).

Step 1.b: (\mathbf{T}_r -TreeSB) \implies (WP). Consider now a solution π^* to (\mathbf{T}_r -TreeSB). Since $\pi^* \in \mathcal{P}_{T_r}$, we have $\pi^* = \pi_r^* \prod_{(v,v') \in E_r} \pi_{v'|v}^*$ and $\pi_i^* = \mu_i$ for any $i \in S$.

Let us show that $\{\pi_v^*\}_{v \in V}$ is a solution to (WP). Let $\{\nu_v\}_{v \in V} \in \mathcal{P}^{\ell+1}$ such that $\nu_i = \mu_i$ for any $i \in S$.

Let $\{\nu^{(v,v')}\}_{(v,v') \in E_r}$ be a family of probability measures such that $\nu^{(v,v')} \in \mathcal{P}^{(2)}$, $\nu_v^{(v,v')} = \nu_v$, $\nu_{v'}^{(v,v')} = \nu_{v'}$ for any $(v, v') \in E_r$.

Using the gluing lemma, we build the probability measure $\pi = \nu_r \prod_{(v,v') \in E_r} \nu_{v'|v}^{(v,v')}$, such that (i) $\pi \in \mathcal{P}_{T_r}$ and (ii) $\pi_{v,v'}$ and $\nu^{(v,v')}$ have the same distribution for any $(v, v') \in E_r$. We have

$$\begin{aligned} \varepsilon \text{KL}(\pi \mid \pi^0) &= G(\pi_r, \{\pi_{v,v'}\}) && \text{(Lemma 24)} \\ &= G(\nu_r, \{\nu^{(v,v')}\}) && \text{(definition of } \pi) \\ &\geq \varepsilon \text{KL}(\pi^* \mid \pi^0) && \text{(definition of } \pi^*) \\ &= G(\pi_r^*, \{\pi_{v,v'}^*\}) . && \text{(Lemma 24)} \end{aligned}$$

By taking the infimum in the previous inequality over the families $\{\nu^{(v,v')}\}_{(v,v') \in E_r}$, we obtain by (25) that

$$F(\{\nu_v\}) \geq G(\pi_r^*, \{\pi_{v,v'}^*\}) \geq F(\{\pi_v^*\}),$$

and therefore, $\{\pi_v^*\}_{v \in V}$ is a solution to (WP).

Step 2. We now assume A2. By Proposition 4, there exists a unique solution $\pi^* \in \mathcal{P}^{(\ell+1)}$ to (TreeSB) such that we π^0 -a.s. have $(d\pi^*/d\pi^0) = \exp[\bigoplus_{i \in S} \psi_i^*]$, where $\{\psi_i^*\}_{i \in S}$ are measurable potentials with $\psi^* : \mathbb{R}^d \rightarrow \mathbb{R}$. Since $\pi^0 \in \mathcal{P}_{T_r}$, we also have $\pi^* \in \mathcal{P}_{T_r}$, i.e., the potentials $\{\psi_i^*\}_{i \in S}$ do not modify the Markovian nature of π^0 . Therefore, π^* is also the unique solution to (\mathbf{T}_r -TreeSB). Using the equivalence between (\mathbf{T}_r -TreeSB) and (WP) established in Step 1, we finally obtain the result of Proposition 25. \square

Finally, Proposition 8 is a particular case of Proposition 25, when T is a star-shaped tree, and r is chosen as the central vertex of this tree.

D.4 Comparison with Haasler et al. (2021)

In their work, Haasler et al. (2021) study the *discrete-state* counterpart of our approach. Given a state space X such that $|X| = n + 1$ with $n \in \mathbb{N}$, they establish a correspondence between multi-marginal EOT with a general tree-based cost and discrete-time multi-marginal Schrödinger bridge, and provide an efficient method to solve these problems. In this section, we provide details on their framework and give a precise comparison between our theory and their results.

To be coherent with the setting of Haasler et al. (2021), we adapt here some of our notation. Let us define $Z^{(q)} = \mathbb{R}_+^{(n+1)^q}$. For any $q \in \mathbb{N}^*$, the set of probability measures on X^q is defined as $\mathcal{P}^{(q)} = \{M \in Z^{(q)} : \langle M, \mathbf{1} \rangle = 1\}$. We denote $\mathcal{P} = \mathcal{P}^{(1)}$. For any tensors $M, P \in Z^{(q)}$, the Kullback-Leibler divergence between M and P is defined as $\text{KL}(M \mid P) = \langle M \log(M/P) - M + P, \mathbf{1} \rangle$ and the entropy of M is defined as $H(M) = -\text{KL}(M \mid \mathbf{1})$, where the operations are meant componentwise. In the rest of the section, we consider an undirected tree $T = (V, E)$ with $|V| = \ell + 1$ such that V may be identified with $\{0, \dots, \ell\}$.

Details on the results of Haasler et al. (2021). In their paper, the authors consider a cost tensor $C \in Z^{(\ell+1)}$ that factorizes along T , i.e., for any $\{j_0, \dots, j_\ell\}$ with for any $i \in \{0, \dots, \ell\}$, $j_i \in \{0, \dots, n\}$, we have

$$C_{j_0, \dots, j_\ell} = \sum_{(v, v') \in E} C_{j_v, j_{v'}}^{\{v, v'\}},$$

where $C^{\{v, v'\}} \in Z^{(2)}$ is a cost matrix for transportation between the marginals at vertices v and v' , see (Haasler et al., 2021, Eq. (3.1)). In particular, this cost can be seen as the discrete counterpart of the tree-based cost introduced in (1) in the quadratic setting.

Given a subset $S \subset V$ with $|S| = K$ and a set of marginals $\{\mu_i\}_{i \in S} \in \mathcal{P}^K$, Haasler et al. (2021) study the EOT problem associated to T , see (Haasler et al., 2021, Eq. (2.4)), which is given by

$$\text{argmin}\{\langle C, M \rangle - \varepsilon H(M) : M \in \mathcal{P}^{(\ell+1)}, \text{proj}_i(M) = \mu_i, \forall i \in S\}. \quad (\text{discrete-EOT})$$

This problem may be solved with Sinkhorn algorithm (Cuturi, 2013; Knight, 2008; Sinkhorn & Knopp, 1967), for which the authors provide an efficient implementation adapted to the tree-based setting, see (Haasler et al., 2021, Algorithm 3.1). Moreover, they state the convergence of their method in (Haasler et al., 2021, Theorem 3.5), as a direct consequence of the results presented in Luo & Tseng (1992).

In (Haasler et al., 2021, Section 4.2), it is assumed that S corresponds to the set of the leaves of T , as we do, and it is shown an equivalence between (discrete-EOT) and the discrete-state SB problem stated in (Haasler et al., 2021, Eq 4.2), which is given by

$$\begin{aligned} & \text{argmin}\{\sum_{(v, v') \in E_r} \text{KL}(M^{(v, v')} \mid \text{diag}(\nu_v) A^{(v, v')}) : \\ & M^{(v, v')} \in \mathcal{P}^{(2)}, \{\nu_v\}_{v \in V} \in \mathcal{P}^{\ell+1}, M^{(v, v')} \mathbf{1} = \nu_v, M^{(v, v')}^\top \mathbf{1} = \nu_{v'}, \nu_i = \mu_i, \forall i \in S\}, \end{aligned} \quad (\text{discrete-TreeSB})$$

where $T_r = (V, E_r)$ is the directed version of T rooted in an arbitrary vertex $r \in S$, and $A^{(v, v')} = \exp(-C^{(v, v')}/\varepsilon) \in Z^{(2)}$ for any $(v, v') \in E_r$. Remark that $A^{(v, v')}$ may not necessarily be a transition probability matrix.

Finally, Haasler et al. (2021) provide two main numerical experiments. In (Haasler et al., 2021, Section 5.2), they consider a tree with 15 vertices, 14 edges and 8 leaves, combined to the state-space $X = \{0, 1\}^{50 \times 50}$, and solve the corresponding (discrete-EOT) problem for the quadratic cost. In (Haasler et al., 2021, Section 6), they apply their methodology to estimate ensemble flows on a hidden Markov chain. Given $\tau \in \mathbb{N}^*$, they consider a tree T with τ internal vertices (modeling the distribution of N agents at time $t \in \{1, \dots, \tau\}$), that are linearly linked, and such that each of these vertices is independently linked to S leaves of T (modeling observations at time $t \in \{1, \dots, \tau\}$). In this setting, the state space is given by $X = \{1, \dots, 100\}^N$. They solve the formulation (discrete-TreeSB) where the reference measure is chosen as a random walk.

Comparison with our results. We now establish remarks on the main differences between our methodology and the work of Haasler et al. (2021).

First of all, the continuous state-space counterpart of (**discrete-TreeSB**) is given by

$$\operatorname{argmin}\{\mathrm{KL}(\pi \mid \pi^0) : \pi \in \mathcal{P}_{T_r}, \pi_i = \mu_i, \forall i \in S\}, \quad (27)$$

where π^0 is a reference measure which factorizes along T_r . In this case, $\pi_{v,v'}$, π_v and $\pi_{v'|v}^0$ in (27) respectively correspond to the continuous version of $M^{(v,v')}$, ν_v and $A^{(v,v')}$ in (**discrete-TreeSB**). In contrast, our formulation of the multi-marginal Tree Schrödinger Bridge problem given in (**TreeSB**) is a minimization problem over all probability measures $\pi \in \mathcal{P}^{(\ell+1)}$, and is not restricted to the distributions that admit a Markovian factorization along T as in (27). Hence, our framework may be considered more general. Remark that under **A1**, **A2** and **A3**, Proposition 4 states that (**TreeSB**) admits a unique solution $\pi^* \ll \pi^0$ such that $(d\pi^*/d\pi^0)$ can be written with potentials. Then, $\pi^* \in \mathcal{P}_{T_r}$ since $\pi^0 \in \mathcal{P}_{T_r}$, and (**TreeSB**) is then equivalent to (27).

Furthermore, (**EmOT**) is more general than the continuous version of (**discrete-EOT**), which we can recover by taking any measure ν of the form $(d\nu/d\mathrm{Leb}) = \exp[\bigoplus_{i \in S} \varphi_i]$ in (**EmOT**), where $\{\varphi_i\}_{i \in S}$ is a family of potentials such that $|\int_{\mathbb{R}^d} \varphi_i d\mu_i| < \infty$ for any $i \in S$. As a consequence, our setting allows us to choose the root $r \in V \setminus S$ for the SB problem, whereas Haasler et al. (2021) only consider the case where $r \in S$. In the latter case, we establish in Appendix E that r can be chosen arbitrarily, as stated by (Haasler et al., 2021, Corollary 4.3).

Finally, we present some advantages of the method proposed by Haasler et al. (2021) compared to ours. First, Haasler et al. (2021) may choose any kind of tree-based cost in practice, while our methodology only holds for the quadratic cost. This limitation is shared with all approaches based on the DSB De Bortoli et al. (2021) methodology. Indeed, since the cost is determined by the reference path measure, we often choose quadratic costs associated with Brownian motions or Ornstein-Uhlenbeck processes. Moreover, Haasler et al. (2021) may consider various inhomogeneous state spaces for the vertices of T , as presented in their numerical experiments. In our case, this approach is not compatible with our diffusion-based method. Finally, unlike Haasler et al. (2021), our method is not scalable with the number of vertices or edges in T due to computational limits. This limitation is common to all multimarginal approaches which rely on neural networks to parameterize the potential and/or the distributions of the multimarginal OT method, see Li et al. (2020); Fan et al. (2020); Korotin et al. (2022, 2021) for instance.

E Additional details on Tree DSB

Choice of the root r for π^0 . We recall that the reference measure π^0 considered in (**TreeSB**), which is defined in (2), verifies $\pi^0 \in \mathcal{P}_{T_r}$ for some fixed root $r \in V$ and $\pi_r^0 \ll \mathrm{Leb}$ with density φ_r . Moreover, we have $\pi_{v'|v}^0(\cdot \mid x_v) = N(x_v, \varepsilon/(2w_{v,v'})I_d)$ for any $(v, v') \in E_r$, and thus, π^0 is entirely determined by the choice of the root r and the density on the corresponding vertex φ_r .

As presented in Appendix D.1, we recall that (**TreeSB**) is equivalent to any multi-marginal Tree-SB problem with a reference measure $\bar{\pi}^0$ given by (14), i.e., $\bar{\pi}^0$ writes as $(d\bar{\pi}^0/d\pi^0) = \exp[\bigoplus_{i \in S} \psi_i^0]$, where $\{\psi_i^0\}_{i \in S}$ is a family of measurable potentials with $\psi_i^0 : \mathbb{R}^d \rightarrow \mathbb{R}$ such that $|\int_{\mathbb{R}^d} \psi_i^0 d\mu_i| < \infty$ for any $i \in S$. Hence, this result implies that (**TreeSB**) is unchanged if r is arbitrarily chosen in S , and if φ_r is such that $|\int_{\mathbb{R}^d} \varphi_r d\mu_r| < \infty$. By assuming that $H(\mu_{i_{K-1}}) < \infty$, the setting chosen in Section 3 is thus justified.

Consider now the case where $r \in S^c$, i.e., r is not a leaf of T , as done in Section 7. Then, the choice of φ_r can not be made arbitrarily anymore, since it determines a further regularization on the r -th marginal of the solution to (**TreeSB**). In this setting, the sequence defined by (**mIPF**) is unchanged. Hence, TreeDSB proceeds in the same manner as presented in Section 3, except for the first iteration, which we detail now.

Let us define $P = \mathrm{path}_{T_{i_0}}(i_0, r)$, where $T_{i_0} = (V, E_{i_0})$ is the directed version of T rooted in i_0 . We recall that first iterate of (**mIPF**) is defined by

$$\pi^1 = \operatorname{argmin}\{\mathrm{KL}(\pi \mid \pi^0) : \pi \in \mathcal{P}^{(\ell+1)}, \pi_{i_0} = \mu_{i_0}\}.$$

Following the proof of Lemma 13, it is clear that

$$\pi^1 = \mu_{i_0} \bigotimes_{(v,v') \in P} \pi_{v'|v}^0 \bigotimes_{(v,v') \in E_{i_0} \setminus P} \pi_{v'|v}^0 = \mu_{i_0} \bigotimes_{(v,v') \in E_{i_0}} \pi_{v'|v}^0,$$

where we emphasize that $P = \{(v, v') \in E_{i_0} : (v', v) \in E_r\}$. Therefore, Proposition 3 still applies between r and i_0 , by considering r instead of i_{K-1} . In practice, this means that the first iteration of TreeDSB consists in computing the time reversal of the path measures $\mathbb{P}_{(v',v)}^0$ for any $(v, v') \in P$.

Details on Section 5. Consider the entropic-regularized Wasserstein barycenter problem given by $(\mu_0\text{-regWB})$. As explained above, one way to get rid of the parameter μ_0 is to arbitrarily choose $r \in \{1, \dots, \ell\}$ and set $\varphi_r = d\mu_r/d\text{Leb}$ (or set φ_r such that $|\int_{\mathbb{R}^d} \varphi_r d\mu_r| < \infty$). In this case, we would obtain the following regularized Wasserstein barycenter problem

$$\mu_\varepsilon^\star = \arg \min \left\{ \sum_{i=1}^{\ell} w_i W_{2,\varepsilon/w_i}^2(\mu, \mu_i) + (\ell - 1)\varepsilon H(\mu) : \mu \in \mathcal{P} \right\}. \quad (\text{leaf-regWB})$$

Under A2, we know from Proposition 25 that (leaf-regWB) has a unique solution given by the marginal at vertex 0 of the solution to (TreeSB). Note that in that case, we also recover the $(\ell\varepsilon, (\ell - 1)\varepsilon)$ doubly regularized Wasserstein barycenter problem Chizat (2023). However, solving (TreeSB) with π^0 initialized at a leaf (instead of the central vertex) incurs the choice of a leaf r . In practice, since the optimization at each step of TreeDSB does not reach equilibrium, such a choice leads to approximate solutions which are biased towards the starting dataset on the leaf r , while the problem $(\mu_0\text{-regWB})$ is *agnostic* to the leaves of the tree.

F Algorithmic details

Choice of μ_0 in $(\mu_0\text{-regWB})$. Consider an undirected star-shaped tree T with $K + 1$ vertices and leaves $\{1, \dots, K\}$. In order to incorporate the marginal constraints in the penalization brought by μ_0 , we choose μ_0 as a Gaussian distribution with mean equal to $\sum_{i=1}^K \mathbb{E}[\mu_i]/K$ and diagonal covariance matrix computed as $(\sum_{i=1}^K \text{diag}(\text{Cov}[\mu_i])^{-1}/K)^{-1}$, where the inverse operation is component-wise. In this setting, (TreeSB) verifies A1 and A3 by Proposition 17.

Time discretization in Tree-DSB. Denote $k_n = (n - 1) \bmod(K)$ for any $n \in \mathbb{N}$. Let $T = (V, E)$ be a weighted undirected tree and consider the multi-marginal Schrödinger bridge problem (TreeSB) associated to this tree. We recall that for any $\{v, v'\} \in E$, we define $T_{v,v'} = \varepsilon/(2w_{v,v'})$.

Consider the path measures $\{\mathbb{P}_{(v,v')}^n\}_{n \in \mathbb{N}, (v,v') \in E_{k_n}}$ provided by Proposition 2. By combining Proposition 1, Proposition 3 and results on time reversal theory (Haussmann & Pardoux, 1986), we obtain by recursion that for any $n \in \mathbb{N}$, any $(v, v') \in E_{k_n}$, $\mathbb{P}_{(v,v')}^n$ is associated with a Stochastic Differential Equation on $[0, T_{v,v'}]$ given by

$$d\mathbf{X}_t = f_{t,v,v'}^n(\mathbf{X}_t)dt + d\mathbf{B}_t, \quad \mathbf{X}_0 \sim \pi_v^n. \quad (28)$$

Let $N \in \mathbb{N}^*$. In order to sample from the dynamics (28) at iteration $n \in \mathbb{N}$, we consider its Euler-Maruyama discretization on $(N + 1)$ time steps,

$$X_{m+1} = X_m + \gamma_{m+1} f_{t_m,v,v'}^n(X_m) + \sqrt{\gamma_{m+1}} Z_{m+1}, \quad X_0 \sim \pi_v^n, \quad (29)$$

where $Z_m \sim N(0, I_d)$ for any $m \in \{1, \dots, N\}$, $t_m = \sum_{i=1}^m \gamma_i$, and $\{\gamma_m\}_{m=1}^N \in (0, \infty)^N$ is a time schedule such that $\sum_{m=1}^N \gamma_m = T_{v,v'}$. This results in approximating the path measure $\mathbb{P}_{(v,v')}^n$ by the joint distribution $\pi_{(v,v')}^{n,N} \in \mathcal{P}^{(N+1)}$ defined by

$$\pi_{(v,v')}^{n,N} = \pi_v^n \otimes_{m=0}^{N-1} \pi_{(v,v'),m+1|m}^{n,N},$$

where $\pi_{(v,v'),m+1|m}^{n,N}(\cdot|x_m) = N(x_m + \gamma_{m+1} f_{t_m,v,v'}^n(x_m), \gamma_{m+1} I_d)$ for any $m \in \{0, \dots, N - 1\}$. If N is chosen large enough, then $\pi_{(v,v'),m}^{n,N}$ and $\mathbb{P}_{(v,v'),t_m}^n$ have approximately the same distribution for any $m \in \{0, \dots, N\}$. Consequently, $(\mathbb{P}_{(v,v')}^n)^R$ is naturally approximated by the joint distribution $\tilde{\pi}_{(v,v')}^{n,N} \in \mathcal{P}^{(N+1)}$ defined by

$$\tilde{\pi}_{(v,v')}^{n,N} = \pi_{v'}^n \otimes_{m=0}^{N-1} \pi_{(v,v'),N-m-1|N-m}^{n,N}.$$

If N is chosen large enough, we obtain that

$$\pi_{(v,v'),N-m-1|N-m}^{n,N}(\cdot|x_{N-m}) = N(x_{N-m} - \gamma_{N-m} f_{t_{N-m},v,v'}^n(x_{N-m}) + \gamma_{N-m} \nabla \log p_{v,v',t_{N-m}}(x_{N-m}), \gamma_{N-m} \mathbf{I}_d),$$

where $p_{v,v',t}$ is the density of $\mathbb{P}_{(v,v'),t}^n$ w.r.t. the Lebesgue measure.

Following Proposition 3, we now explain how the sequence $\{\pi_{(v,v')}^n\}_{n \in \mathbb{N}^*, (v,v') \in E_{k_n}}$ is recursively defined. Let $n \in \mathbb{N}$, $k = (n-1) \bmod(K)$. Define the path $P = \text{path}_{T_{i_k}}(i_k, i_{k+1})$. Then, for any $(v, v') \in E_{k+1}$,

- (a) if $(v, v') \in E_k \setminus P$, then $\pi_{(v,v')}^{n+1,N} = \pi_v^{n+1} \bigotimes_{m=0}^{N-1} \pi_{(v,v'),m+1|m}^{n,N}$,
- (b) if $(v', v) \in P$, then $\pi_{(v,v')}^{n+1,N} = \pi_v^{n+1} \bigotimes_{m=0}^{N-1} \pi_{(v',v),N-m-1|N-m}^{n,N}$.

These computations may be obtained by considering the sequence given by (mIPF) to solve the multi-marginal Tree-SB problem associated to $T^{(N)} = (V^{(N)}, E^{(N)})$, the N -discretized version of T (see Appendix B) with weights $w_{e_m}^{(N)} = 2\gamma_m/\varepsilon$, which is given by

$$\pi^* = \text{argmin}\{\text{KL}(\pi|\pi^{0,N}) : \pi \in \mathcal{P}^{(V^{(N)})}, \pi_i = \mu_i, \forall i \in S\},$$

with $\pi^{0,N} = \pi_r^0 \bigotimes_{(v,v') \in E_r} \pi_{(v,v'),1:N|0}^{0,N}$.

To approximate the IPF recursion given by (a) and (b), we use **on each edge** of T the score-matching approach of De Bortoli et al. (2021), which avoids heavy computations of score approximations. The next proposition is direct adaptation of (De Bortoli et al., 2021, Proposition 3).

Proposition 26. Assume that for any $n \in \mathbb{N}$, any $(v, v') \in E_{k_n}$, we have

$$\pi_{(v,v'),m+1|m}^{n,N}(\cdot|x_m) = N(F_{m,v,v'}^n(x_m), \gamma_m \mathbf{I}_d).$$

Let $n \in \mathbb{N}$, $k = (n-1) \bmod(K)$. Consider the path $P = \text{path}_{T_{i_k}}(i_k, i_{k+1})$. Let $(v, v') \in E_{k+1}$.

Define $p^n = \pi_{(v,v')}^{n,N}$ and $m_N = N - m - 1$. Then, if $(v', v) \in P$, we have

$$F_{m,v,v'}^{n+1} = \text{argmin}_{F \in L^2(\mathbb{R}^d, \mathbb{R}^d)} \quad (30)$$

$$\mathbb{E}_{p_{m_N, m_N+1}^n} [\|F(X_{m_N+1}) - (X_{m_N+1} + F_{m_N, v', v}^n(X_{m_N}) - F_{m_N, v', v}^n(X_{m_N+1}))\|^2],$$

otherwise, we have $F_{m,v,v'}^{n+1} = F_{m,v,v'}^n$.

In practice, we use two neural networks per edge $\{v, v'\} \in E$, one for each possible direction of the edge, such that $F_{v,v'}(\theta_{v,v'}^n, m, x) \approx F_{m,v,v'}^n(x)$ and $F_{v',v}(\theta_{v',v}^n, m, x) \approx F_{m,v',v}^n(x)$. For any $\{v, v'\} \in E$, the parameter $\theta_{v,v'}^n$ is updated at iteration n via the score matching loss defined by (30) in Proposition 26 if $(v, v') \in \text{path}_{T_{i_{k_n}}}(i_{k_n}, i_{k_{n-1}})$, see Algorithm 1.

G Details on the experiments

The numerical experiments presented in Section 7 are obtained by our own Pytorch implementation, which is inspired from the code⁷ provided by De Bortoli et al. (2021). In this section, we first provide information on the general setting of our experiments, and then give details on each of them. We define an IPF cycle as a subset of K consecutive iterations of (mIPF) and recall that the order of the leaves given by $\{i_0, \dots, i_{K-1}\}$ is randomly shuffled at each new IPF cycle.

G.1 General experimental setup

Implementation of Algorithm 1 in practice. Let $n \in \mathbb{N}$, with $k = (n-1) \bmod(K)$, $k+1 = n \bmod(K)$. Consider the path $P = \text{path}_{T_{i_k}}(i_k, i_{k+1})$. Assume that we are provided with a dataset D_{i_k} , which contains M samples from $\pi_{i_k}^n$. Following Lines 7-9 in Algorithm 1, we apply processes (a) and (b) recursively on the edges $(v, v') \in P$.

⁷https://github.com/JTT94/diffusion_schrodinger_bridge

(a) **Sampling process (Line 7).** For any $x_0 \in D_v$, we first sample from the diffusion trajectory (29) given by the Euler Maruyama discretization of $\mathbb{P}_{v,v'}^n$ starting from x_0 , which gives $m \times N$ time samples. We then store the last iterate of each trajectory in a new dataset $D_{v'}$, which thus approximates $\pi_{v'}^n$.

(b) **Training process (Lines 8-9).** In order to avoid heavy computation, we approximate the *mean-matching* loss (30) by an unbiased estimator obtained by subsampling b elements from the *full* trajectories obtained in the sampling process, see (De Bortoli et al., 2021, Eq. (97)-(98)). Here, b refers to the *batch-size* parameter of the neural networks.

To avoid any bias issue, the whole trajectories obtained at process (a) are refreshed at a certain frequency over the training iterations of the neural networks by once again simulating the diffusion (29). In our experiments, this refresh occurs each 500 iterations.

Choice of π^0 . We recall that the reference measure π^0 of each Tree-SB problem that we consider in our experiments is given by (2) where the root r is chosen as the central vertex of the star-shaped tree and π_r^0 is provided in Appendix F.

Setting of the time discretization introduced in Appendix F. The number of time-steps N in the time discretization of the diffusions is chosen to be even and identical for each of the edges of the tree. Let $\{v, v'\} \in E$. We now give details on the design of the time schedule $\{\gamma_k\}_{k=1}^N$ related to the edge $\{v, v'\}$, see Appendix F. Following De Bortoli et al. (2021), we choose this sequence to be invariant by time reversal and consider $\gamma_k = \gamma_0 + (2k/N)(\bar{\gamma} - \gamma_0)$ for any $k \in \{0, \dots, N/2\}$ (the rest of the sequence being obtained by symmetry) where γ_0 is a free parameter and $\bar{\gamma}$ is determined by $\sum_{k=1}^N \gamma_k = T_{v,v'}$. In our experiments, we set $N = 50$ and $\gamma_0 = 10^{-5}$.

Choice of the architectures of the neural networks. In the case of the experiments related to synthetic datasets (two-dimensional toy datasets, Gaussian distributions) and to the subset posterior aggregation task, we implement the same architecture as presented in (De Bortoli et al., 2021, Figure 3). We refer to this model as “Basic Model” and detail it in Figure 8. In the “Basic Model”, the PositionalEncoding block applies the sine transform described in Vaswani et al. (2017), with output dimension equal to 32, and each MLP Block represents a Multilayer Perceptron Network. In particular, MLPBlock (1a) has shape $(d, 128, \max(256, 2d))$, MLPBlock (1b) has shape $(32, 128, \max(256, 2d))$, and MLPBlock (2) has shape $(2 \times \max(256, 2d), \max(256, 2d), \max(128, d), d)$, where d denotes the dimension of input data. We optimize the networks with ADAM (Kingma & Ba, 2014) with learning rate 10^{-4} and momentum 0.9. For each of the networks, we set the batch size to 4,096 and choose the number of iterations as 15,000 for the synthetic datasets and 20,000 for the subset posterior aggregation task. Our experiments ran on 1 Intel Xeon CPU Gold 6230 20 cores @ 2.1 Ghz CPU.

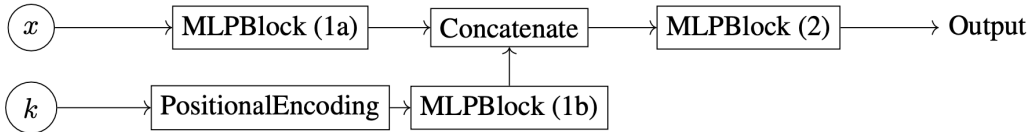


Figure 8: Architecture of the “Basic Model”.

In the case of the experiments related to MNIST dataset, we use a reduced UNET architecture based on Nichol & Dhariwal (2021), where we set the number of channels to 64 rather than 128. We implement an exponential moving average of network parameters across training iterations, with rate 0.999. We optimize the networks with ADAM (Kingma & Ba, 2014) with learning rate 10^{-4} and momentum 0.9. Finally, we set the batch size to 256 and the number of training iterations to 30,000. Our experiments ran using 1 Nvidia A100.

Details on regularized state-of the art methods. We run the fsWB algorithm (Cuturi & Doucet, 2014) with the implementation provided by Flamary et al. (2021). For each experiment, we run 100 Sinkhorn iterations with 1500 samples for each dataset (*i.e.*, the maximum number of samples that it can generate) and set the regularization parameter ε to its lowest value such that the algorithm is stable. Finally, for sake of fairness with our method, we initialise the barycenter measure with

π_r^0 . To run the crWB algorithm (Li et al., 2020), we use the code provided by the authors. We consider the quadratic regularization, which is shown to be empirically more stable than entropic regularization. Following Fan et al. (2020), we choose the potential networks to be fully connected neural networks with 3 hidden layers of shape $(\max(128, 2d), \max(128, 2d), \max(128, 2d))$. The activation functions are ReLu. We optimize the networks with ADAM (Kingma & Ba, 2014) with learning rate 10^{-4} for the subset posterior aggregation task and 10^{-3} for the Gaussian experiment. Finally, we set the batch size to 4,096 and the number of training iterations to 50,000.

Details for experiments on the two-dimensional datasets. We consider three different datasets that contain 10,000 samples from Swiss-roll (vertex 1), circle (vertex 2) and moons (vertex 3). We run TreeDSB for 20 IPF cycles with regularization parameter $\varepsilon = 0.2$ and report the results in Figure 4 and Figure 5. In our early results, we observed a decreasing performance by taking $\varepsilon < 0.2$ or by considering a “Basic Model” which is not expressive enough, see Figure 9.

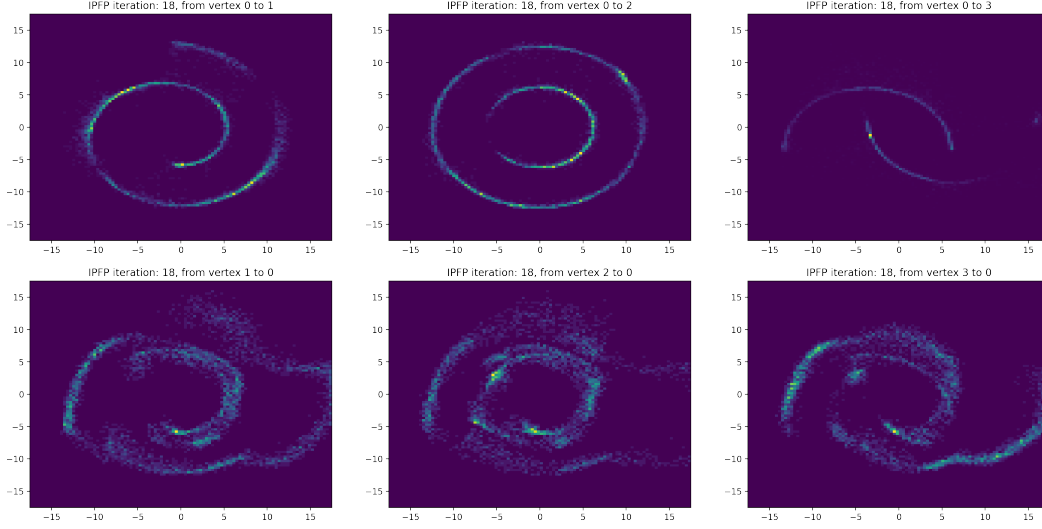


Figure 9: From left to right: estimated densities on the leaves (above) and estimated density for the barycenter by diffusing from the leaves (below) after 18 IPF cycles. In this setting, $\varepsilon = 0.2$, MLPBlock (1a) has shape (2, 16, 32), MLPBlock (1b) has shape (16, 16, 32), and MLPBlock (2) has shape (64, 64, 64, 2). We observe that the procedure does not converge well.

Details for experiments on synthetic Gaussian datasets. For each dimension that we consider, we generate three different triplets of random non-diagonal covariance matrices whose condition number is less than 10. We then run the algorithms on each triplet and aggregate the obtained results. The Gaussian datasets contain 1,500 samples for fsWB, and 10,000 samples for crWB and TreeDSB. We run fsWB with the following settings $(d, \varepsilon) \in \{(2, 0.1), (16, 0.2), (64, 0.5), (128, 1.0), (256, 2.0)\}$. We run TreeDSB for 10 IPF cycles with regularization parameter $\varepsilon = 0.2$, and keep, for each of the three settings, the best result among the 30 IPF iterations.

Details for experiments for subset posterior aggregation. When considering a dataset splitted into several subdatasets, a common paradigm in bayesian inference consists in running Monte Carlo Markov Chain methods separately on these subdatasets, and then merge the obtained posteriors to recover the full posterior. The barycenter of these subdataset posteriors is proved to be close to the full data posterior under mild assumptions (Srivastava et al., 2018). In our setting, we consider the posterior aggregation problem for the logistic regression model associated to the wine dataset⁸ ($d = 42$) with 3 subdatasets. We consider here two splitting methods: (i) either, data is uniformly splitted between 3 subdatasets with respect to the label distribution, denoted by wine-homogeneous, or (ii) data is splitted with some heterogeneity according to a Dirichlet distribution whose parameter is randomly chosen, denoted by wine-heterogeneous. Following Korotin et al. (2021), we use the stochastic approximation trick so that the subset posterior samples do not vary consistently from the

⁸<https://archive.ics.uci.edu/ml/datasets/wine>

full posterior in covariance (Minsker et al., 2014). We implement the Unadjusted Langevin Algorithm (ULA) to sample from each subdataset posterior and from the full posterior. In each case, we run ULA for $5.5 \cdot 10^6$ iterations with a well chosen step-size, and obtain 9,900 samples after applying a *burn-in* of order 10% and then a *thinning* of size 500. We provide in Figure 10 some metrics which assess the quality of this sampling process. We recall that the full posterior samples serve as ground truth in this experiment.

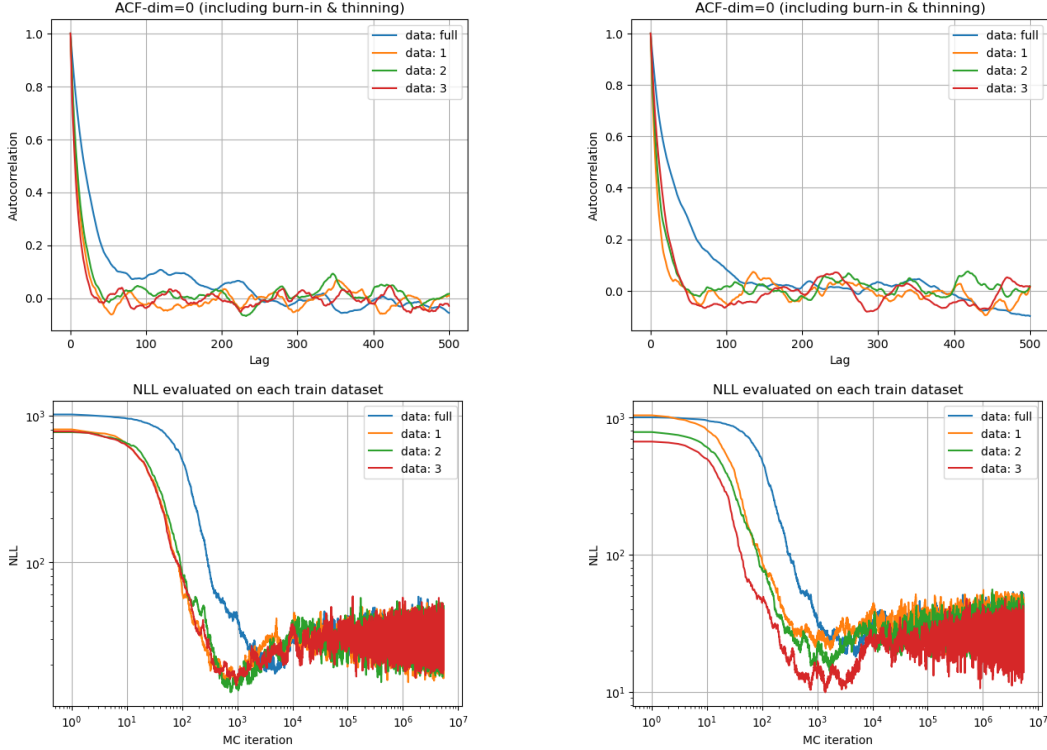


Figure 10: Evaluation of the sampling process for wine-homogeneous (left) and wine-heterogeneous (right). We display the Autocorrelation function on 500 lags (above) and the evolution over the iterations of ULA of the negative log-likelihood (NLL) evaluated on each training dataset (below). In particular, the samples are decorrelated and the NLL has a satisfying profile.

The results presented in Table 2 were computed as follows. For fsWB, we first subsample 1,500 samples out of the 9,900 samples from each posterior, and then run the algorithm with $\varepsilon = 0.5$. We repeat three times this procedure and then aggregate the results. In the case of crWB and TreeDSB, we run the algorithms three times with various seeds. Similarly to the Gaussian setting, we run TreeDSB for 10 IPF cycles with regularization parameter $\varepsilon = 0.2$, and keep, for each of the three settings, the best result among the 30 IPF iterations.

Details for experiments for MNIST Wasserstein barycenter. We recall that the dimension of MNIST data is $d = 28 \times 28 = 784$. In this setting, we have 1,000 samples per dataset. We run TreeDSB for 3 IPF cycles with regularization parameter $\varepsilon = 0.5$. In our early results, we observed a decreasing performance of our method when we chose $\varepsilon < 0.5$ or when running TreeDSB for more than 3 IPF cycles, due to the accumulation of numerical errors over the iterations of the algorithm. We provide in Figure 11 a further illustration of the result presented in Section 7, along with an additional experiment in Figure 12.

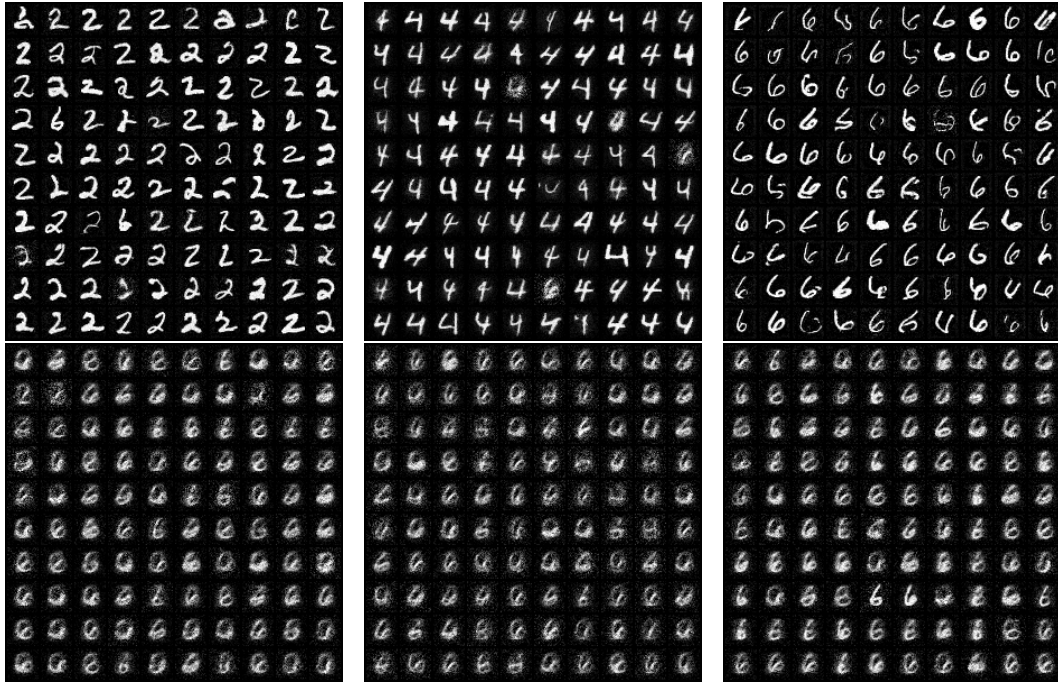


Figure 11: Tree-DSB Wasserstein barycenter between the digits 2, 4 and 6. From left to right: samples from the leaves (above) and samples from the barycenter by diffusing from the leaves (below).

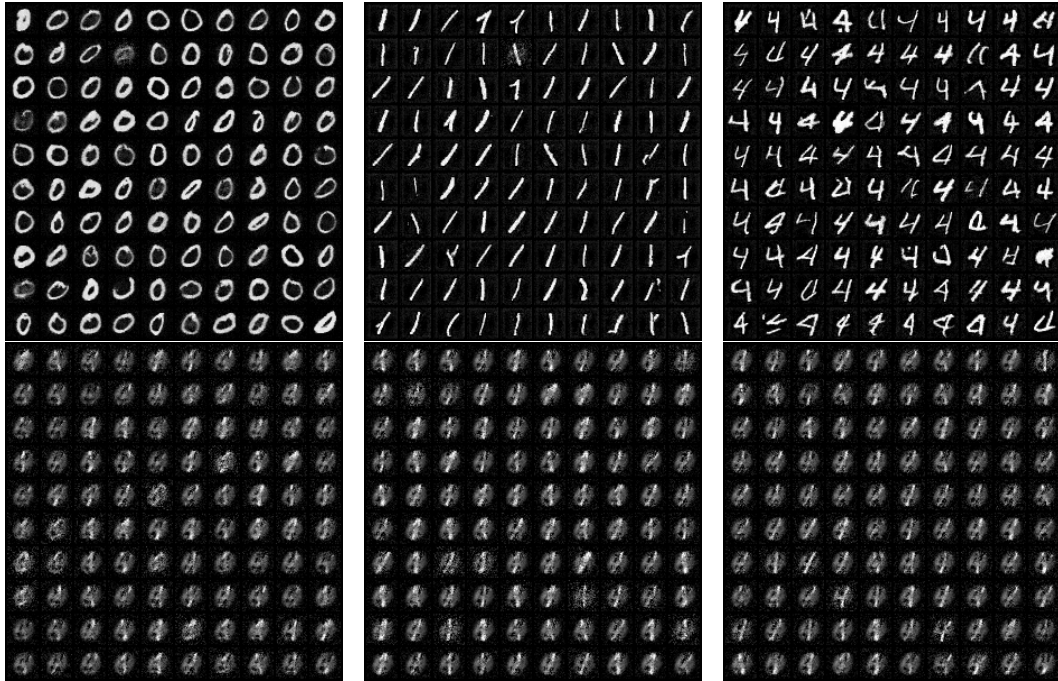


Figure 12: Tree-DSB Wasserstein barycenter between the digits 0, 1 and 4. From left to right: samples from the leaves (above) and samples from the barycenter by diffusing from the leaves (below).